

**DEF6 is associated with the  
translational initiation regulating  
protein synthesis of eIF4E, 4E-T and  
PABP and colocalises with eIF4E and  
PABP in the immunological synapse**

By

Maha Mohammed Alsayegh

Thesis submitted to The University of Nottingham for the degree of Doctor  
of Philosophy

**October 2017**

# Acknowledgements

By the grace of almighty Allah, I have completed my thesis. This research would not have been possible without the financial support of the Ministry of Higher Education in the Kingdom of Saudi Arabia.

This thesis could not be completed without the great guidance and support which I have received from many people over the years of my research. I would like to extend my sincere thanks to the following:

First and foremost, I am extremely thankful to my supervisor, Professor Fred Sablitzky, for his patience, guidance, advice, and support which enabled me to complete this PhD. Thank you for keeping your office door open and being so readily available. Thank you for all the chats and enjoyable moments over these past years.

I must also remember to thank Dr Peter Jones for his useful feedback and expert technical knowledge.

During my PhD I was blessed to make such good friends and work within such a cooperative atmosphere. I would like to acknowledge lab members: Huaitao, Tamil, Chen and Kerry; thank you for your friendship and help during my work in the lab.

To Deniz, from my first day in the lab you became one of my best friends. You are an amazing person in too many ways. We have supported and helped each other through both good and bad times. I will always remember the great times we have had over the years.

Thank you to all of you for giving me precious memories and years of fun. I hope our friendship will continue to be strong in the future.

Also, I would like to thank all my family members who supported me. To my parents, thank you for your love, prayers and encouragement. I would not be who I am today without you. You have always been my biggest supporters and I am proud to be your daughter.

To my brother Ghassan, words cannot express how grateful I am for all of the sacrifices you have made. Without your patience and sacrifice, I could not have completed this

thesis. I am truly lucky to have a big brother like you who is always supporting me. I wish Allah to fulfil all your wishes. Thank you very much from the bottom of my heart.

A special word of thanks also goes to my brother Rajab for his continuous help which kept me going through many struggles to reach this goal. Thank you for your cheering me up when I needed it most.

To my sister Jacqueline, thank you for your encouraging words, love, and faith in me; for being always there for me and when I need a listening ear and wise opinion. I am glad and blessed to be your sister. I also want to thank my brothers Jawdat and Mazen for their love and support.

Finally I would like to thank, project students Christian Tuckwell-Smith and Elspeth Meakin for making Serine and threonine mutations for me; and all the member of the C5 lab.

To anyone that may I have forgotten, thank you sincerely, I am indebted to you all.

## Abstract

DEF6 is an atypical guanine nucleotide exchange factor (GEF) for Rho GTPases Rac1 and Cdc42, which is highly expressed in mature T cells. DEF6 is recruited to the immunological synapse (IS) following phosphorylation by LCK in response to T cell receptor (TCR) stimulation during inflammation. In resting Jurkat T cells, DEF6 has been known to associate with polysomes and under cellular stress conditions to form cytoplasmic granules colocalising with mRNA decapping enzyme subunit 1 (DCP1), a marker of P-bodies. Hence DEF6 has been linked to mRNA regulation, which includes mRNA translation initiation and repression by P-body formation. To elucidate the structural requirements for P-body localisation of DEF6, N-terminal truncation mutants lacking either the C-terminal coiled coil domain or the pleckstrin homology (PH) domain in conjunction with the coiled coil domain were established and coexpressed with DCP1 in COS7. Both GFP-tagged mutant DEF6 proteins spontaneously colocalised with DCP1 indicating that the N-terminal end of DEF6 is sufficient for P-body association and that the coiled coil domain facilitates a confirmation that masks the N-terminal end of DEF6. Exchange of serine and/or threonine residues in the C-terminal end with either phosphomimic or phosphosilent amino acids resulted in formation of GFP-DEF6 aggregates or granules, respectively. While GFP-DEF6 granules partly overlapped with DCP1, GFP-DEF6 aggregates appeared to trap DCP1. In resting Jurkat cells endogenous DEF6 associated with nascent mRNA translation and colocalised with eukaryotic translation initiation factor 4E (eIF4E) as well as poly A binding protein (PABP). eIF4E and the eIF4E-binding protein 4E-T but not PABP were shown to interact with DEF6 *in vitro*. Moreover, siRNA-mediated knockdown and ectopic overexpression of DEF6 in Jurkat cells established a positive

correlation of DEF6 expression and eIF4E, PABP and 4E-T protein expression. RT-PCR revealed that the alteration in expression of these proteins was not due to transcriptional regulation and inhibition of protein degradation pathways could not rescue downregulation of eIF4E. Colocalisation of DEF6 with eIF4E and PABP but not with 4E-T was also observed in the IS upon TCR-mediated signalling. Together these results strongly suggest that DEF6 is involved in active mRNA translation in resting and activated Jurkat T cells controlling expression of components of the translational initiation complex as well as P-bodies.

## Abbreviations

4E-T	Eukaryotic translation initiation factor 4E transporter
APS	Ammonium persulfate
APC	Antigen Presenting Cell
ARP 2/3	Actin-Related Protein 2/3 complex
BSA	Bovine Serum Albumin
Cdc42	Cell Division Control Protein 42 homolog
CTL	Cytotoxic T lymphocyte
DAG	Diacylglycerol
DN	Double negative
DCP 1/2	Decapping Enzyme 1/2
DEF6	Differentially Expressed in FDCP6
DH	Dbl Homology Domain
DHL	Dbl Homology-Like Domain
DOCK	Dedicator of Cytokinesis
DMEM	Dulbecco's Modified Eagle's Medium
DMSO	Dimethyl Sulfoxide
DSH	DEF6/SWAP70 Homology Like Domain
EAE	Experimental Autoimmune Encephalitis
EAU	Experimental Autoimmune uveitis
ECL	Enhanced Chemiluminescence

EDTA	Ethylenediaminetetraacetic acid
eIF	Eukaryotic Initiation Factor
eIF4E	Eukaryotic translation initiation factor 4E
F-actin	Filamentous Actin
FBS	Foetal Bovine Serum
GEF	Guanine nucleotide Exchange Factor
GTP	Guanosine triphosphate
GDP	Guanosine Diphosphate
GDI	Guanine nucleotide dissociation inhibitor
GAP	GTPase-activating protein
GFP	Green Fluorescent Protein
GTPase	Guanosine Triphosphate Hydrolase
IBP	IRF4 Binding Protein (alternative name for DEF6)
ICAM-1	Intercellular Adhesion Molecule-1
IP3	Inositol Triphosphate
IRF4	Interferon Regulatory Factor 4
IS	Immunological Synapse
ITAM	Immunoreceptor Tyrosine-based Activation Motif
ITK	Interleukin-2 Inducible T cell Kinase
IgG etc	Immunoglobulin G etc
LAT	Linker for Activation of T cells

LCK	Lymphocyte-specific Protein Tyrosine Kinase
LFA-1	Lymphocyte Function Associated Antigen-1
LB	Luria-Bertani medium
IL-	Interleukin
mCherry	Red fluorescent proteins
MAPK	Mitogen-activated protein kinase
MHC	Major Histocompatibility Complex
MTOC	Microtubule organising centre
mRNA	Messenger RNA
miRNA	Micro RNA
mRNP	Messenger Ribonuclear Proteins
pMHC	Epitope Presenting MHC
NFAT <sub>c1/2</sub>	Nuclear Factor of Activated T cells
NF- $\kappa$ B	Nuclear Factor $\kappa$ B
NMD	Nonsense-Mediated mRNA Decay
PABP	Poly (A) Binding Protein
P-body	Processing Body
PBS	Phosphate Buffered Saline
PBST	Phosphate Buffered Saline with Tween-20
PFA	Paraformaldehyde
PH	Pleckstrin Homology Domain

PIP3	Phosphatidylinositol 3, 4, 5, Triphosphate
PLC $\gamma$ 1	Phospholipase C $\gamma$ 1
PMSF	Phenylmethylsulfonyl fluoride
PVDF	Polyvinylidene fluoride
Rac1	Ras-Related C3 Botulinum Toxin Substrate 1
RPMI	Roswell Park Memorial Institute medium
SP	Single positive
SDS	Sodium Dodecyl Sulphate
SDS-PAGE	Sodium Dodecyl Sulphate Polyacrylamide Gel Electrophoresis
SE A/B	<i>Staphylococcus aureus</i> enterotoxin A and B
SLAT	SWAP-70 Like Adapter of T cells (alternative name for DEF6)
SLE	Systemic Lupus Erythematosus
SMAC	Supramolecular Activation Cluster
cSMAC	Central Supramolecular Activation Cluster
dSMAC	Distal Supramolecular Activation Cluster
pSMAC	Peripheral Supramolecular Activation Cluster
SWAP70	Switch-Associated Protein-70
TCR	T cell Receptor
T <sub>H</sub>	T Helper
TEMED	Tetramethylethylenediamine
TIA-1	T-cell restricted Intracellular Antigen 1

TIA-R	TIA-1 Related protein
tRNA	Transfer RNA
WASP	Wiskott–Aldrich Syndrome Protein
WAVE2	WASP-family Verprolin-homologous Protein-2
XRN1	5'-3' Exoribonuclease 1
ZAP-70	ζ-chain associated protein of 70kDa

## List of Contents

Acknowledgements .....	I
Abstract .....	III
Abbreviations .....	V
List of Contents .....	X
List of Figures .....	XVI
List of tables .....	XVIII
<b>Chapter 1 Introduction .....</b>	<b>1</b>
<b>1.1 Discovery, protein structure, role and function of DEF6.....</b>	<b>2</b>
1.1.1 Discovery and identification of DEF6.....	2
1.1.2 Structure of DEF6.....	3
1.1.3 Rho family GTPases and role of DEF6 as a guanine nucleotide exchange factor (GEF).....	4
<b>1.2 Role of DEF6 in TCR-mediated cytoskeletal remodelling.....</b>	<b>6</b>
1.2.1 Development, differentiation, activation and survival of T-cells.....	6
1.2.2 Antigen presentation and T cell signalling.....	8
1.2.3 Phosphorylation and Ca <sup>2+</sup> signalling cascades in TCR signalling pathways.....	10
1.2.4 Effect of DEF6 on pathways and various proteins responsible for the formation of the actin cytoskeleton.....	12
<b>1.2.5 The formation and function of the immunological synapse.....</b>	<b>16</b>
1.2.5.1 The structure immunological synapse.....	16
1.2.5.2 The immature and mature immunological synapse.....	19

1.2.5.3 The role of cytoskeletal remodelling in the formation of the immunological synapse .....	21
<b>1.3 The role of DEF6 in P-body formation and mRNA regulation.....</b>	<b>23</b>
1.3.1 Aggregation as a result of phosphorylation of DEF6 by ITK at the tyrosine residues 210 and 222 .....	23
1.3.2 Different domains of DEF6 with unique function during aggregation.....	25
1.3.3 Association of DEF6 with Polysomes in Jurkat T cells.....	26
<b>1.4 mRNA regulations at the transcriptional and translational level.....</b>	<b>29</b>
1.4.1 Post-transcriptional regulation of mRNA.....	29
1.4.2 Initiation process of mRNA translation.....	31
1.4.3 Cytoplasmic foci targeting proteins, P bodies, stress granules, eIF4E, 4E-T and other proteins involved in mRNA regulation and aggregation.....	33
1.4.4 Knock down of protein expression using small interfering RNA (siRNA) technology.....	36
1.4.5 The mRNA cycle.....	37
1.4.6 The role of DEF6 in P-body formation and mRNA regulation.....	39
<b>1.5 DEF6 knockdown and its role in various physiological processes.....</b>	<b>40</b>
1.5.1 Role of DEF6 in autoimmune response.....	40
1.5.2 Role of DEF6 in other processes.....	45
1.6 Research Objective.....	47
<b><i>Chapter 2 Material and methods.....</i></b>	<b>48</b>
2.1 Cell Culture.....	49
• 2.1.1 Cells line.....	49
• 2.1.2 Cells culture media.....	49

- 2.2.1-1 Antibiotic.....50
- 2.1.2-2 Treatments .....50
- 2.2 Bacterial Growth Media.....50
- 2.3 Buffers and solution.....51
  - 2.3.1 Electrophoresis Buffers.....51
  - 2.3.2 Western blots buffer and solution.....51
  - 2.3.3 Co-immunoprecipitation Buffers.....51
  - 2.3.4 Sodium Dodecyl Sulphate Polyacrylamide Gel Electrophoresis Buffers and Solutions.....52
  - 2.3.5 Gel fixer.....52
  - 2.3.6 Immunofluorescence Solutions.....52
  - 2.3.7 Flow cytometry Solution.....53
- 2.4 Cells culture Techniques.....54
  - 2.4.1 Thawing of cell.....54
  - 2.4.2 Passaging of Adherent Cell.....54
  - 2.4.3 Passaging of Suspension Cell.....55
  - 2.4.4 Counting Cell lines using a Haemocytometer.....55
  - 2.4.5 Cryopreservation of Cell Lines.....55
  - 2.4.6 Transfection of Adherent Cell.....55
  - 2.4.7 Transfection of Jurkat T Cell.....56
  - 2.4.8 siRNA Knockdown DEF6.....57
  - 2.4.9 Immunological Synapse Formation.....57
  - 2.4.10 Immunofluorescence.....58
  - 2.4.11 Translation and newly synthesised protein assay.....59
  - 2.4.12 Flow cytometry.....60
- 2.5 Cell Treatments.....60
- 2.6 Bacterial Culture techniques.....61

- 2.6.1 Bacterial transformation.....61
- 2.6.2 Bacterial colony picked.....61

2.7 DNA Techniques.....61

- 2.7.1 Plasmid DNA extraction from bacteria.....61
- 2.7.2 Determination of DNA or RNA Concentration.....63
- 2.7.3 DNA Sequencing.....64

2.8 RNA Techniques.....64

- 2.8.1 RNA extraction.....64
- 2.8.2 cDNA Synthesis.....65
- 2.8.3 Designing primers.....65

2.9 Polymerase Chain Reaction.....65

- 2.9.1 Reverse transcription polymerase chain reaction (RT-PCR).....65
- 2.9.2 Agarose Gel Electrophoresis.....66
- 2.9.3 Site-directed Mutagenesis.....67

2.10 Proteins Techniques.....68

- 2.10.1 Preparation of Protein sample.....68
- 2.10.2 Protein pull down.....69
- 2.10.3 Co-Immunoprecipitation (Co-IP).....69
- 2.10.4 Sodium Dodecyl Sulphate Polyacrylamide Gel Electrophoresis.....70
- 2.10.5 Western blot.....71
- 2.10.6 Re-probing of PVDF Membranes.....72

2.11 Imaging Methods.....72

- 2.11.1 Confocal microscope.....72
- 2.11.2 Image analysis.....72
- 2.11.3 Flow Cytometry analysis.....72
- 2.11.4 Statistical Analysis.....73

<b>Chapter 3 Results</b> .....	<b>74</b>
3.1 Deletion of the coiled coil domain results in spontaneous colocalisation of DEF6 N-terminal mutants with P-body marker DCP1.....	75
3.2 Serine and/or Threonine phosphorylation in the C-terminal end of DEF6 results in aggregates that trap DCP1.....	80
3.3 Endogenous DEF6 is highly expressed in Jurkat T cells but absent in other cell lines.....	94
3.4.1 DEF6 colocalises with sites of translational initiation.....	97
3.4.2 DEF6 does not bind to the Cap 5' mRNA .....	99
3.4.3 DEF6 colocalises with translational initiation factors eIF4E and 4E-transporter .....	100
3.4.4 DEF6 also colocalises with PABP and ARP2/3 but to a much lesser extent than observed for eIF4E and 4E-T.....	104
3.4.5 DEF6 physically interacts with eIF4E and 4E-T but not with PABP.....	106
3.5 siRNA-mediated knockdown of DEF6 expression in Jurkat T cells.....	108
3.5.1 siRNA-mediated DEF6 knockdown resulted in down regulation of eIF4E, 4E-T and PABP protein expression in Jurkat cells.....	114
3.5.2 Increase of eIF4E, 4E-T and PABP protein expression upon DEF6 overexpression in Jurkat cells.....	120
3.5.3 Neither overexpression nor knockdown of DEF6 affect gene expression of eIF4E, 4E-T or PABP.....	123
3.5.4 DEF6 siRNA-mediated downregulation of eIF4E does not seem to be due to protein degradation via autophagy or ubiquitination pathways.....	125
3.6 DEF6 colocalises with eIF4E and PABP at the Immune synapse (IS).....	127
• 3.6.1 Presence of DEF6 at the IS.....	127

- 3.6.2 DEF6 colocalises with translational initiation complex during IS formation.....129

**Chapter 4 Discussion**.....135

4.1 Structure-function analysis of DEF6.....136

4.1.1 The coiled coil domain constrains the N-terminal end of DEF6 to target P-bodies.....136

4.1.2 Serine/threonine phosphorylation in the C-terminal end of DEF6 results in coiled coil-mediated aggregation that trap DCP1.....137

4.2 DEF6 function in mRNA translation.....140

4.2.1 DEF6 is associated with nascent mRNA translation.....140

4.2.2 DEF6 is associated with the translational initiation complex binding eIF4E.....140

4.2.3 DEF6 binds eIF4E-binding protein 4E-T.....141

4.2.5 DEF6 controls protein expression of eIF4E, PABP and 4E-T.....142

4.2.6 DEF6 controls translation of eIF4E.....142

4.3 Translational control in the immunological synapse.....144

4.4 DEF6: a multifunctional signalling hub in T cells.....145

**Conclusion**.....146

**References**.....147

**Appendix**.....162

6.1 Plasmid map.....163

6.2 amino acid and codons.....164

6.3 Primary and Secondary Antibodies.....165

Cell Stain.....166

List of Primer Sequences.....	167
List of Reverse Transcription Polymerase Chain Reaction (RT-PCR) Primers....	168
6.4 Verification of DEF6 by DNA Sequencing.....	169

## List of Figures

Figure 1.1.2 DEF6 domain structure.....	3
Figure 1.2.1 The principle signal transduction pathways triggered by TCR stimulation involved in T helper (T <sub>h</sub> ) cell differentiation.....	7
Figure 1.2.2 Immunologic Synapse (IS) showing LFA-1 on T-cell surface binding to ICAM-1 expressed on Antigen Presenting Cells (APC).....	9
Figure 1.2.4 TCR signal transduction integrating with varied components of the actin polymerization machinery.....	14
Figure 1.2.5.1: Distinct spatial arrangement of components of the immunological synapse (IS). .....	18
Figure 1.2.5.2 Schematic diagram of the mature immunological synapse (IS) and the “bull’s eye”.....	20
Figure 1.3.3 DEF6 associated with Polysomes in Jurkat Cells.....	27
Figure 1.4.4 Schematic representation of the mRNA cycle showing the regulation of mRNA by P-bodies and Stress granules.....	38
Figure 3.1: Schematic representation of DEF6 domain structure and GFP-tagged truncation mutants and their phosphomimic derivatives .....	76
Figure 3.1.1: Coiled coil domain restrains DEF6 from spontaneous colocalisation with P-bodies.....	78
Figure 3.2: Known phosphorylation sites in the DEF6 protein .....	80

Figure 3.2.1: Localisation of DEF6 Threonine or Serine to Glutamic acid mutants.....	82
Figure 3.2.2: Cotransfection of GFP-tagged DEF6 Serine to Glutamic acid GFP tagged mutants with P-body marker (DCP1) .....	83
Figure 3.2.3: Cotransfected DEF6 Threonine to Glutamic acid GFP-tagged mutants either occurring singly or in combination with P-body marker (DCP1).....	86
Figure 3.2.4: Localisation of DEF6 Serine or Threonine to Phenylalanine Mutants.....	88
Figure 3.2.5: Cotransfected of DEF6 Serine mutants to Phenylalanine with P-body marker (DCP1).....	89
Figure 3.2.6: Cotransfected of DEF6 Threonine mutants to Phenylalanine with P-body marker (DCP1).....	91
Figure 3.3: Western blot analysis of DEF6 expression.....	96
Figure 3.4: DEF6 is associated with initiation of mRNA translation in resting Jurkat T cells.....	98
Figure 3.4.1: DEF6 does not bind to the 7-methyl GTP-linker (Cap) at the 5' end of mRNAs.....	99
Figure 3.4.2: Partial colocalisation of DEF6 with eIF4E and 4E-T in Jurkat cells.....	102
Figure 3.4.3: Only a minor fraction of DEF6 colocalise with PABP and Arp2/3 ...	105
Figure 3.4.4: DEF6 interacts with eIF4E and 4E-T but not with PABP.....	107
Figure 3.5: Efficient siRNA-mediated knockdown of DEF6 expression in Jurkat T cells.....	111
Figure 3.5-1: Flow Cytometry analysis confirmed efficient knockdown of DEF6 expression.....	113

Figure 3.5.1: DEF6 regulates expression of eIF4E, 4E-T and PABP proteins in Jurkat T cells.....	117
Figure 3.5.1-1: DEF6 is regulate expression of mRNA translation proteins.....	119
Figure 3.5.2: DEF6 overexpression increases expression of eIF4E, 4E-T and PABP but not Arp2/3.....	122
Figure 3.5.3: RT-PCR analysis of gene expression.....	124
Figure 3.5.4: Inhibition of protein degradation does not rescue eIF4E protein expression in DEF6 siRNA-treated Jurkat T cells.....	126
Figure 3.6.1: DEF6 recruitment to the Immune synapse in Jurkat cells upon antigen presentation by Raji B cells.....	128
Figure 3.6.2: DEF6 colocalisation with proteins of the mRNA initiation complex in the IS.....	132
Figure 6.1: Plasmid map of GFP-tagged DEF6. eGFPC2.....	163
Figure 6.4: Verification of DEF6 by DNA Sequencing.....	169

## **List of tables**

Table 1: PCR program for RT-PCR reactions.....	66
Table 2: PCR program for Quick Change Mutagenesis.....	67
Table 3: Table 3: Summary of behaviour and localisation of Serine/Threonine mutant DEF6 proteins ectopically expressed in COS7 cells .....	92
Table 4: List of amino acids, their single and three letter abbreviations and codons.....	163
Table 5: List of Primary and Secondary Antibodies.....	165
Table 5.1 List of Secondary antibodies used.....	166

Table 6: Cell Stain.....166

Table 7: List of Primer Sequences.....167

Table 8: List of Reverse Transcription Polymerase Chain Reaction (RT-PCR)  
Primers.....168

# **Chapter 1: Introduction**

## **1.1 Discovery, protein structure, role and function of DEF6**

### **1.1.1. Discovery and identification of DEF6**

DEF6 was first identified as a novel Rho-family GEF in mouse haematopoietic tissues (Hotfilder *et al.*, 1999). DEF6 is also known as interferon regulatory factor 4-binding protein (IBP) (Fanzo *et al.*, 2006) and has been described as Swap-70-like adapter of T cells (SLAT) (Tanaka *et al.*, 2003) due to its close homology with Swap-70 (Borggreffe *et al.*, 1998). However, Swap-70 is mainly expressed in mature B cells (Masat *et al.*, 2000), whereas DEF6 is primarily expressed in T cells and to a lesser extent in B cells (Borggreffe *et al.*, 1999). From AD10, T Cell Receptor (TCR) transgenic mouse Th2 cells SLAT/DEF6 cDNA was isolated. Human peripheral T cell, Jurkat cells and THP-1 was shown to express SLAT/DEF6 (Tanaka *et al.*, 2003). DEF6 cDNA, which was 2.3kb in length, was also isolated from a human lymph node cDNA library. The open reading frame encoded a protein of 631 amino acids with a molecular weight of 74 kDa (Gupta *et al.*, 2003).

### 1.1.2. Structure of DEF6.

To date 89 GEFs have been identified in the human genome which are characterized into three main families according to their domain architecture: the Dbl family is the largest of these, comprising of 69 family members with a Dbl homology (DH) domain at the N-terminus and a pleckstrin homology (PH) domain at the C-terminus; the Dock family contains 11 members which not have a DH homology; the third family comprises of only two family members, Swap-70 and DEF6, which exhibit the converse domain arrangement to the Dbl family, with a PH domain at the N-terminus and a DH-like (DHL) domain at the C-terminus (Figure 1.1.2). Two putative  $\text{Ca}^{2+}$  binding EF-hand motifs at the N-terminus are separated from the PH domain by a DEF6/Swap-70 homology (DSH) domain. The DH domain is responsible for Rho GTPase activation, the PH domain mediates lipid-binding via PIP3 signalling pathways (Gupta *et al.*, 2003b; Mavrakis *et al.* 2004 Rossman *et al.*, 2005; Tybulewicz and Henderson 2009, Bécart *et al.*, 2008).



**Figure 1.1.2: DEF6 domain structure**

Schematic diagram of the domain structure of DEF6. The N-terminal EF-hand that binds  $\text{Ca}^{2+}$  is followed by the Immunoreceptor Tyrosine-based Activation Motif (ITAM; also known as the DEF6/Swap70-homology domain (DSH)). The central Pleckstrin Homology domain (PH) binds phosphatidylinositol (3, 4, 5)-triphosphate (PIP3) and the C-terminal Dbl Homology-like domain (DHL) contains a coiled-coil domain and facilitates guanine nucleotide exchange (GEF) activity. Tyrosine residues Y133 and Y144 are phosphorylated by the lymphocyte specific protein tyrosine kinase LCK and Tyrosine residues Y210 and Y222 are phosphorylated by the Interleukin-2 inducible T cell Kinase (ITK). Numbers refer to amino acid positions. (Mavrakis *et al.*, 2004; Bécart *et al.*, 2008a; Hey *et al.*, 2012)

### **1.1.3 Rho family GTPases and role of DEF6 as a guanine nucleotide exchange factor (GEF):**

Rho GTPases are small signalling G-proteins (20–25 kDa) that belong to the larger Ras superfamily. They act as molecular switches and play pivotal roles in signal transduction in response to external stimuli. GTPases are active in their GTP (guanosine triphosphate) form and inactive in their GDP (guanosine diphosphate) form (Wennerberg and Der 2004). The switch from their GDP to GTP form is catalysed by GEFs. At the same time, GTP exchange is inhibited by GDP dissociation inhibitors (GDI) and GTPase activating proteins (GAP) induce GTP dissociation/hydrolysis. Their diverse biological activities have been attributed to variations in their C-termini, which define their physicochemical characteristics, subcellular location and membrane interactions (Wennerberg and Der 2004; Tybulewicz and Henderson 2009).

Of all the Rho GTPases, Rac1, Cdc42 and RhoA are the best characterised and have been shown to coordinate TCR-actin-dependent mechanisms: Rac1 promotes actin polymerisation; Cdc42 facilitates the formation of filopodia and extracellular recognition; and RhoA is involved in actin-myosin dynamics (Hall, 1998). In addition, cytoskeletal reorganisation, Rho GTPases mediate gene expression through actin dependent initiation of the  $\text{Ca}^{2+}$ -calmodulin-calcineurin pathway (Rivas *et al.*, 2004) by activating signalling molecules, such as NF- $\kappa\beta$ , and stress-activated MAP kinases (Gupta *et al.*, 2003; Fanzo *et al.*, 2006). Rho GTPases have also been implicated in anti-apoptotic actions via Cyclin D1 pathways (Wennerberg and Der, 2004).

*In vitro* studies have demonstrated that DEF6 could specifically interact with Rho GTPases Rac1, Rac2, Cdc42 and RhoA (Mavrakis *et al.*, 2004). For

example, the specificity of DEF6 for Cdc42 and Rac1, which are also localised in the immunological synapse (IS) that forms in T cells upon activation via antigen-presenting cells APCs (more detail provided in section 1.2.5), suggests that DEF6 plays a role in linking PH domain-induced cytoskeletal rearrangement with  $Ca^{2+}$ /NFAT signalling, and thereby differentiation of  $CD4^+$   $T_h$  subtypes (Bécart *et al.*, 2007). DEF6 activates Rac1 and Cdc42 following its recruitment to the IS (Altman and Bécart, 2009). This necessitates a conformational change by phosphorylation of selected tyrosine residues, which is triggered by the upstream lymphocyte specific protein tyrosine kinase (LCK)/ T cell Kinase (ITK) phosphorylation cascade (Altman and Bécart, 2009). Initially phosphorylation of Tyr133, Tyr144 and Tyr210 had been attributed to LCK; however, it has recently been revealed that tyrosine phosphorylation of DEF6 at Tyr210 and Tyr222 is directly mediated by ITK demonstrating that DEF6 was a direct substrate for ITK (Hey *et al.*, 2012). However, ITK is itself activated by LCK phosphorylation, indicating that LCK can contribute to DEF6 phosphorylation both directly and indirectly. As such, it was also proposed that LCK and ITK might act as joint regulators in actin-dependant TCR responses (Singleton *et al.*, 2011; Hey *et al.*, 2012). DEF6 has also been implicated in the clonal expansion of  $CD8^+$  T cells to cytotoxic T lymphocytes (CTL) (Feau *et al.*, 2013).

## 1.2 Role of DEF6 in TCR-mediated cytoskeletal remodelling

### 1.2.1 Development, differentiation, activation and survival of T cells

Leukocytes formed in the bone marrow are delivered to the thymus as uncommitted thymocytes where they develop and differentiate into naïve CD4<sup>+</sup> T-helper (T<sub>h</sub>) cells or CD8<sup>+</sup> cytotoxic T cells. During their development, thymocytes undergo a series of selection stages, commonly referred to as double negative (DN), double positive (DP) and single positive (SP), before their final differentiation into CD4<sup>+</sup> T helper (T<sub>h</sub>) cells, regulator (Treg) or CD8<sup>+</sup> cytotoxic T cells. The major T<sub>h</sub> subtypes, Th1, Th2 and Th17, perform distinct functions according to their specific cytokine signatures (Nakayama and Yamashita 2010): Th1 cells target pathogens via secretion of interleukin IL-2 and IFN $\gamma$ ; Th2 cells are involved in humoral immunity and secrete IL-4, IL-5, IL-6, IL-13 and IL-10; and Th17 cells are involved in inflammatory response via secretion of IL-17, IL-17B and IL-22 (Bécart *et al.*, 2007; Canonigo-Balancio *et al.*, 2009). The development, differentiation and eventual activation of naïve T cells to effector T cells require precise and timely coordination between multiple regulatory molecules and pathways. These are controlled by T cell receptor (TCR)-mediated signalling following antigen recognition (Figure 1.2.1) (Nakayama and Yamashita, 2010). Disruption of any of these events can result in abnormal T cells, suppression of cytokine production or extended inflammatory response (Fanzo *et al.*, 2006). Importantly, reactive peripheral T cells must be eliminated following prolonged activation to prevent their accumulation and subsequent over-production of cytokines, which may lead to autoimmune disorders (Sprent, 2001).

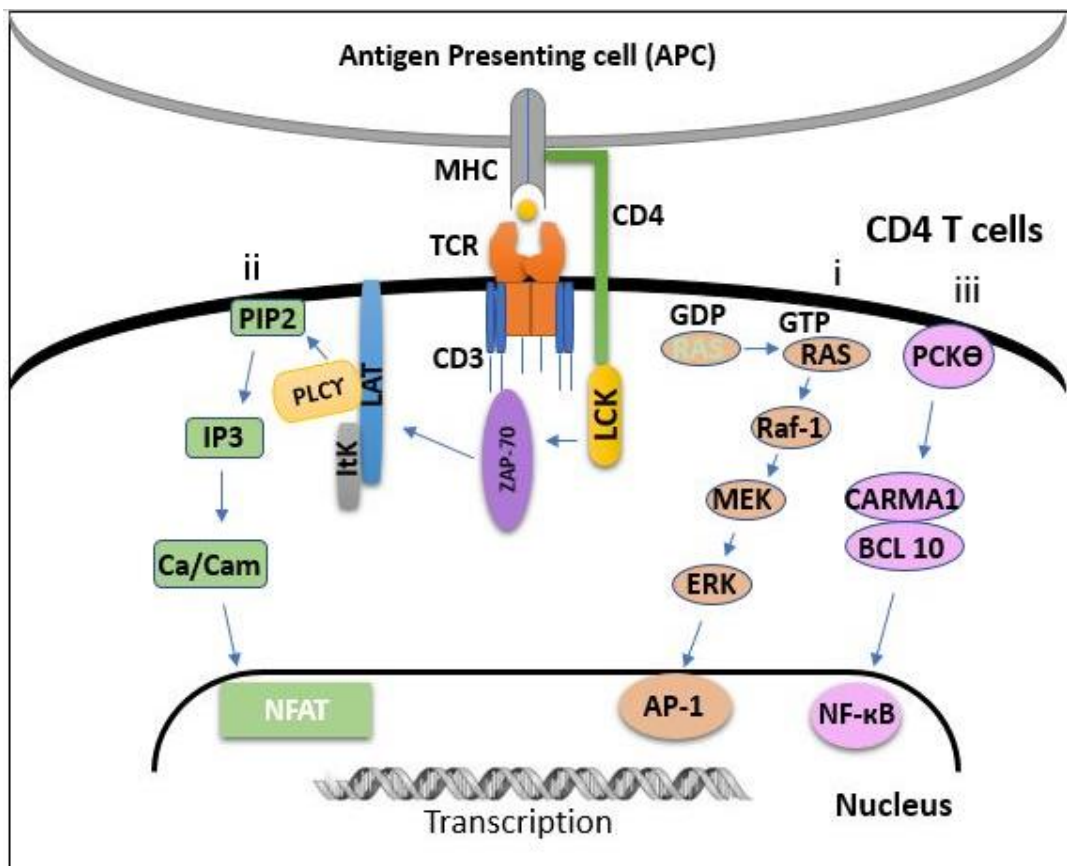


**Figure 1.2.1: The principle signal transduction pathways triggered by TCR stimulation involved in T helper ( $T_H$ ) cell differentiation**

Summary of three main signalling cascades in T cells activated after antigen presentation through the major histocompatibility complex (MHC) of antigen presenting cells (APCs). Antigen-binding by the T cell receptor (TCR) triggers various downstream events initiated by activation of tyrosine kinase LCK that phosphorylates tyrosine residues in Immunoreceptor tyrosine-based activation motifs (ITAMs) of the TCR. ZAP70 which is src family kinase is then recruited to the phosphorylated ITAMs resulting in phosphorylation of (LAT) molecules. This in turn activates the downstream pathways Ras/ERK MAPK cascade (i), the Ca/calcineurin/NFAT pathway (ii), and the PKC/NF- $\kappa$ B pathway (iii) resulting in transcriptional activation of target genes. ZAP-70: Zeta-chain-associated protein kinase 70, ERK: extracellular signal-regulated kinases, MAPK: A mitogen-activated protein kinase, NFAT: Nuclear factor of activated T cells, PKC: Protein kinase C and NF- $\kappa$ B: nuclear factor kappa-light-chain-enhancer of activated B cells. (Reproduced from Nakayama and Yamashita, 2010).

### 1.2.2 Antigen presentation and T cell signalling

T cell based signalling needs to be highly regulated since the number of self-antigens greatly outnumbers the non-self-antigens, hence in order to prevent any damage to our own tissues and cells, strict regulation of T cell mediated activities are required. Before encountering an Antigen Presenting Cell (APC), a T cell is highly mobile and keeps scanning the cellular environment for an APC carrying an antigen (Friedl and Gunzer, 2001). APCs express major histocompatibility complexes MHCs, which bear epitopes from antigen molecules. These epitopes are known as pMHC and these are recognised by mobile T cells by using their T cell receptor (TCR) and Filamentous actin (F-actin) an invadosome like protrusion (Sage *et al.*, 2012). The degree at which the TCR and pMHC are complementary to each other decides the stability of this interaction. This results in the formation of a TCR-pMHC complex that securely attaches the T cell to the APC (Sage *et al.*, 2012). Expressed on the surface of T cell are integrin based Lymphocyte Function associated Antigen-1 (LFA-1), which reduce the motility and enhance the sensitivity of T cell by recognising Intercellular Adhesion Molecule-1 (ICAM-1) on the APC surface (Figure 1.2.2). Increased TCR sensitivity of T cell for APC causes reduction of the amount of antigen required by T cell in order to generate an immune response (Bachmann *et al.*, 1997).

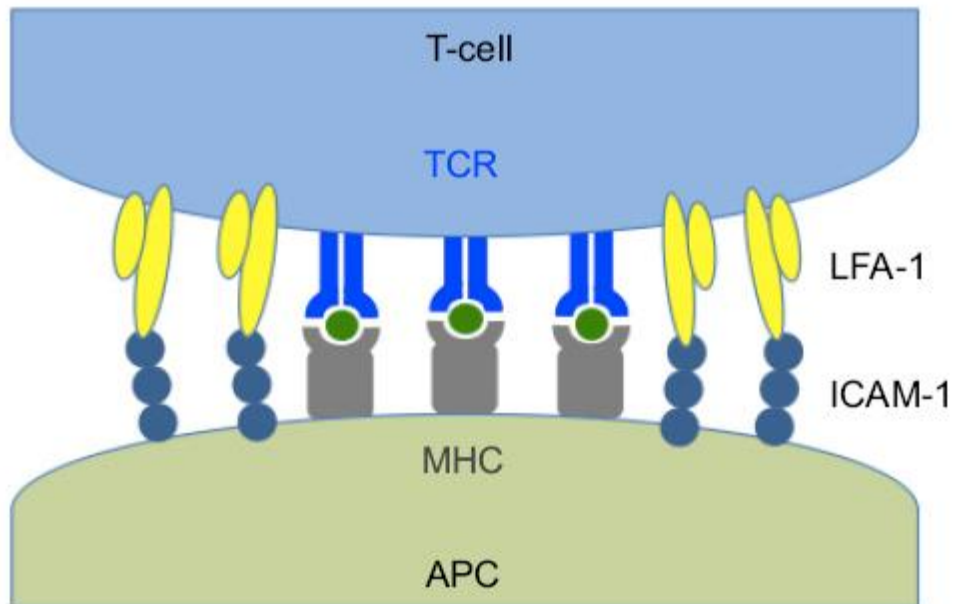


**Figure 1.2.2: Immunologic Synapse (IS) showing LFA-1 on T cell surface binding to ICAM-1 expressed on Antigen Presenting Cells (APC)**

Expressed on the surface of T cells are integrin based Lymphocyte Function associated Antigen-1 (LFA-1), which reduce the motility and enhance the sensitivity of T cells by recognising Intercellular Adhesion Molecule-1 (ICAM-1) on the APC surface. Antigen (green) presented by the major histocompatibility complex (MHC; brown) expressed by APCs is bound by the T cell receptor (TCR; blue) leading to stimulating intracellular signals that cause activation and proliferation of T cells and release of inflammatory cytokines. (Reproduced from Semba *et al.*, 2016).

### 1.2.3 Phosphorylation and Ca<sup>2+</sup> signalling cascades in TCR signalling pathways

Both phosphorylation and Ca<sup>2+</sup> signalling pathways are integral in TCR mediated events. TCR-mediated signalling triggers the release of Ca<sup>2+</sup> from endoplasmic reticulum (ER) through ion channels. This elevates the level of cytosolic Ca<sup>2+</sup>, which in turn triggers an influx of Ca<sup>2+</sup> through calcium release-activated channels (CRAC) in the plasma membrane (Lewis, 2001). Ca<sup>2+</sup> signalling initiates various TCR-related functions, including activating the Ca<sup>2+</sup> calmodulin-calcineurin pathway, which promotes nuclear translocation of critical transcription factors, such as nuclear factor  $\kappa\beta$  (NF- $\kappa\beta$ ) and nuclear factor for activated T cells (NFAT). Both these are essential for Th differentiation and cytokine expression, including IL-2 and TNF- $\alpha$  (Lewis, 2001; Marangoni *et al.*, 2013).

Phosphorylation signalling cascades are involved in multiple TCR-stimulated events, such as cytoskeletal remodelling, formation of the IS, including triggering Ca<sup>2+</sup> pathways, and importantly, activation of guanine nucleotide exchange factors (GEF) and Rho GTPases (Schulze-Luehrmann and Ghosh, 2006). Upstream phosphorylation activates lymphocyte protein tyrosine kinase (LCK) and other Src family tyrosine kinases leading to phosphorylation of the TCR/CD3 signalling molecule complex. Z-chain associated protein kinase (Zap-70) contributes to the downstream phosphorylation pathway following its recruitment to the TCR/CD3 complex (Schulze-Luehrmann and Ghosh, 2006). These actions lead to the downstream phosphorylation and activation of inducible T cell kinase (Itk). Phosphatidylinositol 4, 5-bisphosphate (PIP<sub>2</sub>), itself a product of phosphatidylinositol (3, 4, 5)-

triphosphate (PIP3) hydrolysis, is hydrolysed by Itk via phosphorylation of phospholipase C $\gamma$ 1 (PLC $\gamma$ 1). This results in the production of important second messengers, inositol triphosphate (IP3) and diacylglycerol (DAG). IP3 triggers the release of Ca<sup>2+</sup> from the ER; and DAG promotes NF- $\kappa$ B and NFAT (Schulze-Luehrmann and Ghosh, 2006).

#### **1.2.4 Effect of DEF6 on pathways and various proteins responsible for the formation of the actin cytoskeleton**

Rho GTPases have been identified as playing key roles in the TCR-mediated immune response. In addition to their roles in regulating  $\text{Ca}^{2+}$  signalling mechanisms, they play key roles in cytoskeletal organisation and IS assembly (Yu *et al.*, 2013; Kumari *et al.*, 2014). Figure 1.2.4 shows a signal transduction cascade generated by binding of MHC II to TCR when APC presents an antigen to the T cell. In terms of DEF6, when MHC forms the pMHC complex with TCR, the LCK is activated, which results in phosphorylation of DEF6 at residues Y133 and Y144 that causes DEF6 activation. Both Cdc42 and Rac have been implicated in the formation of actin filopodia and lamellipodia (Nobes and Hall, 1995). These are fine projecting protrusions extending from the IS, and flat polymerised actin sheets that can appear as “ruffles” at the edge of the IS, respectively (Nobes and Hall, 1995; Dustin and Chan, 2000). In order to carry out their TCR-stimulated functions, they must first be activated by GEFs.

DEF6 functions as GEF by catalysing the GDP-GTP exchange for Cdc42 and also facilitates Vav1 in the activation of Rac1 that results in intracellular calcium release (Tybulewicz and Henderson, 2009). This also causes activation and translocation of NFAT<sub>c1/2</sub> to the nucleus thereby promoting T cell activation and proliferation (Bécart *et al.*, 2007). F-actin is formed at the IS upon activation of Cdc42 and Rac1, which then causes the formation of filopodia and lamellipodia thus increasing the surface area of IS and in turn stabilising the interaction between the T cell and APC (Billadeau *et al.*, 2007).

Once activated, Cdc42 and Rac1 bind to their respective Rho-GTPase effector proteins. Among the best characterised are Wiskott-Aldrich syndrome protein (WASp) and p21-activated protein kinase (PAK) (Daniels and Bokoch, 1999; Snapper and Rosen, 1999), which are involved in actin polymerisation and the regulation of myosin, respectively. Cdc42 binds to WASp promoting a structural change to an open conformation. This allows WASp to activate Arp2/3 which links the actin cytoskeleton to microtubule structures thereby facilitating IS assembly (van der Merwe, 2002). WASp also interacts with WIP, a novel proline-rich adaptor protein that enhances actin polymerisation through its actin and profilin binding sites (Ramesh *et al.*, 1997). A deficiency in WASp was found to induce aberrant actin polymerisation (Snapper and Rosen, 1999), further demonstrating the importance of Rho GTPases, and by implication GEFs, in TCR stimulated actin dynamics. Furthermore, DEF6 deficient T cells were shown to have reduction in F-actin polymerisation and lamellipodia formation and IS stabilisation and maturation was rescued by activation of Rac1 providing additional evidence of the importance of DEF6 in regulation of F-actin polymerisation (Fanzo *et al.*, 2006). In addition, deficiencies in both Vav and DEF6 resulted in impaired formation of the IS (Bécart *et al.*, 2008; Feau *et al.*, 2013). The recruitment of Vav1 and DEF6 to the IS (Kumari *et al.*, 2014), and subsequent activation of Arp2/3, is believed to be rapid following TCR engagement, suggesting that these GEFs are central in establishing maximal contact between the TCR and APC, which in turn will enhance the sensitivity of TCR stimulation (Delon, 2000; Dustin and Chan, 2000). The spatiotemporal organisation of the actin cytoskeleton and recruitment of DEF6 to the IS facilitates phosphorylation of DEF6 by LCK and

ITK resulting in activation of Cdc42. Impaired localisation of DEF6 or Cdc42 to the IS was found to result in defective interaction between the actin cytoskeleton and the IS, thereby reducing the efficiency of T cell activation in response to TCR signalling (Singleton *et al.*, 2011). These pathways are shown schematically in Figure 1.2.4.

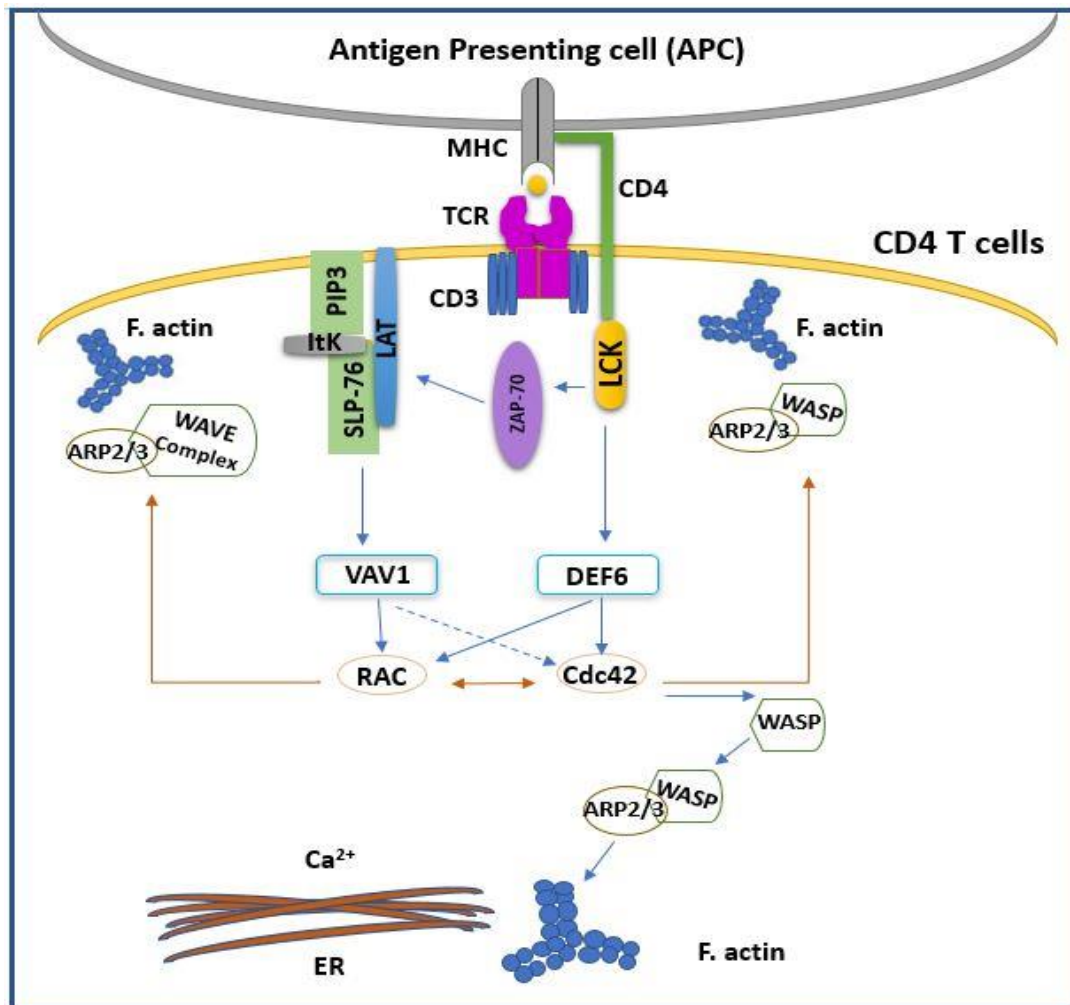


**Figure 1.2.4 TCR signal transduction integrating with varied components of the actin polymerisation machinery.**

Schematic diagram showing the inter-relationships between TCR-mediated signalling pathways (see also Figure 1.2.1) and the molecular components involved in spatiotemporal organisation of the actin cytoskeleton. VAV1 and DEF6 activation leads to activation of Rac1 and Cdc42. Cdc42-induced activation of Arp2/3 promotes actin polymerisation and activation of Rac1 leads to the mobilisation of lamellipodia, which in turn enables Ca<sup>2+</sup> transport from the extracellular milieu. In addition, release of Ca<sup>2+</sup> from endoplasmic reticulum (ER) is triggered by activation of Wiskott-Aldrich syndrome protein (WASP) and the actin-binding protein Arp2/3. Rac1: Ras-related C3 botulinum

toxin substrate 1 and Cdc42: Cell division control protein 42 homolog. (Reproduced from Kumari *et al.*, 2014)

NFAT<sub>c1/2</sub> nuclear translocation was shown to be dependent on DEF6 since DEF6-deficient mice failed to translocate NFAT<sub>c1/2</sub> to the nucleus since they were less dependent on Cdc42 for intracellular calcium release due to the fact that activation of Cdc42 requires DEF6 (Bécart *et al* 2007). Furthermore, translocation of DEF6 to IS after LCK mediated phosphorylation of DEF6 at residues 133 and 144 was also shown to result in activation of NFAT<sub>c1/2</sub> (Bécart *et al* 2008a). Nuclear translocation of NFAT<sub>c1/2</sub> is a significant event for T cell activation since Th1 and Th2 cell responses are dependent on DEF6 since mouse deficient in DEF6 were unable to mount these responses and also had reduced number of peripheral T cells (Bécart *et al.*, 2007).

## 1.2.5 The formation and function of the immunological synapse

### 1.2.5.1 The structure immunological synapse

An effective immune response requires accurate communication between regulatory molecules and signalling pathways and cross-talk between cells (Monks *et al.*, 1998). This can be achieved by assembling a complex of contributory proteins, kinases, adhesion proteins and other contributory molecules at an interface between the TCR on the surface of the T cell and an antigen-presenting cell (APC). This TCR-APC interface has been termed the immunological synapse (IS) (Monks *et al.*, 1998). In addition to its role in the initiation and orchestration of TCR signalling events, the IS has recently been proposed as sustaining and terminating TCR signalling (Lee *et al.*, 2002; Bécart and Altman, 2009). For example, Yokosuka *et al.*, (2005) demonstrated that TCR containing micro clusters (a complex consisting of the T cell receptor, CD3 and associated signalling proteins) that were generated at the initial contact site between the T cell and APCs initiated and sustained T cell activation (Yokosuka *et al.*, 2005). However, the mechanisms are not fully understood and require further investigations. The precise definition of the IS has been under debate. Dustin *et al.*, (2010) defined it as being a stable contact between the T cell and APC. Stinchcombe *et al.* (2006) described it as the contact between the CTL (activated CD8<sup>+</sup> cell) and target pathogen or tumourigenic cell (Stinchcombe *et al.*, 2001); however, Monks *et al.* (1998) suggested the term referred to reorganisation of the IS complex into concentric rings, termed the “bull’s eye” (Monks *et al.*, 1998). This is shown as a schematic diagram in Figure 1.2.5.1 (Yu *et al.*, 2013). Despite these

variations, the bull's eye model is the most commonly accepted. Simply, each ring is attributed to a distinct set of functions: the central ring or central supramolecular activation cluster (cSMAC) contains the TCRs and co-stimulatory molecules, such as CD28. cSMAC lacks any F-actin molecule but is enriched with TCR micro clusters, co-stimulatory receptors and protein-tyrosine kinases (Yu *et al.*, 2013). The second peripheral ring (pSMAC) is made up of integrins such as lymphocyte function associated antigen 1 (LFA-1) that binds to intercellular adhesion molecule 1 (ICAM1), and many cytoskeletal linker proteins (such as talin) (Yu *et al.*, 2013); and the distal ring (dSMAC) contains adhesion molecules, such as CD45 (Alarcón *et al.*, 2011). TCR micro clusters are formed at the dSMAC, which is also rich in F-actin (Kaizuka *et al.*, 2007). This arrangement of membrane proteins would facilitate directed secretion of cytokines.

There is a centripetal flow of F-actin from dSMAC to pSMAC, causing movement of TCR micro clusters and so generating a mechanical force exerted on the TCR-pMHC complexes formed in the IS. This force can also dissociate the TCR-pMHC complex if it becomes stronger compared to the bonding affinity between TCR and pMHC (Kaizuka *et al.*, 2007; Kim *et al.*, 2012). The mechanical force thus generated by movement of F-actin molecules acts as a regulatory mechanism, which reduces the probability of T cells disseminating a response towards self-antigens and causing damage to our own body cells and tissues (Kaizuka *et al.*, 2007; Kim *et al.*, 2012).

An additional debate has been conducted as to whether the organisation of the IS is a "cause or consequence" of TCR stimulation. Although this arrangement of SMACs has classically been associated with maintaining TCR

signalling, Alarcon *et al.*, (2011) reported that the formation of the cSMAC was not essential for full TCR-mediated activation of T cells, and suggested that the cSMAC may instead play a role in the down regulation of the TCR dependant on the intensity of TCR signalling (Alarcón *et al.*, 2011). Furthermore, they noted that this typical arrangement of SMACs was not found in the IS formed with the APCs of dendritic cells.

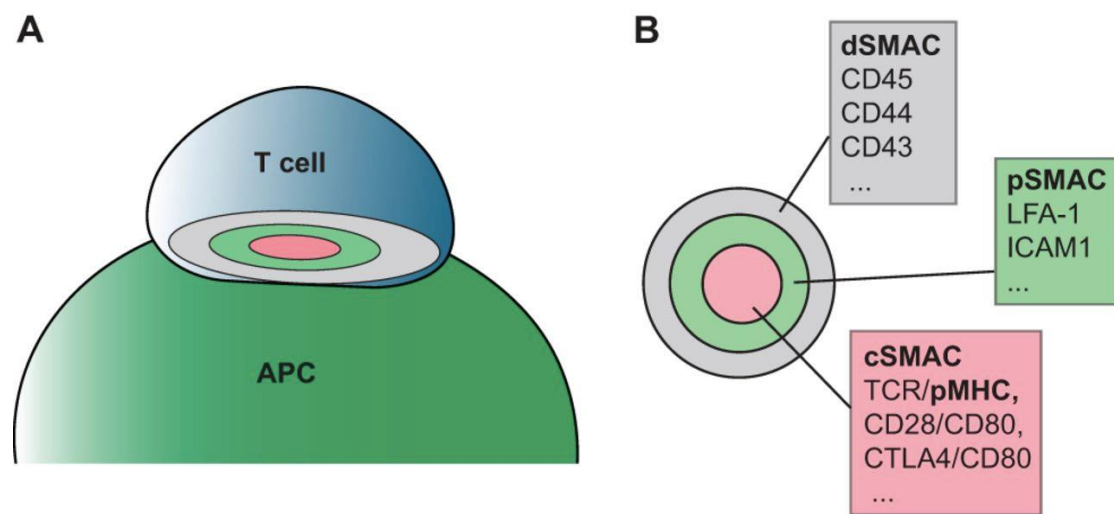


**Figure 1.2.5.1: Distinct spatial arrangement of components of the immunological synapse (IS).** (A) Schematic diagram of the immunological synapse (IS) formed at the junction of T cell and the antigen presenting cell (APC). Distinct spatial arrangements of the components shown in (B) through translocation and differential sorting of the proteins result in “Bull’s Eye” formation consisting of several concentric domains known as supramolecular activation clusters (SMACs). The central ring (cSMAC; pink) is reinforced with TCR and co-stimulatory molecules such as Cluster of Differentiation 28 (CD28) and 80 (CD80). The peripheral ring (pSMAC; green) consist of integrins, such as Lymphocyte Function associated Antigen-1 (LFA-1) that bind to Intercellular Adhesion Molecule-1 (ICAM1), and many cytoskeletal proteins. Distal ring (dSMAC; grey) contains proteins with large extracellular domains, including Cluster of Differentiation 45 (CD45), 44 (CD44), and 43 (CD43) (Reproduced from Yu *et al.*, 2013).

### 1.2.5.2 The immature and mature immunological synapse

The formation of the IS is a dynamic process: an “immature” IS is first assembled when a naïve T cell interacts with an APC; this is reorganised into a “mature” IS during construction of the bull’s eye (Figure 1.2.5.2) (van der Merwe, 2002; Huppa and Davis, 2003). This progression can evolve over several minutes, whereas a TCR stimulate response is triggered within seconds. This suggests that the mature IS is involved in functions further downstream in the TCR signalling pathway (Delon, 2000). It was originally proposed that the function of the mature IS was to enhance or sustain TCR signalling (Davis and Dustin, 2004). However, Lee et al. (2002) showed that the mature IS only formed as TCR signalling began to diminish, thereby disproving this hypothesis (Lee *et al.*, 2002). The alternative proposal is that the arrangement of the bull’s eye in the mature IS enables polarised secretion of cytokines (van der Merwe, 2002). Interestingly, the position of the pMHC appears to correspond with the orientation of the microtubule organising centre (MTOC). This would facilitate transportation of the necessary molecular components to the site of the IS (Kuhn and Poenie, 2002). As yet, the specialised roles of the immature and mature IS are unclear, and the distinct functions of the different regions in the bull’s eye remain to be established.

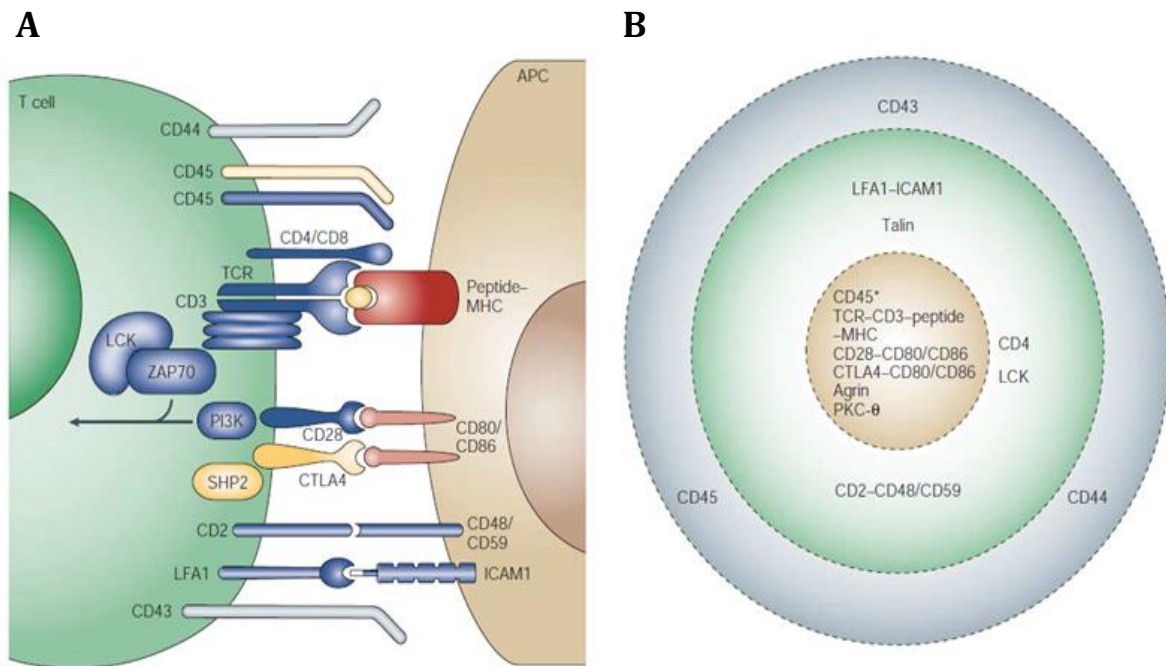


**Figure 1.2.5.2: Schematic diagram of the mature immunological synapse (IS) and the “bull’s eye”**

**A)** Side view of the Immunological synapse showing the principle ligand pairs and signalling molecules that are involved in T cell-APC recognition. The pMHC is shown in red; other key molecules include the activating/co-stimulatory molecules such as TCR, CD3 and CD28 (Blue), inhibitory molecules like CTLA4 (Yellow) and non-signalling molecules CD43 and CD44 (Grey; see also Figure 1.2.5.1). The arrow indicates that the interaction of TCR with pMHC assemble signals that lead to T cell activation. **B)** Top view of the IS showing the “bull’s eye” with the central supra-molecular activation cluster (cSMAC; yellow) that contains major components including the TCR and one of the downstream signalling effectors protein kinase C zeta (PKC-zeta). cSMAC is surrounded by peripheral supra-molecular activation cluster (pSMAC; green) which is enriched with LFA-1 and cytoskeletal linker talin that is critical for cell adhesion. Large molecules such as CD44 and CD45 are localised in the region outside of the pSMAC known as the distal supra-molecular activation cluster (dSMAC; grey). Other key molecules and ligand pairs are also indicated like CD80/CD86, PKC: Protein kinase C, Agrin, ICAM-1: Intercellular Adhesion Molecule-1, Cluster of Differentiation 4 (CD4); CD2, CD48, CD59 and CD43. (Reproduced from Huppa and Davis, 2003).

### **1.2.5.3 The role of cytoskeletal remodelling in the formation of the immunological synapse**

Cytoskeletal organisation is required to transport and assemble contributory proteins and molecules to the IS and redistribute surface effectors in response to TCR stimulation (Dustin and Chan, 2000). Although there has been considerable progress in determining the various roles and functions of the different cytoskeletal structures during the construction of the IS, the underlying details are poorly understood. Both passive and dynamic processes are involved; the passive functions are generally involved in receptor ligand binding; whereas the active mechanisms are primarily associated with cytoskeletal mobilisation and polarised secretion of cytokines (van der Merwe, 2002). The different mechanisms rely on proteins from different “rings” of the bull’s eye: ligand binding requires integrins and adhesion proteins from the pSMAC and dSMAC regions, respectively, whereas cytoskeletal organisation is dependent on a large variety of proteins and effectors, including Rho GTPases and GEFs which are located in the centre of the IS (pSMAC), and cytoskeletal molecules, such as talin which is required for the mobilisation of integrin receptors and is located in the pSMAC (Alarcón *et al.*, 2011). The actin cytoskeleton in particular is essential for these processes. T cells must be highly sensitive to small dense clusters of pMHC complexes located on the surface of the APC in order to trigger an effective response. This requires the precise alignment of the membrane surfaces between the TCR on the T cell and APC. By ensuring tight adhesion between the membranes, TCR clusters can be driven against the APC, thereby expanding the area of contact (Dustin and Chan, 2000). During

assembly of the IS, each of the molecular components must be directed to its appropriate “ring” (Delon, 2000). Furthermore, several effectors need to be mobilised within the first few seconds to trigger a rapid response, whereas others can be assembled over minutes. This requires accurate spatiotemporal organisation of actin cytoskeletal elements (Delon, 2000). The role and dynamics of the microtubule cytoskeleton in the immune response are less well known than those associated with actin structures. The orientation of the MTOC alongside the IS is thought to perform a critical role in transporting specialized cellular machinery towards the IS, and transporting secretory lysosomes and directing cytokine secretions to the infected cells (Beal *et al.*, 2009). In addition, there are specific interactions between the actin and microtubule cytoskeletons during TCR signalling; for example, the actin-binding protein Arp2/3 has been implicated in transporting secretory lysosomes from the MTOC to the plasma membrane along actin “highways” (van der Merwe, 2002).

## **1.3 The role of DEF6 in P-body formation and mRNA regulation**

### **1.3.1 Aggregation as a result of phosphorylation of DEF6 by ITK at tyrosine residues 210 and 222**

There is increasing evidence that mRNA regulation is central to the immune response (Hey, *et al.*, 2012). The importance of mRNA localisation as a mechanism to exert temporal and spatial control in gene expression is also becoming apparent (Martin and Ephrussi, 2009; Blower, 2013). Proteins that are involved in mRNA regulation are frequently found to co-localise within transient cytosolic structures known as stress granules and processing bodies (P-bodies) (Kedersha *et al.*, 2005). Whereas stress granules are associated with delaying mRNA translation, and can thereby control the timing of gene expression (Besse *et al.*, 2009), P-bodies contain decapping enzymes such as DCP1/2 and are therefore associated with mRNA degradation and translation (Kedersha *et al.*, 2005). An additional cellular advantage in packaging mRNA regulatory components within dynamic cytoplasmic granules is the ability to transport them along cytoskeletal pathways, such as actin filaments, to their required location (Martin and Ephrussi, 2009).

Post-translational modifications frequently play a key role in the aggregation and accumulation of proteins during granule formation (Eulalio *et al.*, 2007); and a glutamine (Q)-rich region within a coiled-coil domain is a characteristic of aggregating proteins. By carrying out systematic bioinformatics searches, Hey *et al.* (2012) revealed that DEF6 contained such a region in its DHL domain. They had previously reported that DEF6 was phosphorylated at Tyr210 and Tyr220 as a consequence of the LCK/ITK signalling cascade.

Exposure of the negative charges at these residues would induce a conformational change in DEF6 making it susceptible to self-aggregation (Hey *et al.*, 2012). They proposed that ITK-induced phosphorylation promoted this effect by unmasking the Q-rich region in its C-terminal. Mutants Y210E-Y222E DEF6 were tagged with GFP and looked at their cellular localisation. It was found that this mutant protein formed cytoplasmic granules upon stimulation with using anti-CD2, CD3 and CD28 coated magnetic beads in both untreated and sodium pervanadate treated Jurkat T cells. The GFP-tagged mutant Y210E-Y222E was also shown to co-localise with DCP1 in COS7 cells, which is a marker for Processing Bodies (P-bodies) (Hey *et al.*, 2012) thus suggesting a role of DEF6 in P-body formation (Hey *et al.*, 2012).

### **1.3.2 Different domains of DEF6 with unique function during aggregation**

The DHL domain of DEF6 lacks amino acids proline in the same area that is rich in glutamine and asparagine (see figure 1.1.2). When only the DHL domain of DEF6 is endogenously expressed in COS7 cells, it aggregated and formed cytoplasmic foci but was not found to co-localise with P-body marker dsRed DCP1 (Mollett, 2014). DEF6 lacking 39 amino acids at the C-terminus (DEF6  $\Delta$ C) however aggregated with the P-body marker dsRed DCP1 in COS 7. This result indicated that the C-terminal DHL domain can form aggregates in the form of cytoplasmic foci but the N-terminal domain is responsible for targeting and co-localising with the P-body (Mollett, 2014). Mollet also showed that DEF6 formed granules which were present at the IS indicating that DEF6 granules have a role in establishing T cell and APC contact. Mollet also provided evidence for the movement of DEF6 granules at a velocity similar to actin and tubulin indicating that the mechanism of movement of the DEF6 formed aggregates in the cell occurs along with actin and tubulin.

### **1.3.3 Association of DEF6 with Polysomes in Jurkat T cells**

The process of differential centrifugation of a Jurkat cell lysate results in the separation of DEF6 associated polysomes. In the experiment conducted by Dr Peter Jones (unpublished data) a sucrose cushion was used through the formation of a density gradient that facilitated the separation of Jurkat T cell lysates through the use of the ultracentrifugation process. Based on size and density, particles were able to deposit as sediments. This resulted in further increase of the gradient that existed before the state of equilibrium was successfully achieved. Different fractions were then separated from the various samples of sucrose concentrations used for the experiment through the use of SDS separation technique through immunoblotting. The experiment also involved ribosomal protein L7a used as an antigen for the detection of the 60S subunit (Uchiumi et al., 1980). In addition to this, the detection of DEF6 was conducted with the use of Anti-DEF6 in each sample separated.

DEF6 associated polysomes and their co-immunoprecipitation was obtained through the separation of polysomes obtained from Jurkat T cells previously done with the help of sucrose cushion ultracentrifugation. The resulting polysomes were then incubated with anti-DEF6 as well as without the use of the antibody. This was done earlier to the precipitation of DEF6 with the help of magnetic beads. Absorbance of the polysomes was calculated for the amount of DEF6 that underwent precipitation along with the control samples calculated for the experiment (Remon, PhD thesis, 2016).

The technique of cellular fractionation was used for the separation of membrane and cytosolic polysomes. The associated polysomes were then separated from the samples using ultracentrifugation technique. SDS-Page

was used for separation of proteins, and were then immunoblotted for identifying the presence of ribosomal protein L7a and DEF6 (Remon, PhD thesis, 2016).

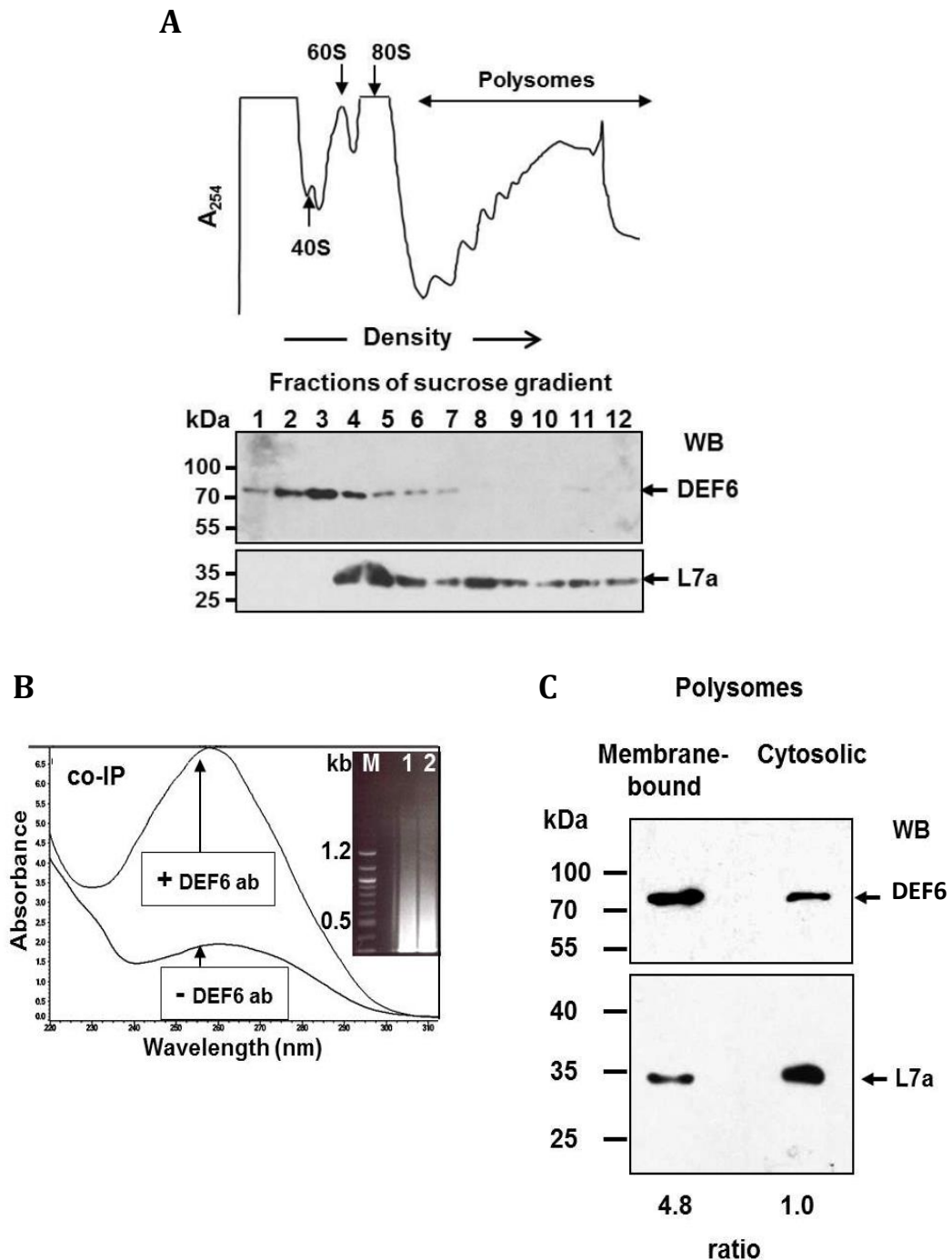


**Figure 1.3.3: DEF6 associated with Polysomes in Jurkat Cells.**

(A) Jurkat T cells were lysed with the help of the centrifugation process at 4 degrees. The use of the supernatant increase the gradient of sucrose cushion by 10%, with the greatest concentration of sucrose at the base of the ultracentrifugation tube. Fractions obtained were separated for conducting

relative absorbance at 254nm. The samples separated were then applied with SDS-PAGE with the use of the immunoblotting technique with the help of the ribosomal protein L7a as an identity for 60S subunit. (B) Polysomes obtained through ultracentrifugation were incubated with anti-DEF6 as well as control sample without the antibody. The overall precipitation rate increased at 254nm when compared with the control sample. (C) The membrane was isolated from the cytosol through the use of the technique of cellular fractionation. Polysomes were then separated through the sucrose cushion formed with the help of ultracentrifugation by applying SDS-PAGE. Presence of ribosomal protein L7a was used for the detection of polysomes whereas the presence of DEF6 was detected by anti-DEF6 in the different fractions of polysomes used in the experiment (Reмон, PhD thesis, 2016).

Differential centrifugation allows the fractionation of polysomes of the 40S, 60S and 80S subunits along with subunits of various sizes as well. It is important to state here that ribosomal protein 7a belongs to the category of 60S subunit present in polysomes (Figure 1.3.3 A). The use of SDS-PAGE accompanied with immunoblotting led to the conclusion that DEF6 is a protein that can collectively sediment ribosomes, with a significant DEF6 signal identical with the 40S subunit (Figure 1.3.3 A). Use of immunoprecipitation technique resulted in an increase in the absorbance rate at 254nm indicating an increase in the amount of ribosomes when compared with the control sample used (Figure 1.3.3 B). Furthermore, the use of ultracentrifugation used for the separation of membrane bound and cytosolic polysomes also verified an increase of the DEF6 protein, especially in the fraction of the samples that were membrane bound (Figure 1.3.3 C) (Reмон, PhD thesis, 2016). On the basis of the result obtained, DEF6 was linked with the ribosomes and the translation process of protein synthesis leading to the foundation of this study.

## **1.4 mRNA regulations at the transcriptional and translational level**

### **1.4.1 Post-transcriptional regulation of mRNA**

Post-transcriptional regulation of mRNA plays an important role in the control of protein synthesis: this includes mRNA transport, splicing and maturation, localisation and degradation.

RNA transcription is a process, which takes place in the nucleus, whilst translation to proteins is a cytoplasmic process. The RNA molecules must first be transported through nuclear pores. The equilibrium of RNA synthesis in the nucleus and RNA degradation in the cytoplasm and during transport determines mRNA levels in the cytoplasm. Both the 5'-7-methyl-guanosine cap and the 3' poly-adenylate tail on the transcribed RNA serve to avert premature degradation, especially during transport from the nucleus to the cytoplasm (Kohler & Hurt, 2007). The eukaryotic initiation factor 4E (eIF4E) is bound to the 5'-7-methyl-guanosine cap, this has been suggested to stabilise mRNA. The 3' poly-adenylated tail of mRNAs in eukaryotes is vital for the stability of the mRNA in the cytoplasm. The 3' poly-adenylated tail remains bound to poly (A)-binding protein (PAPB). During decay, the mRNA is de-adenylated (Guhaniyogi & Brewer; 2001). These processes can decrease or increase the rate of decay of newly transcribed mRNA, thereby regulating its availability.

Another post transcriptional regulation mechanism is splicing, which involves the deletion of introns, non-coding sequences, and the joining up of exons to a single strand. Alternative splicing permits the manufacture of completely different mRNA transcripts from the same pre- mRNA by a process of

selecting alternative introns to be spliced. This way, a single gene can encode several different proteins.

The rate at which mRNAs degrade is an important control mechanism for gene expression, the stability of mRNA varies widely. mRNAs with a long half-life allow for stable translation, whereas short-lived mRNAs are often found in processes initiated by inflammation or hormonal stimuli. When mRNA is de-capped or de-adenylated, it will undergo degradation. Other means of mRNA decay include nonsense-mediated degradation (Garneau *et al.*, 2007). Various protein factors indicated in the 5' end to the 3' end have been shown to accumulate in P-bodies, including factors required for de-capping and de-adenylation as well as those involved in nonsense-mediated decay. These factors do, however exist in the cytoplasm outside of P-bodies as well. In eukaryotic cells, degradation of mRNAs typically begins by the shortening of the 3' end by an mRNA deadenylase. This is then followed by decapping by DCP1/2 and break down from the 5' end to the 3' end by Xrn, an exonuclease. The fast degradation of mRNAs which do not encompass a translation termination codon is called non-stop decay and starts from the 3' end to the 5' end (Frischmeyer *et al.*, 2002).

### 1.4.2 Initiation process of mRNA translation

Translation in eukaryotic cells is the process of translating mRNA into proteins. The first and rate-limiting step in translation is translation initiation. Translation initiation is the process of assembling the 40S and 60S ribosomal subunits into an 80S ribosome with Met-tRNA at the start codon. This is a highly-controlled step which involves several different protein initiation factors. The amino acid encoded by the start codon is methionine in eukaryotes. Met-tRNA is delivered to the start codon, which allows the assembly of the ribosome (Aitken & Lorsch, 2012). Rates of translation initiation vary immensely. Shah *et al.* (2013) found rates between 4 seconds and 4 minutes in yeast cells. The authors concluded that the availability of free ribosomes was rate limiting for protein synthesis. Eukaryotic translation initiation factors (eIFs) are protein factors that stabilise the ribosome at the start codon. Furthermore, eIFs are involved in controlling the initiation of translation.

At the beginning of translation, the two complexes that include eIF2 ternary and 40S subunit complex get associated with each other. This results in the formation of the 43 pre-initiation complex, which binds to the activated mRNA and begins the 5'-3' scanning of the mRNA. The Met associated t-RNA anticodon then recognises the AUG start codon and this causes GTP hydrolysis to take place releasing phosphate and resulting in the formation of the 48S complex, which then associates with 60S ribosomal subunit. Finally, through a series of GTP hydrolysis resulting in release of phosphate group, the competent 80S ribosome is formed. Translation then goes through elongation and then reaches the termination phase where the 60S and 40S complexes get dissociated causing release of t-RNA and mRNA (Jackson *et al.* 2010).

Another protein associated with mRNA at every stage of translation process is PABP, which binds to the 5' mRNA cap & circularises the mRNA forming a closed loop model thus regulating the translation process (Kahvejian *et al.*, 2001). Using atomic force microscopy, the closed loop structure has been visualised (Wells *et al.*, 1998).

### **1.4.3 Cytoplasmic foci targeting proteins, P-bodies, stress granules, eIF4E, 4E-T and other proteins involved in mRNA regulation and aggregation**

Stress granules are made up of Ribonuclear Proteins (mRNPs), which are actually cytoplasmic aggregates whose main function is to store mRNA during unfavourable conditions, that include: cells deprived of glucose or amino acids, oxidative stress, viral infection, heat shock, ultraviolet radiation exposure and several others (Anderson and Kedersha, 2002). The amount of non-translating mRNAs also determines the assembly of cytosolic stress granules. Stress granules are the loci of translation initiation factors (Franks & Lykke-Anderson, 2008). Translational factors such as eIF4A, eIF4E and eIF4G accumulate in stress granules along with PABP and small ribosomal subunits. As the name suggests, stress granules accumulate under cellular stress, but they have been noted under other conditions that inhibit translation, such as drug treatment or an over-abundance of translation inhibitors (Buchan and Parker, 2009).

P-bodies are similar to stress granules in the sense that they also consist of mRNA but the function of P-body is different from stress granules since they are involved in mRNA decay, Nonsense-Mediated mRNA Decay (NMD) and translational repression in contrast to mRNA storage function as carried by stress granules (Sheth and Parker, 2003; Sheth and Parker, 2006; Teixeira *et al.*, 2005). P-bodies form cytoplasmic foci that comprises of sequestered mRNA along several mRNA decay factors that include aggregating mRNPs, decapping enzymes that include DCP1 and DCP2, 5'-3' exonuclease Xrn1, the decapping activating Lsm1-7 complex and translational initiation factor

eIF4E and 4E-T which acts as a transporter of eIF4E (van Dijk *et al.*, 2002; Bashkirov *et al.*, 1997; Ingelfinger *et al.*, 2002; Andrei *et al.*, 2005; Ferraiuolo *et al.*, 2005). Whilst P-bodies increase in response to cellular stress, they do exist at baseline conditions as well. The amount of non-translating mRNA determines the assembly of P-bodies.

The eukaryotic translation factor 4E (eIF4E) is one of the three subunits of eIF4F, the other two are the DEAD box helicase eIF4A and the scaffolding factor eIF4G. Eukaryotic mRNAs are blocked with a 5'-7-methyl-guanosine cap. The translation initiation factor eIF4E recruit ribosomes to this cap. eIF4F identifies the cap structure, where eIF4E is its cap-binding protein and eIF4E is regulated by phosphorylation (Gingras *et al.*, 1999). For example, cytokines can activate p38, a mitogen-activated protein kinase (MAPK) and p38 in turn activates MAPK interacting kinase 1 and 2 (Mnk1 and Mnk2). Growth factors, on the other hand, activate ERK1 and ERK 2, also leading to Mnk1 and Mnk 2 activation (Waskiewicz & Flynn 1997). Mnk1 and Mnk 2 in turn phosphorylate eIF4E and therefore regulate its activity (Ueda *et al.*, 2004). eIF4E has been implicated in tumorigenesis where it is involved in the regulation of several mRNAs implicated in metastasis and is over-expressed in malignant tumours (Mamane *et al.*, 2004). The absence of phosphorylated eIF4E prevents tumour formation in a mouse model of prostate cancer (Furic *et al.*, 2010).

The translation initiation factor 4E transporter (4E-T) is an eIF4E binding protein which is required for P-body formation in the cytosol. 4E-T shuttles between the nucleus and the cytoplasm, however, it's nuclear function is unclear. Interestingly, 4E-T is enriched in the P-bodies of mammalian cells (Kamenska *et al.*, 2014). The authors showed that ectopic 4E-T leads to a

reduction in mRNA translation and protein synthesis, whereas 4E-T depletion enhanced it.

mRNA has been shown to be targeted by various proteins to different cytoplasmic foci that includes structures like polysomes, P-bodies and also to stress granules. The process includes proteins first binding to mRNA and then shuttling mRNA to the foci. Proteins can alternatively induce aggregation along with mRNA (Anderson and Kedersha, 2006). Cytotoxic T Lymphocyte (CTL) granule mediated apoptosis is caused by two proteins, TIA-1 and TIA-R, which although are expressed ubiquitously in the cell are primarily focused in the role of apoptosis. Their mechanism of action involves causing nucleolysis of the target cell. Structurally these proteins contain three RNA Recognition Motif (RRM) by the help of which they bind to mRNA. They also possess at their C terminus, a Glutamine rich region that helps them to form aggregates resulting in bundling of the target mRNA along with any associated pre-initiation factors to form stress granules (Tian *et al.*, 1991; Kawakami *et al.*, 1992).

#### **1.4.4 Knock down of protein expression using small interfering RNA (siRNA) technology**

Small interfering RNAs (siRNAs) (also termed as silencing RNAs or short interfering RNAs) are commonly used as a RNA interference tool to knock down protein expression (Wittrup and Lieberman, 2015). siRNA molecules are double stranded and between 20 to 25 base pairs long. siRNAs base pair with complementary mRNAs that results in specific degradation of the target mRNAs through the RISC complex thus interfering with gene expression and protein production (Wittrup and Lieberman, 2015). Synthetic siRNAs are mostly made through the methods of solid-phase chemical synthesis that gives a readily, stable and highly pure modified siRNAs (Wen and Meng, 2014). siRNAs are transfected into cells by various methods including polymer or cationic lipid based artificial membranes or electroporation that induces holes in the plasma membrane of the cells allowing siRNA molecules to enter the cells (Valiunas and Brink, 2015).

### 1.4.5 The mRNA cycle

mRNA post synthesis needs to be regulated since not every mRNA is used for translation into proteins. This regulation is achieved by a process known as mRNA cycle that involves P-bodies, polysomes and stress granules (Figure 1.4.4). Nascent mRNA produced inside the nucleus is shuttled outside into the cytoplasm by bound nuclear proteins (Buchan and Parker, 2009). In case the transcript was found to be defective it is incorporated into P-bodies for decay (Eulalio *et al.*, 2009b). Alternatively, stress granules get associated with mRNA transcript resulting in dissociation of RNA degradation proteins (e.g. decapping enzymes 1 and 2-DCP1/2) and RNA helicases. Incorporation of mRNA transcript into stress granules also attracts eukaryotic initiation factors thus forming the pre-initiation complexes (Decker and Parker, 2012). The pre-initiation complex thereby goes through a series of sequential steps that includes formation of translation initiation complex, then establishment of ribosomal complex and finally aggregation into polysomes. At this stage the mRNA undergoes several rounds of translation resulting in the expression of protein polypeptides. Once the expression demand has been met, the ribosomal complex gets disintegrated by the degradation machinery, which cause deadenylation and 3'-5' exosomal decay. Alternatively, the ribosomal complex can be incorporated into P-bodies (Buchan and Parker, 2009). Based on the demand of protein by the cell this translation machinery can be turned on and off by degrading the degradation machinery and re-establishing the eukaryotic initiation factors or vice versa (Eulalio *et al.*, 2007b, Buchan and Parker, 2009).

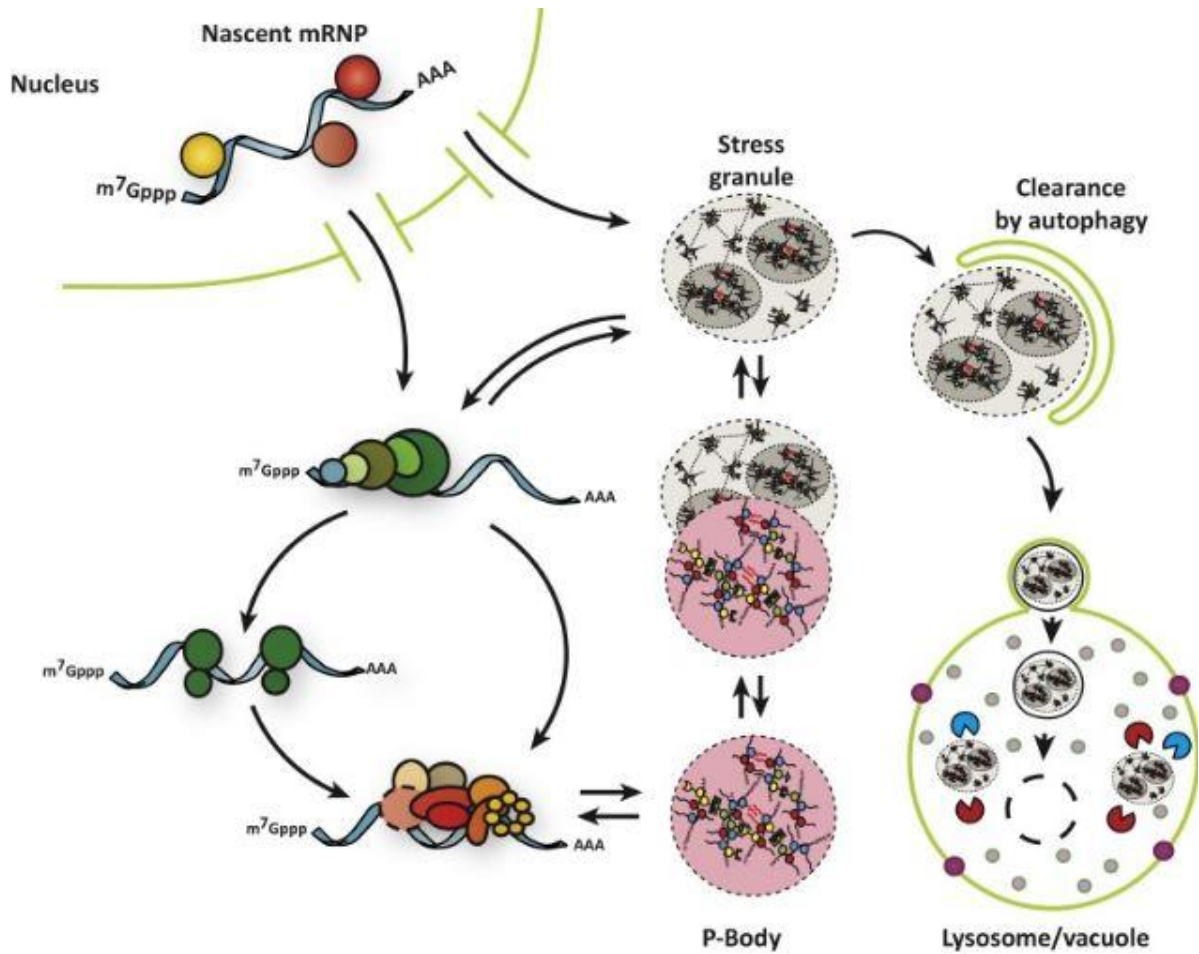


**Figure 1.4.4: Schematic representation of the mRNA cycle showing the regulation of mRNA by P-bodies and Stress granules.**

The figure showing how nascent mRNA synthesized inside the nucleus is shuttled outside into the cytoplasm by nuclear proteins and then incorporated into p-bodies if found to be defective or undergoes rounds of translation. The figure also shows the incorporation of mRNA into stress granules and how it maintains a balance between translation and degradation (Reproduced from Protter *et al.*, 2016)

#### **1.4.6 The role of DEF6 in P-body formation and mRNA regulation**

Whilst DEF6 is spread throughout the cytoplasm, it has been shown to form granules in stressed cells and these granules then co-localise with P-bodies. This suggests a role for DEF6 in post-transcriptional mRNA degradation (Hey *et al.*, 2012).

DEF6 has been found to involve with both TCR-mediated polymerisation leading to IS formation and also has been associated with mRNA translation initiation involving stress granules and P-bodies. Thus these two seemingly different processes might be functionally connected via DEF6 for which further investigation is required. In other words, the role of stress granules and P-body is TCR mediated IS formation requires attention.

## **1.5 DEF6 knockdown and its role in various physiological processes**

### **1.5.1. Role of DEF6 in autoimmune response**

Autoimmune disorders are characterised by the accumulation of reactive T cells in the periphery and chronic inflammation in the target organs. They cover a broad spectrum of diseases, including vasculitis, reactive and rheumatoid arthritis, multiple sclerosis and systemic lupus erythematosus (SLE); however, the pathogeneses of these diseases are often unknown. As such, the molecular mechanisms autoimmune responses are the subject of considerable research. Animal models, including experimental autoimmune encephalomyelitis (EAE) and experimental autoimmune uveitis (EAU) have played key roles in these studies.

In order to maintain T cell homeostasis, activated T cells must be subjected to programmed cell death or apoptosis following engagement with pathogens. This necessitates a precise balance of T<sub>h</sub> subtypes, accurate timing of multiple TCR signalling pathways, and coordination between regulatory molecules (Fanzo *et al.*, 2006; Bécart *et al.*, 2007; Canonigo-Balancio *et al.*, 2009; Biswas *et al.*, 2012). There has been significant progress in identifying the specific CD4<sup>+</sup> T cells and their corresponding cytokines that have the greatest influences in autoimmune events; recent investigations have identified interleukin-21 (IL-21) and IL-17 as being amongst the most influential cytokines in promoting an autoimmune response (Chen *et al.*, 2008; Canonigo-Balancio *et al.*, 2009). Although IL-21 is primarily expressed in follicular helper T cells (T<sub>fh</sub>) (Crotty, 2011), it has also been identified in extra follicular T<sub>h</sub> cells and murine Th17 cells (Korn *et al.*, 2007).

The role of DEF6 in the autoimmune events appears paradoxical and has been the subject of contradictory reports (Chen *et al.*, 2008; Altman and Bécart, 2009).

Fanzo *et al.* (2006) found that DEF6-deficient mice developed spontaneous systemic autoimmune disorders, such as lupus-like syndrome, and rapidly developed organ specific disorders, such as rheumatoid arthritis-like joint disease (Fanzo *et al.*, 2006). These were characterised by diminished levels of ERK1/2 and c-Fos, enhanced production of auto-antibodies and the accumulation of T and B cells. Furthermore, both actin polymerisation and IS formation were found to be impaired in DEF6-deficient mice, and these effects were more pronounced in the absence of Vav1. They concluded that not only were DEF6 and Vav1 both essential for the assembly of the IS, but that they may cooperate in sustaining the IS in order to ensure optimal production of IL-2 (Fanzo *et al.*, 2006). Whether this was a consequence of their distinct homologies will be a subject for future investigation.

By identifying a potential role for GEFs Vav1 and DEF6, in the control and regulation of peripheral T cells, Fanzo *et al.*, (2006) postulated that there might be a genetic link between DEF6 and autoimmunity. This hypothesis was supported by the observation that many autoimmune disorders exhibit a sex bias and are more prevalent in females, particularly human SLE, (Fanzo *et al.*, 2006). However, this effect has not always been observed in mice models, but was associated with IBP/DEF6. This suggested that a potential genetic link will need to be further verified by further investigations.

Consistent with the findings of Fanzo *et al.* (2006), Chen *et al.* (2008) found that DEF6-deficient mice developed a lupus-like syndrome, rheumatoid

arthritis-like disease and large-vessel vasculitis that was accompanied by enhanced expression of both IL-17 and IL-21. Conversely, the up regulation of IL-21 and IL-17 could be abrogated by the absence of IFN regulatory factor 4 (IRF-4), indicating that IRF-4 was a key regulator of IL-21 gene expression and by inference that IRF-4 might also be essential in Th17 development (Huber *et al.*, 2008). Based on these findings, they hypothesised that DEF6 was able to sequester IRF-4 and thereby inhibit overexpression of pro-inflammatory cytokines IL-21 and IL-17 (Chen *et al.*, 2008). Furthermore, they proposed that DEF6 performed this role independently of its GEF activity but the details of such a mechanism are unclear.

Previous studies had demonstrated the importance of IRF-4 as a regulator of IL-21 production in T<sub>h</sub> cells (Chen *et al.*, 2008) and an essential contributor in plasma cell generation in B cells (Klein *et al.*, 2006). These findings demonstrated that DEF6 not only suppressed IRF-4 function in T<sub>h</sub> cells, in agreement with Chen *et al.* (2008), but was also involved in IL-21 B cell responsiveness through cooperation with its homologue, Swap-70. Previous reports had also indicated that loss of DEF6 alone could induce an autoimmune response in mice (Fanzo *et al.*, 2006; Chen *et al.*, 2008). However, Biswas *et al.* (2012) demonstrated that the development of lupus-like syndrome in female mice could be enhanced by the loss of both DEF6 and Swap-70 (Biswas *et al.*, 2012). Consequently, they proposed that Swap-70 might be involved in fine-tuning the response. Further investigations suggested that DEF6 may play a dual role in B cells by regulating immunoglobulin class switching, a process by which activated B cells can alter antibody production between different isotopes. They found this was

dependent on the ability of DEF6 to regulate expression of activation-induced cytidine deaminase (AID), which is required for B cell differentiation. Of note, DEF6 has also been implicated in a genetic relationship between B cell development and AID mRNA (Muramatsu *et al.*, 1999).

Conversely, other authors have suggested that DEF6-deficiency can enhance autoimmune resistance (Bécart *et al.*, 2007; Canonigo-Balancio *et al.*, 2009; Vistica, Shi *et al.*, 2012). Bécart *et al.* (2007) found that Th1 and Th2 inflammatory responses were suppressed in DEF6<sup>-/-</sup> T cells and diminished both the number of peripheral T cells and the production of IL-2. They found that these effects were linked to a deficiency in Ca<sup>2+</sup> release from intracellular stores, resulting in impaired nuclear translocation of NFAT and suppression of Th cell differentiation. These findings confirmed that DEF6 was not only crucial to the development and differentiation of Th1 and Th2 cells via activation of Rho GTPases, but also that loss of DEF6 promoted resistance to pro-inflammatory diseases due to a reduction in peripheral T cells.

Canonigo-Balancio and Fos (2009) reported similar effects, by showing that DEF6<sup>-/-</sup> T cells produced lower levels of IL-2, IFN and IL-17 compared to their wild-type counterparts and that this correlated with enhanced resistance to Th1/Th2 inflammation (Canonigo-Balancio *et al.*, 2009). In agreement with Bécart *et al.* (2007) they attributed this effect to a decrease in cytosolic Ca<sup>2+</sup> leading to a reduction in Th1, Th2 and Th17 differentiation. In contrast, DEF6-positivity enhanced the capacity for T<sub>h</sub> cell differentiation. Canonigo-Balancio and Fos (2009) also demonstrated that DEF6-positivity was associated with increased generation of encephalitogenic Th1 and Th17 cells, promoting the development of EAE in a mouse model. Conversely, the number of migrating

auto reactive T cells was decreased in DEF6-deficient mice. This was taken to imply that DEF6 was involved in the progression of naïve T cells to pathogenic Th17 cells in the presence of IL-6, a secretory product of Th2 (Canonigo-Balancio *et al.*, 2009). Consistent with both these reports, Vistica *et al.* (2012) demonstrated that knockout of DEF6 could inhibit the development of EUA in mice and that this was correlated with reduced production of IFN $\gamma$  and IL-17, reflecting impaired differentiation of Th1 and Th17 (Vistica *et al.*, 2012)

### 1.5.2. Role of DEF6 in other processes

CD4<sup>+</sup> cells from DEF6<sup>-/-</sup> mice showed diminished adhesion to ICAM-1 compared to CD4<sup>+</sup> cells from wild type mice (Cote *et al.*, 2015). The authors showed that DEF6 mediates adhesion after TCR binding via the GTPase Rap1. DEF6 deficiency in CD8<sup>+</sup> cells led to a reduction in TCR induced nuclear translocation of NFAT. However, DEF6 deficiency did not result in any impairment in the differentiation of cytotoxic T cells (Feau *et al.*, 2013).

DEF6 has been shown to be an inhibitor of osteoclast formation in patients suffering from rheumatoid arthritis (Binder *et al.*, 2017). A deficit in DEF6 in mice increased the development of osteoclasts in response to TNF- $\alpha$  stimulus both in vivo and in vitro. Furthermore, lack of DEF6 caused an increase in bone resorption. In patients suffering from rheumatoid arthritis, high TNF- $\alpha$  levels in their serum were accompanied by lowered DEF6 expression. Taken together, these findings suggest that DEF6 might inhibit the degradation of bone typically found in rheumatoid arthritis.

Haematopoietic stem cells express both Swap-70 and DEF6. Ripich *et al.* (2016) investigated the effect of Swap-70 and DEF6 on the ability of stem cell precursors to rebuild haematopoietic stem cell lines. They transferred precursor cells from Swap70<sup>-/-</sup>, DEF6<sup>-/-</sup> and double knock-out mice into irradiated mice. Precursor stem cells from Swap70<sup>-/-</sup> showed a reduced potential to rebuild haematopoietic stem cell lineage. DEF6<sup>-/-</sup> derived haematopoietic stem cells were as abundant as wild type. Interestingly, the stem cell precursor from double knockouts were less abundant than wild type, showing an opposing effect of Swap-70 and DEF6. Furthermore, double knockout DEF6<sup>-/-</sup> Swap<sup>-/-</sup> mice spontaneously developed an auto-immune

disease which was similar to systemic lupus erythematosus and showed an up-regulation in IL-10 release (Manni *et al.*, 2015).

## Research Objectives:

- Establish whether the PH and/or DH-like domains containing a coiled coil region are constraining DEF6 from spontaneous colocalisation with P-bodies
- Establish functional consequences of phosphorylation at serine/threonine residues in the C-terminal end of DEF6
- Elucidate the potential role of DEF6 in the control of mRNA translation in Jurkat T cells
  - Test whether DEF6 colocalises with the translation initiation complex
  - Test whether DEF6 interacts with proteins of the translation initiation complex
  - Use siRNA-mediated knockdown and ectopic overexpression of DEF6 to establish whether expression of proteins of the translation initiation complex is altered
  - Determine whether DEF6 colocalises with proteins of the translation initiation complex in the immunological synapse

## **Chapter 2: Material and Methods**

## **2.1 Cell Culture**

### **2.1.1 Cells lines:**

#### **Adherent cell type:**

**COS7 Cells:** it was derived from the kidney of the African Green Monkey, *Cercopithecus aethiops*.

**Hek293 and HeLa cells:** Human embryonic kidney cells 293 and an immortal cancer cell line Hela were kindly provided by Ayoub PhD (E84)

#### **Suspension cell type:**

**Jurkat cells:** Jurkat E6.1 human leukaemic T cell lymphoblasts (ECACC #88042803).

**Raji B cells:** Raji B cell lymphoblasts (Sigma #85011429).

### **2.1.2 Cells culture media:**

**RPMI-1640:** medium supplemented with L-glutamine and sodium bicarbonate; 10% (v/v) Foetal Bovine Serum (FBS) and 1% (v/v) penicillin/streptomycin. Media was stored at 4°C (Sigma Aldrich #R8758).

**Dulbecco's Modified Eagle's Medium (DMEM):** supplemented with 4500mg/L glucose, 110mg/L Sodium Pyruvate, LGlutamine, 10% (v/v) Foetal Bovine Serum (FBS) stored at 4°C (Sigma #D6429).

**10x Trypsin/EDTA:** solution containing 5g Porcine Trypsin and 2g EDTA, sterile-filtered; diluted in sterile 1x PBS (Sigma #T4174).

**1x Phosphate Buffered Saline:** prepared from 137M NaCl, 2.7mM KCl, 10mM  $\text{Na}_2\text{HPO}_4$  and 2mM  $\text{KH}_2\text{PO}_4$  pH7.4; Sterilise by autoclaving and stored at 4°C.

**Freezing mix:** 10% (v/v) DMSO in FBS.

### **2.1.2-1 Antibiotic:**

**Penicillin and Streptomycin:** 10,000 units Penicillin and 10,000µg Streptomycin per ml (Lot #1864845, gibco by life technologies).

**Kanamycin:** Kanamycin stock solution was prepared by dissolving kanamycin monosulphate in ddH<sub>2</sub>O to a concentration of 50 mg/ml. The solution was filter sterilised through a 0.2 µm filter and stored at -20°C. Kanamycin was used at a working concentration of 50 µg/ml (K1637, Sigma).

### **2.1.2-2 Treatments:**

**Cycloheximide:** 200mg/ml of Cycloheximide dissolved in DMSO (Calbiochem #239763).

**Phorbol-12-myristate-13-acetate:** 1.62mM of PMA dissolved in DMSO (Calbiochem #524400).

**Ionomycin:** 3.1mM *Streptomyces conglobatus* ionomycin calcium salt dissolved in DMSO (Calbiochem #407952).

**MG132 Proteasome inhibitor:** 10mM of MG132 dissolved in DEMSO (Sigma # M7449)

**Bafilomycin A1 inhibitor:** 50 µM of Bafilomycin A1 dissolved in DEMSO (Invivo Gen # tlr1-baf1)

## **2.2 Bacterial Growth Media:**

**Luria Bertani broth (LB):**1%(w/v) tryptone ,0.5%(w/v) yeast extract, 0.5% (w/v) NaCl were dissolved in ddH<sub>2</sub>O, then sterilised by autoclaving for 30 min. To make LB-agar add 1.5% of agar prior to autoclaving

**Super Optimal Broth (SOC):** 2% (w/v) tryptone, 0.5% yeast extract, 8.9mM NaCl 2.5 mM KCl, 20mM MgSO<sub>4</sub> and 20Mm glucose were dissolved in ddH<sub>2</sub>O then sterilise by autoclaving for 30 min.

## **2.3 Buffers and Solutions**

### **2.3.1 Electrophoresis Buffers:**

**Agarose Gel:** 1 or 1.5% agarose was dissolved in 1x TBE by heating, once cool SafeVeiw was added (NBS biologicals ltd#NBS-SV)

**10 x Tris-Borate EDTA (TBE):** 108g Tris, 55g Boric acid and 40ml 0.5M EDTA pH8.

### **2.3.2 Westren blots buffer and solution:**

**10x Phosphate Buffered Saline:** prepared from 1.37M NaCl, 27mM KCl, 100mM  $\text{Na}_2\text{HPO}_4$  and 20mM  $\text{KH}_2\text{PO}_4$  pH7.4;bring up to 1 liter of distilled water before being autoclaved. Stock buffer diluted in distilled water to make 1x working solution.

**10x RIPA buffer:** 20 mM Tris-HCl (pH 7.5), 150mM NaCl, 1mM  $\text{Na}_2\text{EDTA}$ , 1mM EGTA, 1% NP-40, 1% sodium deoxycholate, 2.5 mM sodium pyrophosphate, 1mM beta-glycerophosphate, 1mM  $\text{Na}_3\text{VO}_4$ , 1  $\mu\text{g/ml}$  leupeptin.Diluted in ddH<sub>2</sub>O to make 1x working buffer; aliquoted and stored at -20°C.(Cell Signaling#9806).

**100mM phenylmethylsulphonyl fluoride (PMSF) a protease inhibitor:** MW=174.19g/mol is desolved in 100% Ethanol to the final volume 100mM; Stock stored at -20°C. PMSF used at final concentration of 1mM.

**PhosSTOP™:** inhibitor tablets for phosphatase, phosphatase inhibitor tablets (Sigma #04906845001)

**Laemmli 2X buffer:** 4% SDS, 10% 2-mercaptoethanol, 20% glycerol ,0.004% bromophenol blue and 0.125M Tris HCl (Sigma #S3401).

**Transfer buffer:** 30mM Tris, 24mM Glycine and 25% (v/v) Methanol.

**Blocking Solution:** 5% (w/v) Marvel dried skimmed milk powder dissolved in PBST

**Incubating Solution for antibody:** 3% (w/v) Marvel dried skimmed milk powder dissolved in PBST

**Wash solution:** 1xPBS and 0.1%(v/v) tween-20 (Lot#SZBB1080V, Sigma)

### **2.3.3 Co-immunoprecipitation Buffers**

**10x RIPA buffer:** 20mM Tris-HCl (pH 7.5), 150mM NaCl, 1mM  $\text{Na}_2\text{EDTA}$ , 1mM EGTA, 1% NP-40, 1% sodium deoxycholate, 2.5 mM sodium pyrophosphate, 1mM

beta-glycerophosphate, 1mM Na<sub>3</sub>VO<sub>4</sub>, 1µg/ml leupeptin. Diluted in ddH<sub>2</sub>O to make 1x working buffer; aliquoted and stored at -20°C. (Cell Signaling#9806).

### **2.3.4 Sodium Dodecyl Sulphate Polyacrylamide Gel Electrophoresis Buffers and Solutions**

**Resolving Gel Buffer:** 3.3ml 30% (v/v) bis acrylamide, 2.5ml 1.5M Tris pH 8.8, 100µl 10% (w/v) SDS, 100µl 10% (w/v) APS, 4ml distilled water, and 8µl TEMED.

**Stacking Gel Buffer:** 830µl 30% (v/v) bis acrylamide, 630µl 1M Tris pH6.8, 50µl 10% (w/v) SDS, 50µl 10% (w/v) APS, 3.4ml distilled water, and 8µl TEMED.

**10x SDS Running Buffer:** 1.87M glycine, 250mM Tris and 1% (w/v) SDS diluted dH<sub>2</sub>O to make a 1x working buffer.

### **2.3.5 Gel fixer:**

**Coomassie Blue Stain:** 50% (v/v) methanol, 10% (v/v) acetic acid and 3mM Coomassie Brilliant Blue R (Sigma #B7920).

**Coomassie Blue De-stain solution:** 30% (v/v) methanol and 10% (v/v) acetic acid.

### **2.3.6 Immunofluorescence Solutions:**

**Fixing Solution:** 4% (w/v) PFA in 10ml dH<sub>2</sub>O with 10mM NaOH and heated to 60°C until dissolved. Then add 10ml 2x Tris buffer saline, 4ml 1M Tris HCL PH.8 and 12ml 5M NaCl; fill up to 200ml.

**Permeabilisation Solution:** 0.2% (v/v) Triton X-100 in 1x PBS.

**Blocking Solution:** 3% (w/v) BSA in 1x PBS

**Incubating Solution for antibody:** 3% (w/v) BSA in 1x PBS.

### **2.3.7 Flow cytometry Solution:**

**Fixing Solution:** 4% (w/v) PFA in 10ml dH<sub>2</sub>O with 10mM NaOH and heated to 60°C until dissolved.

**Permeabilisation Solution:** 0.2% (v/v) Triton X-100 in 1x PBS.

**Incubating Solution for antibody:** flow cytometry staining buffer solution (Cat# 00-4222-57, eBioscience).

## **Methods:**

### **2.4 Cells culture Techniques:**

#### **2.4.1 Thawing of cells**

Frozen cells in a cryogenic vial (Corning) were thawed by placing the vial in a 37°C water bath. Cells were centrifuged at 1500 rpm for five minutes, and then the supernatant was removed. Pellets were re-suspended with 1 ml of pre-warmed growth medium by gently pipetting up and down before transferring to a T75 cm<sup>2</sup> flask for suspension cells or to a sterile dish for adherent cells, both containing an appropriate volume of medium. Cells were cultured at 37°C in a 5% CO<sub>2</sub> atmosphere with controlled humidity for 48 hours before being passaged once the cells reached the appropriate density.

#### **2.4.2 Passaging of Adherent Cells**

COS7 cells were grown in Dulbecco's Modified Eagle's Medium (DMEM) in sterile culture dishes at 37°C in a 5% CO<sub>2</sub> atmosphere with controlled humidity. When the cells reached 80% confluency, the DMEM media was removed, and the cells were washed with 5 ml of 1x PBS. The 1x PBS was removed and 1.5 ml of 1x Trypsin-EDTA was added to the cells. The excess trypsin was removed from the dish, and the dish was incubated for three minutes at 37°C in a 5% CO<sub>2</sub> humidified atmosphere to detach the cells. The dish was removed from the incubator and one side was gently tapped. The dish was checked under a light microscope to determine if the cells had detached. If the cells still appeared to be attached to the bottom, the dish was placed in the incubator for an additional three minutes. COS7 cells were re-suspended in 10 ml of DMEM medium, then 1 ml was transferred to a

new sterile culture dish at a 1:9 ratios with fresh DMEM media, and the plate was incubated at 37°C in a 5% CO<sub>2</sub> atmosphere with controlled humidity.

#### **2.4.3 Passaging of Suspension Cells**

Jurkat and Raji cells were cultured using RPMI-1640 media in T75cm<sup>2</sup> flasks in a humidified atmosphere at 37°C containing 5% CO<sub>2</sub>. Cells were maintained at 1 x 10<sup>6</sup> cells/ml. Once the cells reached the required density, they were split and transferred in a ratio of 1:5 into fresh, pre-warmed RPMI-1640 media and placed in the incubator.

#### **2.4.4 Counting Cells using a Haemocytometer**

To count cells, 20µl of the cell solution was added to the haemocytometer and covered by a coverslip. Cells were counted in the 5x5 centre square and in the 4x4 square on the right, including the cells on the bottom and right edges. The average number of cells counted was multiplied by 10,000 to give the number of cells per ml.

#### **2.4.5 Cryopreservation of Cell Lines**

Cells were centrifuged at 1200rpm for 10 minutes, and then re-suspended with 1ml of freezing media. This 1ml was transferred to cryogenic vials and moved to the -80°C freezer overnight before being transferred to liquid nitrogen for storage.

#### **2.4.6 Transfection of Adherent Cells**

Cultured COS7 cells in the logarithmic growth stage were trypsin digested from the plate and placed on sterile, square coverslips in a 6-well plate at density of 1.5 x 10<sup>5</sup> cells/well in 2ml of DMEM media. They were incubated at 37°C in a 5% CO<sub>2</sub>

atmosphere for 24 hours prior to transfection to allow them to reach 50 to 60% confluency. Then, 2µg of DNA plasmid was precipitated by adding one-tenth of 2M NaCl by volume to 80µl of ice-cold 100% ethanol and placing it in a -20°C freezer for 10 minutes. The DNA was recovered by centrifugation at 14,000xg for five minutes at 4°C, the supernatant was aspirated and 500µl of ice-cold 70% ethanol was added. The solution was centrifuged again at 14,000xg for five minutes at 4°C. The DNA pellet was air dried for five minutes inside the Class II tissue culture hood and incubated for five minutes at room temperature with 100µl of Opti-MEM medium (Cat#31985, GIBCO Invitrogen corporation) along with 6µl of GeneJuice (Cat#70967-3, Novagen) transfection reagent. The DNA was added to the cells on the coverslips at a final concentration of 2µg/µl, mixed gently by swirling and incubated for 24 hours at 37°C in a 5% CO<sub>2</sub> atmosphere.

### **2.4.7 Transfection of Jurkat T Cells**

Cultured Jurkat cells in the logarithmic growth stage were transfected by square wave electroporation. Cells were re-suspended at density of  $2 \times 10^7$  in serum-free RPMI-1640 medium. Then 50µg of DNA was precipitated by adding one-tenth of 2M NaCl by volume and two volumes of ice-cold 100% ethanol and placing in a -20°C freezer for fifteen minutes. The DNA was centrifuged at 14,000xg for 10 minutes at 4°C, the supernatant was aspirated and the pellet was washed by 500µl of ice-cold 70% ethanol. The solution was centrifuged again at 14,000xg for 10 minutes at 4°C. The DNA pellet was air dried for five minutes inside the Class II tissue culture hood and re-suspend in 50µl of Opti-MEM medium. 250µl of the cell suspension was gently mixed with 50µg of DNA in a 4 mm Geneflow electroporation cuvette before exposure to a single pulse from the BTX Electro Square Porator ECM 830 machine

(A Division of Genetronics, Inc) at 310 V or 312 V for 10ms. Cells were then re-suspended in 10 ml of pre-warmed complete growth medium and incubated for 24 hours at 37°C in a 5% CO<sub>2</sub> atmosphere.

#### **2.4.8 siRNA Knockdown of DEF6**

Jurkat cells were plated at  $2 \times 10^5$  per well in a 24-well plate using 100µl of RPMI culture medium. Then, 562.5ng of siRNA (DEF6 Silencer Select Pre-Designed siRNA Cat #4392420, ID: s27057, Ambion) were diluted into 100µl of Opti-MEM medium or culture medium without serum, and 9µl of HiPerFect Transfection Reagent (Lot# 154028459, QIAGEN) were added to the diluted siRNA and mixed. This sample was incubated for 10 minutes at room temperature to allow the formation of the transfection complex. This complex was added drop-wise onto the cells, the plate was gently swirled and incubated for six hours at 37°C in a 5% CO<sub>2</sub> atmosphere. After six hours, 400µl of culture medium was added to give a final siRNA concentration of 75nM, and the plate was incubated for 72 hours at 37°C in a 5% CO<sub>2</sub> atmosphere. Fresh medium was added when required.

#### **2.4.9 Immunological Synapse Formation**

Immunological synapses were formed by collecting  $6.6 \times 10^6$  Raji B cells, which were centrifuged for five minutes and re-suspended in 1ml of complete RPMI medium. Calcein (green or blue, see appendix table 6) was added to the B cells at a final concentration of 1µg/ml, and the cells were covered in foil and incubated for 20 min at 37°C in a 5% CO<sub>2</sub> atmosphere. After centrifuging for five minutes, the cells were washed three times in 1x PBS and re-suspended in 1ml of complete RPMI medium plus 1.5µg/ml Staphylococcus aureus enterotoxin A and 1.5µg/ml S. aureus

enterotoxin B. These were incubated for 30 minutes at 37°C in a 5% CO<sub>2</sub> atmosphere, then centrifuged for five minutes before being re-suspended in 250µl of complete RPMI medium.

A total of  $3.3 \times 10^6$  Jurkat T cells were collected following a five minute centrifugation and re-suspended in 250µl of complete RPMI medium. Raji B and Jurkat T cells were mixed together and incubated for one hour at 37°C in a 5% CO<sub>2</sub> atmosphere, then diluted (1:2) in 3% BSA in 1x PBS. A total of 150µl of cells were placed on each Poly-L-Lysine coated coverslip in a 6-well plate and incubated at room temperature for 10 minutes. The cells were washed twice in 3% BSA in 1x PBS and were fixed with 4% PFA for 10 minutes. They were washed three times in 3% BSA in 1x PBS and permeabilised by adding 0.2% Triton X-100. After incubation for 10 minutes at room temperature, the cells were immunostained as described below.

#### **2.4.10 Immunofluorescence**

Immunodetection was performed by adding Jurkat cells onto Poly-L-Lysine coated coverslips for 10 minutes before aspirating the media. Coverslips were washed one time with 1x PBS, then the cells were fixed by incubating them with 4% PFA for 10 minutes at room temperature. After fixation, the cells washed twice with 1x PBS before being permeabilised with 0.2% Triton X-100 for 10 minutes at room temperature. The coverslips were blocked for one hour in 3% BSA in 1x PBS at room temperature. After removing the blocking solution, the primary antibody was diluted (see Appendix table 5) in 3% BSA in 1x PBS and incubated with the cells for one hour in the dark at room temperature. Coverslips were washed three times with 1x PBS for five minutes each, then incubated for 45 minutes or one hour in the dark with diluted fluorescence secondary antibody in 3% BSA in 1x PBS (see Appendix

table 5.1). Cells were washed three times with 1x PBS for five minutes each before being mounted using ProLong™ Diamond Antifade Mountant (lot#1747346, Life Technologies).

#### **2.4.11 Translation and Newly Synthesised Protein Assay**

Protein synthesis experiments were performed using the Click-iT® AHA Alexa Fluor® 488 protein synthesis HCS assay kit (Cat#C10289; Invitrogen). For AHA Alexa Fluor 488 labelling,  $1 \times 10^6$  Jurkat cells were seeded onto Poly-L-lysine-coated coverslips in 24-well plates. The cells were washed with PBS before incubation with RPMI complete medium; the control cells were incubated in methionine-free medium. One well was treated with 100mg/ml of cycloheximide for either 30 minutes or one hour with incubation at 37°C in a 5% CO<sub>2</sub> atmosphere. The cells were then washed with 1x PBS and starved for 30 minutes in methionine-free medium before incubation with methionine-free medium containing 50µM of Click-iT AHA working solution for 30 minutes at 37°C. Subsequently, the cells were washed with 1x PBS and fixed with 4% PFA for 15 minutes at room temperature. The cells were washed twice with 3% BSA/PBS and permeabilised with 0.5% Triton X-100 for 20 minutes at room temperature. The samples were next washed twice with 3% BSA/PBS and incubated with the Click-iT reaction cocktail, protected from light, for 30 minutes at room temperature. The samples were then washed once with 3% BSA/PBS and processed for immunofluorescence, as previously described.

#### **2.4.12 Flow Cytometry**

Jurkat cells were transfected with siRNA knockdown DEF6, and the control cells were transferred into fresh Eppendorf tubes and collected by centrifugation at 900xg for five minutes. The cells were washed once with 3% BSA in 1x PBS and fixed in 100  $\mu$ l of 4% PFA for 10 minutes at room temperature. The cells were centrifuged and washed with 3% BSA/PBS before permeabilisation with 200  $\mu$ l of 0.1% Saponin for 10 minutes. The cells were stained with the primary antibody monoclonal rabbit anti- DEF6 in an appropriate dilution 1/500 in 3% BSA/PBS for one hour in the dark. The cells were collected by centrifugation and washed twice with 300  $\mu$ l of 3% BSA/PBS before the addition of AlexaFluor 488-conjugated anti-rabbit secondary antibody in 3% BSA/PBS for five minutes. Cells were washed twice, re-suspended in 300  $\mu$ l of 1x PBS and stored at 4°C in the dark until required for analysis by flow cytometry via the FL1 Parameter.

#### **2.5 Cell Treatment:**

**Activation of Jurkat cells:** To activate the cells,  $1 \times 10^6$  cells/ml were incubated with PMA (50nM) and Ionomycin (1 $\mu$ M) for 1 hour at 37°C in a 5% CO<sub>2</sub> atmosphere.

**Block translation:** to inhibit translation,  $2 \times 10^6$  cells/ml of Jurkat cells were incubated with 100mg/ml of Cycloheximide for 30min at 37°C in a 5% CO<sub>2</sub> atmosphere.

**Studying cellular degradation of the ubiquitin-proteasome pathway:** treat post-transfection  $2 \times 10^5$  cells with siRNA DEF6 with 50 and 10  $\mu$ M MG-132 proteasome inhibitor to prevent degradation of proteasome for 16 and 24 hours.

**Autophagy studying:** treat post-transfection  $2 \times 10^5$  cells with siRNA DEF6 with 20 $\mu$ M of Bafilomycin A1 inhibitor for 16 and 24 hours.

## **2.6 Bacterial Culture techniques:**

### **2.6.1 Bacterial Transformation**

Chemically competent DH5 $\alpha$  (*Escherichia coli*) cells, NEB 5- $\alpha$  *E. coli* cells or XL10-Gold ultracompetent cells that were used for the site directed mutagenesis were thawed on ice. DNA plasmids (1–100ng) were added to 50 $\mu$ l aliquots of DH5 $\alpha$  *E. coli* and placed on ice for 30 minutes. The cells were transferred to a 42°C water bath and heat-shocked for 45 seconds. After cooling on ice for two minutes, the cells were incubated in 950 $\mu$ l/tube of SOC medium at 37°C for one hour, followed by 30 minutes on an orbital shaker at 220 rpm. A total of 200 $\mu$ l of transformed cells were spread onto an LB agar plate containing 300 $\mu$ l kanamycin antibiotic. The plate was inverted and incubated at 37°C overnight.

### **2.6.2 Bacterial Colony Picking**

A single bacterial colony was picked from an LB agar plate under sterile conditions using a sterilised tip. It was placed into 5 ml of LB medium containing Kanamycin antibiotic and incubated at 37°C in an orbital shaker at 222 rpm overnight.

## **2.7 DNA Techniques:**

### **2.7.1 Plasmid DNA Extraction from Bacteria**

DNA extraction was performed using a GenElute Plasmid Miniprep kit (Cat#PLN70, Sigma) according to the manufacturer's protocol. Briefly, the bacteria from a 5ml overnight culture were harvested by centrifugation to pellet the cells at 12,000xg for one minute (three times). The pellet was re-suspended with 200 $\mu$ l of the resuspension solution by vortexing or pipetting the solution up and down. The cells were lysed by adding 200 $\mu$ l of the lysis solution. This was immediately mixed by

gently inverting the tube 6–8 times before adding 350µl of the neutralization solution to precipitate the cell debris. This tube was gently inverted 4–6 times, and then the debris was pelleted by centrifuging for 10 minutes at 12,000xg. In the meantime, each column was prepared by inserting a GenElute Miniprep column into a microcentrifuge tube and adding 500µl of the column preparation solution. These were centrifuged for one minute, and then the flow-through was discarded. The cleared lysate was transferred to the column and centrifuged for one minute at 12,000xg, and the flow-through was discarded. Next, 500µl of the optional wash solution were added to the column and centrifuged for one minute. The flow-through was discarded. Then, 750µl of the diluted wash solution were added, and it was centrifuged for one minute. The flow-through was discarded, and it was centrifuged again at the maximum speed for one minute to remove the excess ethanol. The column was transferred to a fresh collection tube, 50µl of the elution solution were added and it was centrifuged for one minute at 12,000xg. The final eluent containing the DNA was stored at -20°C.

To obtain a larger amount of DNA, plasmid DNA was isolated from 200 ml cultures using the GenElute HP Endotoxin-free Plasmid Maxiprep Kit (Cat#NA0410, Sigma) according to the manufacturer's protocol. A 5 ml culture of bacteria cells grown overnight were transferred to 200 ml of LB medium containing antibiotic, and the culture was shaken overnight at 250–300rpm at 37°C. A 50 ml sample of the bacterial culture were harvested by centrifugation for 10 minutes at 5000xg (five times), discarding the supernatant each time. Then, 12 ml of the resuspension/RNase A solution was added to the pellet and vortexed. The cells were re-suspended by adding 12 ml of the lysis solution, and the contents were immediately mixed by inverting 6–8 times. Then, 12 ml of the chilled neutralisation

solution were added to the mixture, and it was gently inverted 6–8 times and centrifuged for 10 minutes. The lysate filter was prepared via placing a VacCap firmly into a collection tube. A GenElute HP Endotoxin-free maxiprep filter was attached to the VacCap. The lysate was filtered by attaching the vacuum to the VacCap and allowing the lysate to filter through for at least one minute. A GenElute HP maxiprep binding column was placed onto a falcon tube, and 12 ml of the column preparation solution were added to the column. The vacuum was again applied, and the solution was allowed to pass through. The filtered lysate was mixed with 9 ml of the binding solution by gently inverting 6–8 times. The mixture was transferred to the prepared binding column with the vacuum on, allowing all of the lysate to pass through. Then, 12ml of wash solution 1 were added to the column and allowed to pass through, followed by 12ml of wash solution 2. The vacuum was left on for at least 10 minutes to dry the column to prevent ethanol contamination and allow for efficient elution in the final preparation. The binding column was transferred to a clean 50ml collection tube, and 3ml of endotoxin-free water were added to the column. The collection tube containing the column was centrifuged at 3000xg for five minutes. The centrifugation was repeated for another five min at 1000xg to obtain the maximum concentration of the plasmid. The final eluent containing the DNA was stored at -20°C.

### **2.7.2 Determination of DNA or RNA Concentration**

The DNA concentration was determined using a Nanodrop. The upper and lower pedestals of the Nanodrop were cleaned with ddH<sub>2</sub>O before being initialised and blanked to zero with 1µl of ddH<sub>2</sub>O. Then, 1µl of the DNA sample was carefully pipetted onto the lower optical measurement pedestal. The ratio of the absorbance at 260nm to 280nm was used to assess the purity of the DNA.

### **2.7.3 DNA Sequencing**

DNA sequencing was carried out by Source Bioscience Sequencing. A list of primers and sequences can be found in the appendix.

## **2.8 RNA Techniques:**

### **2.8.1 RNA extraction**

Under sterile conditions, Jurkat T cells were transferred into a fresh tube and collected by centrifugation at 900xg for five minutes. The pellets were washed once with 1x PBS to remove the exceed media before homogenizing with 500µl of Trizol Reagent (lot#14174602, Ambion) that was mixed by pipetting up and down several times. This was followed by the addition of 500µl of Trizol, and the solution was again mixed by pipetting up and down six times. This sample was placed on ice and incubated for 15 minutes. Then, 200µl of chloroform was added to the sample and shaken vigorously for 15 seconds before being incubated for two to three minutes at room temperature. This sample was centrifuged for 15 minutes at 14,000xg at 4°C, and the upper phase was removed and transferred to a fresh tube. One volume of isopropanol was added to the supernatant and mixed by pipetting up and down six times. This was incubated on ice for 10 minutes before again being centrifuged for 30 minutes at 4°C, discarding the supernatant. The pellet was washed with 1 ml of 70% ethanol and centrifuged for five minutes at 4°C. The supernatant was discarded, and the pellet was left to air dry for 10 minutes at room temperature. The pellet was then resuspended in 50µl of nuclease-free water by flicking the tube two to three times before storing the RNA extract at -80°C to prevent degradation. The RNA concentration was determined using a Nanodrop and verified by agarose gel electrophoresis.

### **2.8.2 cDNA Synthesis**

cDNA synthesis was performed on ice by adding the following components into nuclease-free microcentrifuge tube: 1µl of 25µg Oligo (dT) (Lot#1768587, Invitrogen), 1–500 ng mRNA, 1µl of 10mM dNTP mix (Cat# U1511, Promega) and sterile, distilled water up to 12µl. This mixture was heated to 65°C for five minutes and placed on ice for a quick chill. The contents were collected by briefly centrifuging this tube followed by the addition of 4µl of 5x of the first strand buffer, 2µl of 0.1 M DTT and 1µl (40 units/µM) of RNase (Cat#10777-019, Invitrogen). The contents of the tube were mixed gently and incubated for two minutes at 42°C. Next, 1µl (200 units) of SuperScript II (Lot#1653335, Invitrogen) was added and mixed by pipetting up and down before incubating for 50 minutes at 42°C. To inactivate the reaction, this mixture was heated for 15 minutes at 70°C and stored at -20°C.

### **2.8.3 Designing primers**

Primers were designed by IDT Primer Quest Tool and synthesised by Invitrogen. Melting temperatures and GC% content was considered. Nuclease-free water was added to the desalted primers to make a 100µM stock solution. Primers were diluted to 10µM working solution to use in the reactions.

## **2.9 Polymerase Chain Reaction:**

### **2.9.1 Reverse Transcription Polymerase Chain Reaction (RT-PCR)**

Complementary nucleic acid amplifications were performed by PCR in a Takara PCR Thermocycler (Gradient PCR). The standard PCR reaction was carried out in a final volume of 50µl containing 10µl of 5x Q5 reaction buffer, 1µl of 10mM dNTP mix,

10 $\mu$ M of each forward and reverse primers (See Appendix, table 8), 1 ng–1 $\mu$ g of cDNA, 0.5 $\mu$ l of Q5 Hot Start High-Fidelity DNA Polymerase (Lot#0151612, Biolabs), 10 $\mu$ l of 5x Q5 high GC enhancer and filled up to 50 $\mu$ l with sterile, distilled water.

**Table 1: PCR program for RT-PCR reactions:**

Steps	Temperature	Duration	Cycles
Initial Denaturation	94 <sup>o</sup> C	4min	25-35X
Denaturation	94 <sup>o</sup> C	1min	
Primer Annealing	60 <sup>o</sup> C	1min	
Template Extension	72 <sup>o</sup> C	1min	
Final Extension	72 <sup>o</sup> C	1min	

The PCR reaction was held at 4<sup>o</sup>C once completed, and the PCR products were verified by agarose gel or stored at -20<sup>o</sup>C.

### 2.9.2 Agarose Gel Electrophoresis

Nucleic acid electrophoresis was performed using an EPS 300 electrophoresis power supply (Pharmacia Biotech). The gel was prepared by melting 0.45–1.5 g of agarose in 1x TBE buffer to a final concentration of 1.5%, depending on the size of the DNA fragment. Once the gel had cooled, SafeView (nucleic acid stain, code# NBS-SV) was added, the gel was poured and the comb put in place. A 100 base pair (bp) DNA Ladder (NEB#N3231S) was used to estimate the size of DNA fragment. Samples were run at a constant voltage of 140 V for 50 minutes. The DNA was visualised by UV trans-illumination and a digital photograph was taken using the Molecular Imager Gel Doc XR system (Bio-Rad).

### 2.9.3 Site-Directed Mutagenesis

Site-directed mutagenesis was carried out using a plasmid containing the human-derived DEF6 cDNA fused to Green Fluorescent Protein (GFP) and the Quick Change Lightning Multi Site-Directed Mutagenesis Kit (Cat #210515-5, Agilent Technologies). The reaction mixture was assembled on ice, and each reaction condition contained 2.5 $\mu$ l of 10x Quick Change Lightning Multi buffer, 0.75 $\mu$ l Quick solution, 100 ng wild type DEF6 cDNA using GFP-DEF6 as a template for amplification(see Appendix Fig 6.1 plasmid map), 100 ng of each mutagenic primer (primers were designed using Snap Gene viewer, and all mutagenic primers used can be found in the Appendix table 7), 1 $\mu$ l of 10mM dNTP mix, 1 $\mu$ l of Quick Change Lightning Multi enzyme blend and sterile, distilled water to 25 $\mu$ l.

**Table 2: PCR program for Quick Change Mutagenesis:**

Steps	Temperature	Duration	Cycles
Initial Denaturation	95 <sup>o</sup> C	2 min	1
Denaturation	95 <sup>o</sup> C	20 sec	30
Primer Annealing	55 <sup>o</sup> C	40 sec	
Template Extension	65 <sup>o</sup> C	3min:50 sec	
Final Extension	65 <sup>o</sup> C	5 min	1

The PCR reaction was held at 4<sup>o</sup>C once completed, and the PCR products were placed on ice for two minutes to cool the reactions to <37<sup>o</sup>C. DpnI DNase enzyme was used to digest only the methylated DNA by adding 1 $\mu$ l of the DpnI restriction enzyme directly to each amplification reaction tube and gently mixing. This mixture

was spun to the bottom of the tubes by centrifuging at 12,000xg for one minute, and then the tubes were incubated for five minutes at 37°C.

The XL10-Gold ultracompetent cells were incubated for 10 minutes on ice with 1µl of β-mercaptoethanol, and the cells were mixed and swirled gently every two minutes. Then, 4µl of the DpnI-treated DNA was used to transform the ultracompetent cells, which were incubated for 30 minutes on ice. After incubation, these samples were heated in a water bath at 42°C for 30 seconds, then were placed on ice for two minutes before adding 500µl of SOC media and incubating for two hours at 37°C with shaking at 225–250rpm.

DNA was extracted from the bacteria using a GenElute Plasmid Miniprep kit (Sigma#PLN70) as described previously. The extracted DNA was sequencing to confirm the presence of the site-directed mutants.

## **2.10 Protein Techniques:**

### **2.10.1 Preparation of Protein Sample**

Cell extracts were prepared by washing the pellet with 1x PBS and lysing in 1x RIPA buffer (Cat#9806, Cell Signaling) containing one PhosSTOP™ (Cat #04906845001, Sigma) inhibitor tablet and 1mM PMSF, which were added immediately before breaking the pellet by sonication for 10 seconds. The samples were incubated for 30 minutes at 4°C with end-over-end rotation, and then centrifuged at 4°C for 10 minutes at 14,000 rpm. The supernatant was transfer to a cold, fresh tube, and 5µl of all of the extract fraction were taken to determine the protein concentration using a Protein Quantification Kit-Rapid (lot#BCBN0189V, Sigma) according to the manufacturer's instructions. Supernatant containing 40µg of protein was stored at -

20°C or denatured in boiling 2x Laemmli buffer for five minutes at 95°C prior to electrophoresis using a polyacrylamide-SDS gel.

### **2.10.2 Protein Pulldown assay**

To perform protein pull down assay,  $5 \times 10^6$  of Jurkat cells were washed in 1x PBS, then lysed in 1ml of lysis buffer (50mM Tris pH 7.5, 150mM NaCl, 0.1% NP-40, 1 mM PMSF) and broken by sonication for 10 seconds. Lysates were then centrifuged at 14,000rpm at 4°C for 10 minutes, and the supernatant was transferred to a fresh tube containing 20µl of 7-methyl GTP-sepharose beads (GE Healthcare UK) or glutathione sepharose 4B beads (GE Healthcare UK) as a negative control. The samples were incubated for two hours at 4°C with end-over-end rotation. The beads were centrifuged at 600 rpm at 4°C for three minutes and washed three times with lysis buffer (50mM Tris pH 7.5, 150mM NaCl, 0.1% NP-40). The beads were then pelleted before being re-suspended in 20µl of 1x SDS loading buffer to denature the protein by heating for five minutes at 95°C before loading onto an SDS-PAGE gel.

### **2.10.3 Co-Immunoprecipitation (Co-IP)**

This technique was used to analyse the interactions between purified proteins. According to the manufacturer's instructions; 300 µg of Dynabeads Protein G (Lot# 126811600, Novex, Life Technologies) were added to the tube and washed with 0.02% Tween-20 in 1x PBS (PBST). Except for the negative control, the beads were mixed with 200 µl of antibody diluted appropriately (see appendix) in 1x PBST and incubated for 10 minutes at room temperature with end-over-end rotation. The tubes were placed in a magnetic Eppendorf holder to pull the beads out of the solution,

allowing for the supernatant to be discarded, and then washed with 1x PBST. The protein lysates were added to the mixture of antibody bound to the beads and incubated for 30 minutes at room temperature with end-over-end rotation. The supernatant was discarded, the beads were washed three times with 1x PBST and the mixture was transferred to a fresh tube. Then, 20 $\mu$ l of 1x SDS loading buffer was added to denature the protein by boiling for five min at 95°C before loading onto an SDS-PAGE gel.

### **2.10.4 Sodium Dodecyl Sulphate Polyacrylamide Gel Electrophoresis (SDS-PAGE)**

Protein samples were resolved on an 8 or 10% polyacrylamide gel using the Mini-PROTEAN® Tetra system (Bio-Rad). TEMED was directly added to the resolving gel buffer before the gel was poured between the 1.5 mm glass plates, according to manufacturer's instructions. Water-saturated butanol was added to the top of the gel to prevent air bubbles and ensure an even surface, creating an airtight seal for polymerisation. This gel was left for 30 minutes to set, and once set, the butanol was removed. A 5% stacking gel buffer with TEMED was poured on top, and 10-well combs were inserted between the glass plates and left to set for another 30 minutes. The plates were removed from the casting frame after the gel had fully polymerised, placed into the electrode assembly and the clamping frames were closed. The inner chamber assembly was placed in the Mini Tank, which was filled with 1x SDS-PAGE running buffer, and the combs were removed. Equal amounts of protein were loaded into each well, and 2 $\mu$ l of PageRuler™ Prestained Protein Ladder (lot# 00463186, Thermo Scientific) was loaded into the first well. Electrophoresis was run at 35 mA

for one gel or 70 mA for two gels for one hour or until the appropriate separation had been achieved.

### **2.10.5 Western blot**

The proteins were transferred to an 8 cm x 6 cm polyvinylidene fluoride (PVDF) membrane (Cat#10600023, GE Healthcare) by semi-dry transfer (BIO-RAD). Prior to transfer, the PVDF membranes were incubated in 100% methanol for 10 seconds before being washed for 10 minutes with distilled water and then five minutes with transfer buffer, all with agitation. A Whatman sponge soaked in the transfer buffer was placed onto the machine followed by the PVDF membrane, the SDS-page gel and another Whatman sponge. The excess buffer and air bubbles were removed by pressing on the sponges, and the protein was transferred at 15 V for one hour. The membrane was blocked for one hour with 5% marvel in 1x PBST at room temperature with agitation. The membrane was incubated with primary antibody at an appropriate dilution (see appendix) in 3% marvel in PBST for one hour at room temperature or overnight at 4°C. It was then washed in 1x PBST three times for five minutes each with agitation before being incubated with a horseradish peroxidase (HRP)-conjugated secondary antibody (see appendix) diluted in 3% marvel in PBST for 45 minutes or one hour at room temperature with agitation. The washing step was then repeated before the membrane was placed on saran wrap and incubated with a 1:1 mixture of the SuperSignal West Pico Chemiluminescent Substrate for HRP (lot#OA183286, Thermo Scientific) solution for two minutes. The developer was removed and the membrane was wrapped in saran wrap and placed in an autoradiography cassette. In the dark, the membrane was exposed to X-ray film for

two minutes to 10 minutes, depending upon the signal strength. Finally, the membrane was developed until the band appeared, then was fixed until the background cleared before rinsing it in water and leaving it to dry.

### **2.10.6 Re-Probing of PVDF Membranes**

PVDF membranes were washed with 1x PBST and re-activated using methanol for 10 seconds. The membrane was then washed with distilled water then 1x PBST twice for 10 minutes each. The western blotting procedure was then performed as described above.

## **2.11 Imaging Methods:**

### **2.11.1 Confocal Microscopy**

The images were taken using a Zeiss LSM710 Confocal Microscope with a 63x oil-immersion objective. The channels used were UV, 488 and 561 nm lasers. The pinhole diameter was corrected to 1 Airy unit.

### **2.11.2 Image Analysis.**

The images were analysed using ImageJ 1.48v image analysis software.

### **2.11.3 Flow Cytometry Analysis**

Flow cytometry was carried out using an FC500 flow cytometer (BECKMAN Coulter) for green fluorescent protein (GFP) or AlexaFluor 488. Data was analysed using Weasel Analysis Software.

#### **2.11.4 Statistical Analysis**

ImageJ 1.48v software was used to measure band intensities and GraphPad Prism version 7 was employed for analysing the data. An ordinary one-way ANOVA was used to compare multiple samples to the control to determine statistically significant differences.

## **Chapter 3: Results**

### **3.1 Deletion of the coiled coil domain results in spontaneous colocalisation of DEF6 N-terminal mutants with P-body marker DCP1**

Hey *et al.* (2012) showed that DEF6 is phosphorylated by ITK at tyrosine residues Y210 and Y222 and that phosphomimic mutant DEF6 (Y210E/Y222E) formed spontaneously cytoplasmic granules that colocalised with mRNA decapping enzyme subunit 1 (DCP1) a marker of P-bodies. In addition, Sodium Arsenate treatment of COS7 cells transfected with GFP-tagged wild type DEF6 also resulted in accumulation of DEF6 in cytoplasmic granules overlapping with DCP1. Initially it was suggested that formation of DEF6 granules was mediated via the coiled coil domain but it was subsequently shown that the first 108 amino acids of DEF6 are sufficient for spontaneous colocalisation of the N-terminal mutant protein with DCP1 (Mollett, PhD 2014). Furthermore, fellow PhD student Huaitao Cheng established that the first 45 amino acids of DEF6 containing two Ca<sup>2+</sup>- binding EF hand motifs are sufficient for spontaneously colocalisation (Cheng, PhD 2017). To extend this analysis, GFP-tagged N-terminal DEF6 mutants N216 (lacking PH and coiled coil domain) and N312 (lacking just the coiled coil domain; Fig.3.1) were created and expressed in COS7 cells together with mCherry-tagged DCP1 (Fig. 3.1.1). ~70% of the transfected cells exhibited colocalisation of N-terminal mutant proteins with DCP1 (Fig.3.1.1 A & C) indicating that it is the coiled coil domain that constrains wild type DEF6 from spontaneous formation of granules and colocalisation with P-bodies and that phosphorylation of DEF6 at Y210 and Y222 releases this constrain presumably through conformational change. To see whether phosphomimic mutations in the context of the N-terminal DEF6 protein

had any effect, N216E (Y210E) and N312EE (Y210E, Y222E) were established and cotransfected with DCP1 in COS7 cells (Fig. 3.1.1 B & D). ~ 50% of the transfected cells exhibited colocalisation of phosphomimic N-terminal DEF6 mutants with DCP1. Taken together these data establish that phosphorylation of tyrosine residues Y210 and Y222 per se is not required for P-body colocalisation but in the context of the wild type DEF6 protein results in conformational change releasing the N-terminal end from the coiled coil-mediated constrain.

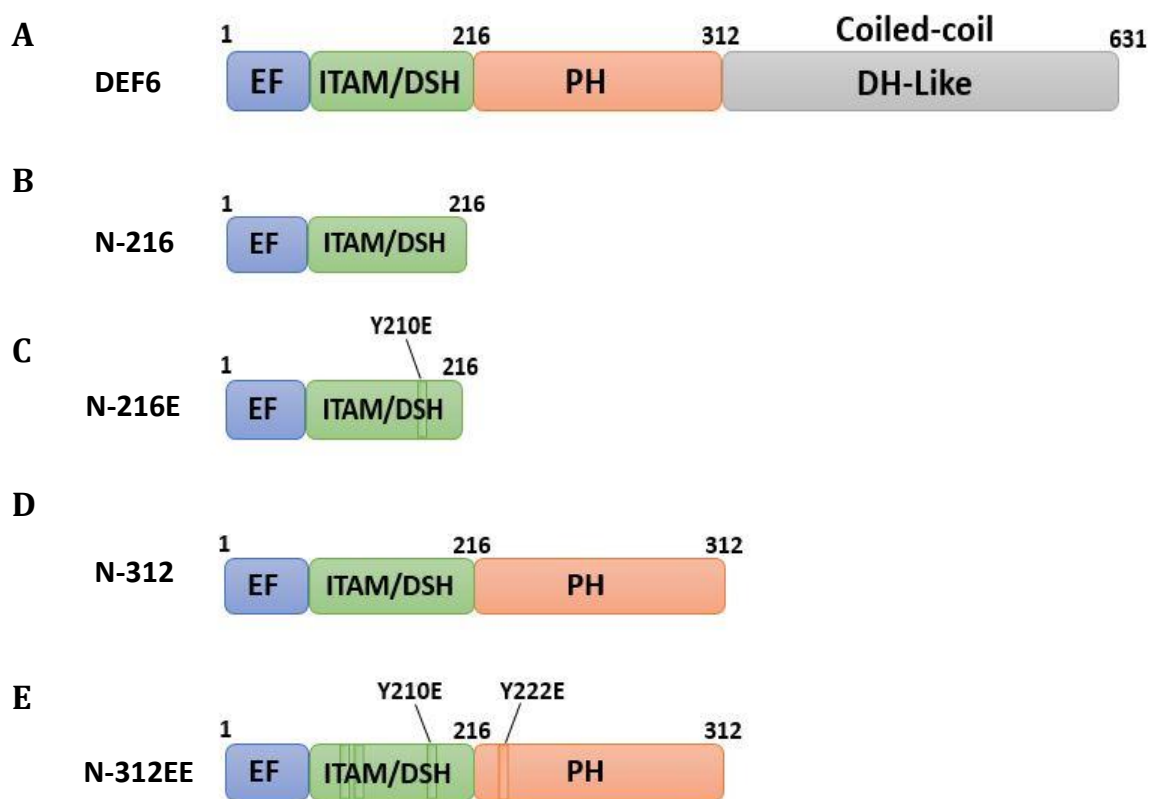


**Figure 3.1: Schematic representation of DEF6 domain structure and GFP-tagged truncation mutants and their phosphomimic derivatives**

**A)** Wild-type full length DEF6 domain structure as shown in figure 1.1.2. The N-terminal EF-hand that binds  $\text{Ca}^{2+}$  is followed by the Immunoreceptor. Tyrosine-based Activation Motif (ITAM: also known as the DEF6/Swap-70 domain (DSH)). The central Pleckstrin Homology domain (PH) binds phosphatidylinositol (3,4,5)-triphosphate (PIP3) and the C-terminal Dbl Homology-like domain (DHL) contains a coiled-coil domain and facilitated nucleotide exchange (GEF) activity. Truncation mutants N-216 (B), N216E (C), N312 (D) and N312EE (E) either lack PH and DH-like domains or just lack the DH-like domain as indicated. Tyrosine residues

positions 210 and 222 were exchanged by Glutamic acid residues (Y210E, Y222E).

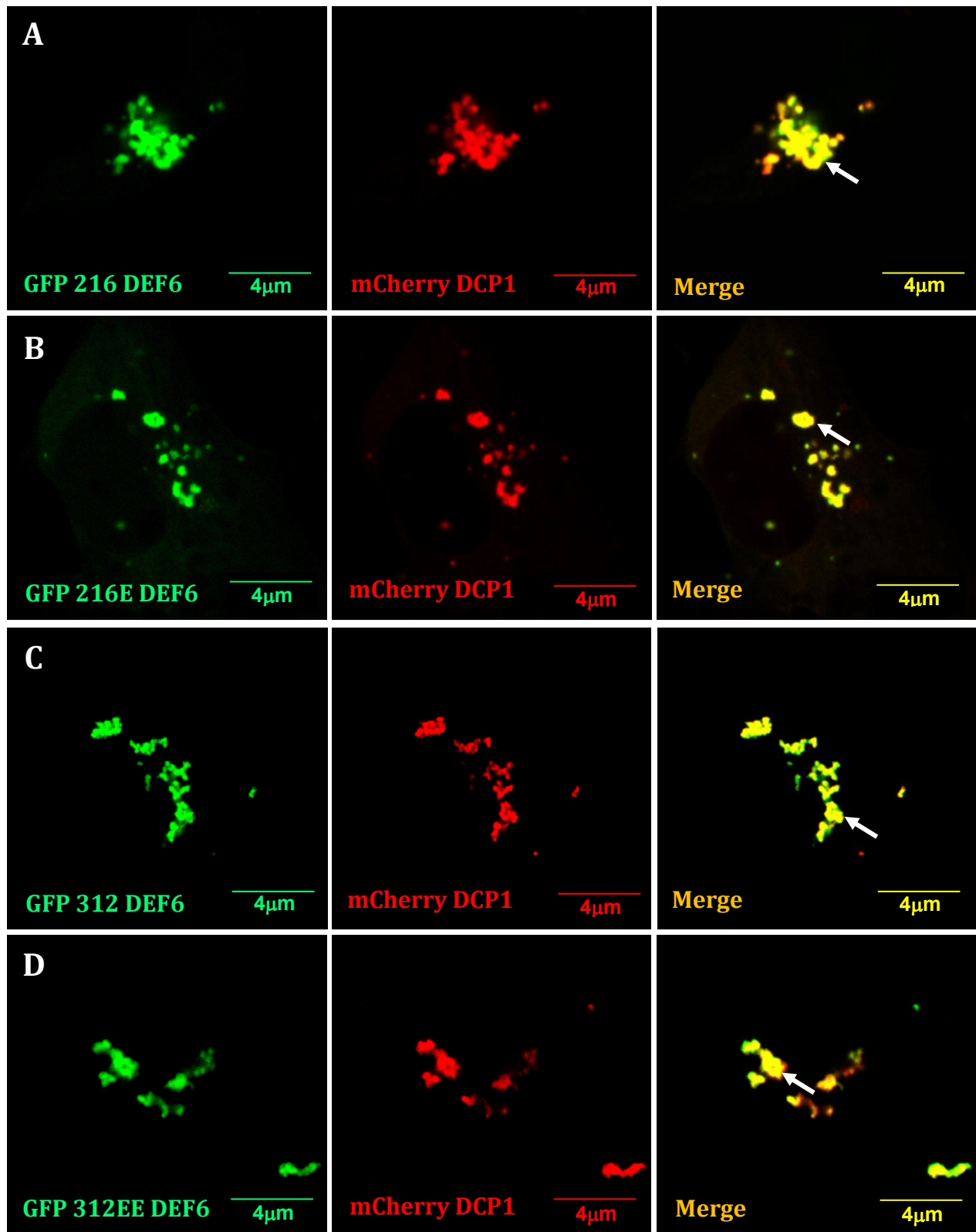


**Figure 3.1.1: Coiled coil domain restrains DEF6 from spontaneous colocalisation with P-bodies**

GFP-tagged N-terminal DEF6 mutants N216 (A) and N312 (C) as well as the corresponding phosphomimetic mutants N216E (B) and N312EE (D) (left column) spontaneously colocalise with mCherry-tagged DCP1 in COS7 cells (middle column) as indicated by white arrows in the merged images (right column). Images were taken

using a Zeiss LSM710 Confocal Microscopy; a single z plane at 63x magnification 2x zoom. Experiments were performed three independent times and scale bars: 4 $\mu$ m

### 3.2 Serine and/or Threonine phosphorylation in the C-terminal end of DEF6 results in aggregates that trap DCP1

DEF6 is phosphorylated by the tyrosine kinases ITK and LCK resulting in conformational change and either granule formation that colocalise with P-bodies (ITK; Hey et al., 2012) or aggregation forming large structure that trap DCP1 (LCK; Cheng, PhD 2017). In addition, it was shown that DEF6 is also phosphorylated by serine/threonine kinases especially at serine (S) and threonine (T) residues in its C-terminal end.

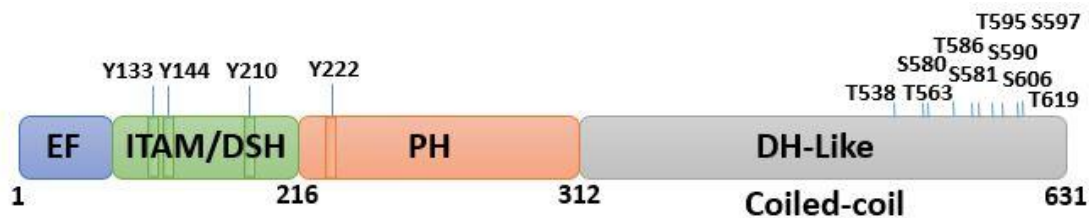


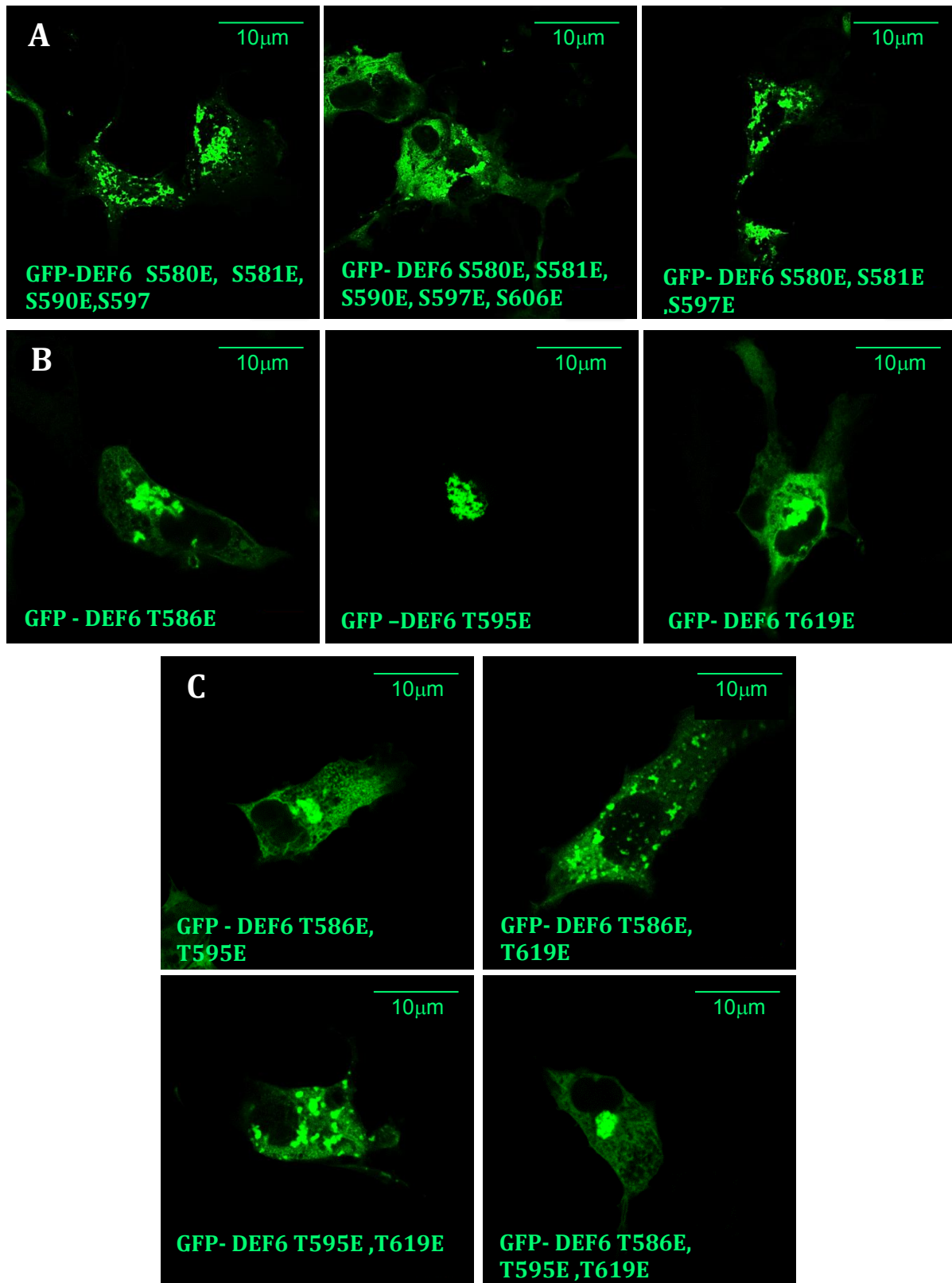
**Figure 3.2: Known phosphorylation sites in the DEF6 protein**

Domain structure of DEF6 as shown in figure 3.1 A and amino acid positions of Tyrosine (Y), Threonine (T) and Serine (S) residues that have been shown to be phosphorylated in vivo.

To test whether S/T phosphorylation at some of these amino acid residues alter structure and function of DEF6, site-directed mutagenesis was performed and S and/or T residues exchanged with either glutamic acid (E) to mimic phosphorylation, or phenylalanine (F) to prevent phosphorylation (See appendix table 4). Residues chosen were: T538, T563, S580, S581, T586, S590, T595, S597, S606 and T619 that had been shown to be phosphorylated in human and/or mice through multiple proteomics analyses (Cell Signalling Technology, Human PhosphoSitePlus@<https://www.phosphosite.org/proteinAction.action?id=21147&showAllSites=true>)

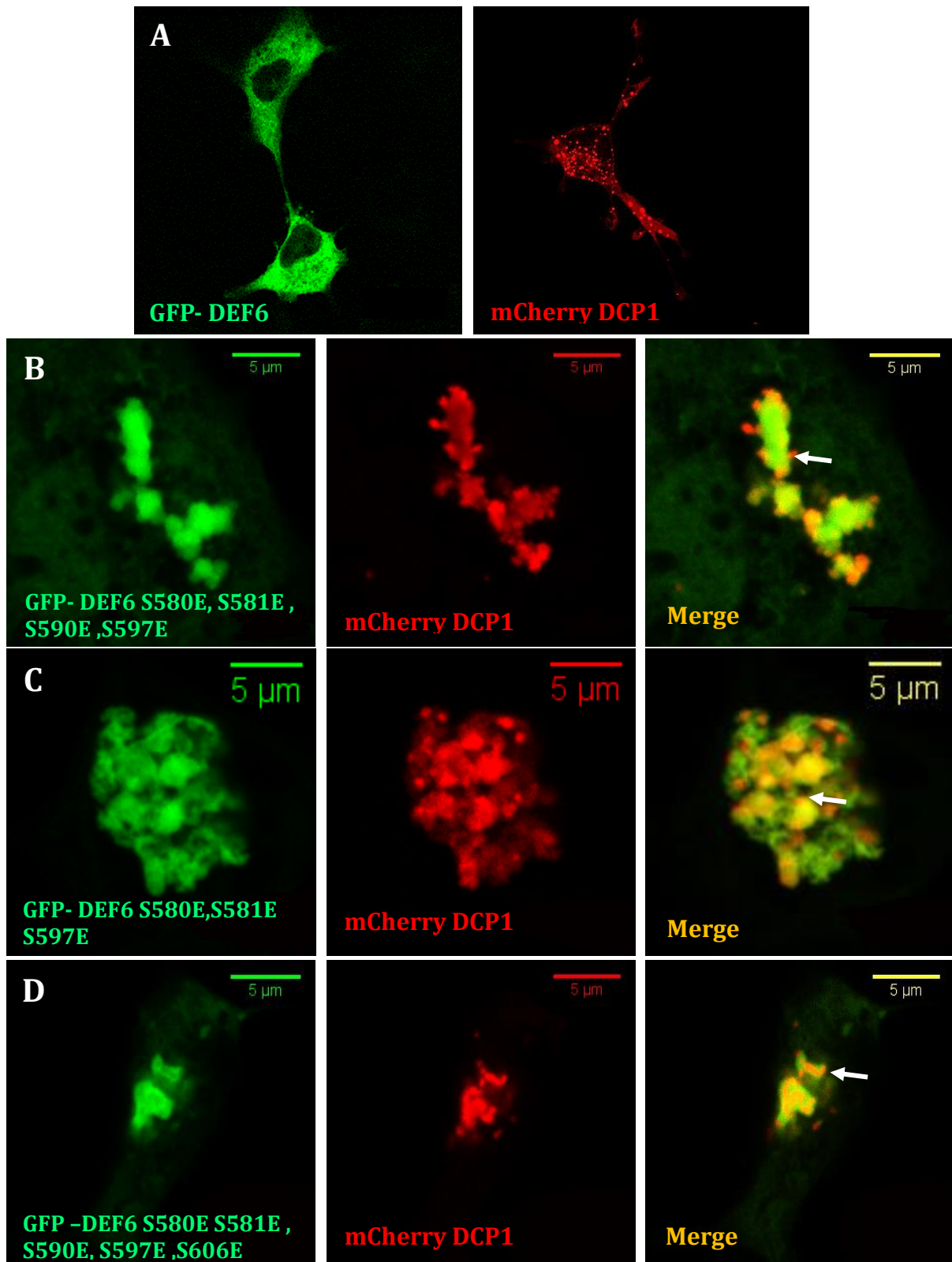
GFP-tagged single or compound S/T mutants were transfected into COS7 cells to determine cellular localisation using confocal microscopy. Remarkably, all S/T mutant DEF6 proteins tested exhibited a cellular localisation that was distinct from the wild type protein which localises diffuse in the cytoplasm (Fig. 3.2.2 A). As summarised in Table 3 and shown in Figures 3.2.2;3.2.3, most phosphomimic mutants formed aggregates in the cytoplasm regardless whether only one T residue was changed (e.g. T586E, T595E; Fig3.2.1 B) or several S/T residues were changed (e.g. T586E, T619E; S580E, S581E, S590E, S597E, S606E; Figures 3.2.1 A and C). Cotransfection COS7 cells with mCherry-tagged DCP1 revealed that 40% of transfected cells with mutant DEF6 proteins that formed aggregates trapped DCP1 (e.g. S580E, S581E, S597E; S580E, S581E, S590E, S597E; S580E, S581E, S590E, S597E, S606E; Figures 3.2.2 and T586E; Figures 3.2.3). Mutant proteins that were diffuse with some granules formation on the other hand did not trap DCP1 but exhibited some association/overlap with it (T586E, T619E; Fig.3.2.3 I) or no overlap at all (T586E, T595E; Fig.3.2-3 H). ~ 29% of transfected cells with mutants that had S or T residues replaced by F showed less aggregation than the phosphomimic mutants and were mostly diffuse with some granule formation (Fig.3.2.4). These mutant proteins exhibited some overlap with DCP1 without trapping it (Fig. 3.2.5; 3.2.6).

Taking together, phosphorylation of serine and/or threonine residues in the C-terminal end results in conformational change and formation of cytoplasmic aggregates that trap DCP1. This is reminiscent of data by Cheng (PhD 2017) who showed that formation of large cytoplasmic aggregates is mediated via the coiled coil domain. One possible explanation could be that S/T phosphorylation in the C-terminal end of DEF6 releases the coiled coil domain that facilitates aggregation.



**Figure 3.2.1: Localisation of DEF6 Threonine or Serine to Glutamic acid mutants**

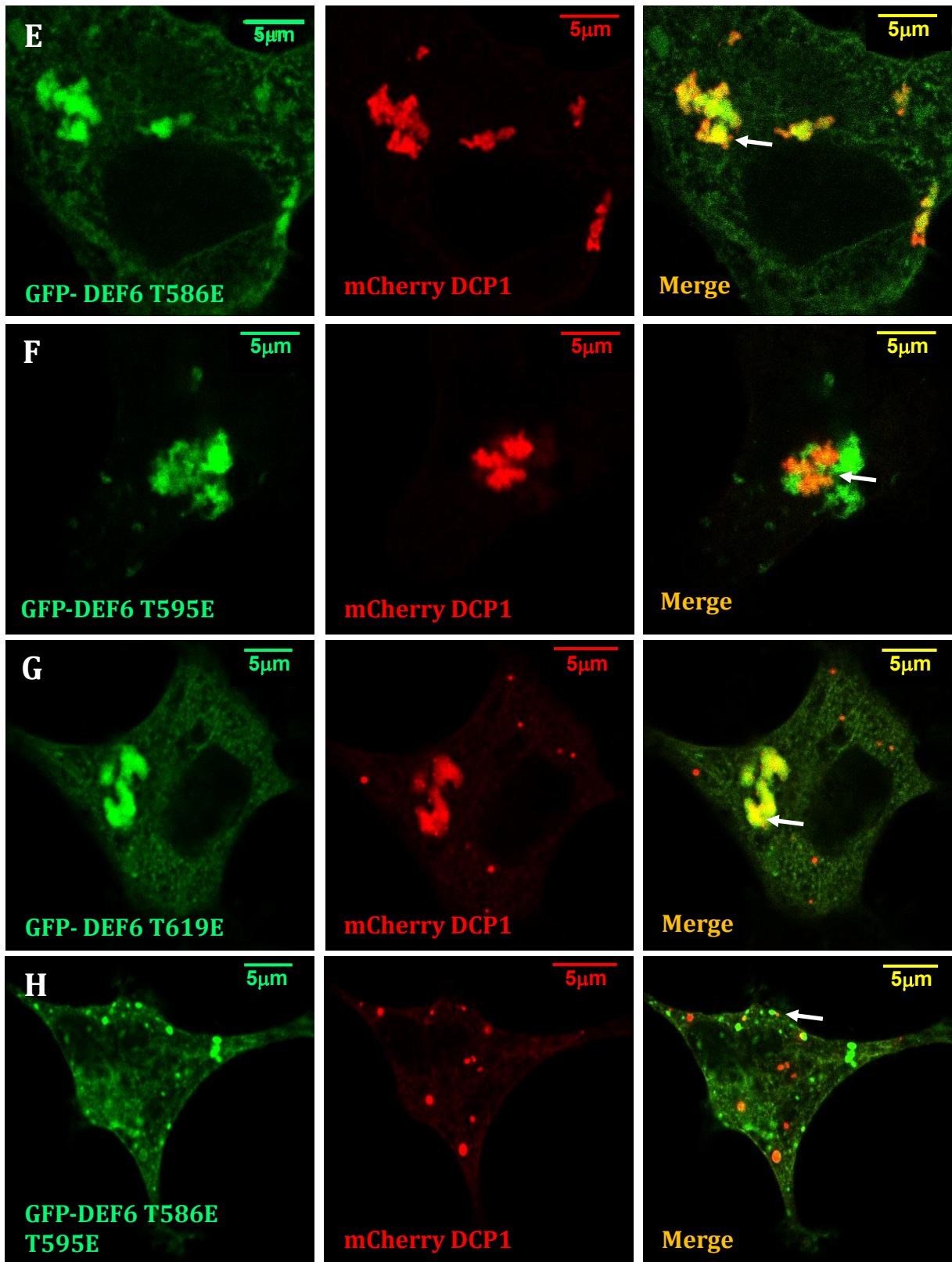
Transfected COS7 cells for 24h with (A) Combined Serine (S) to Glutamic acid (E) mutants as shown in the labels (B) single Threonine (T) to Glutamic acid (E) mutants as labelled-GFP-DEF6-T586E, GFP-DEF6 T595E and GFP-DEF6-T619E.(C) Combined Threonine (T) to Glutamic acid (E) mutants as labelled. Scale bare as shown in the figures. n = 3 replicates

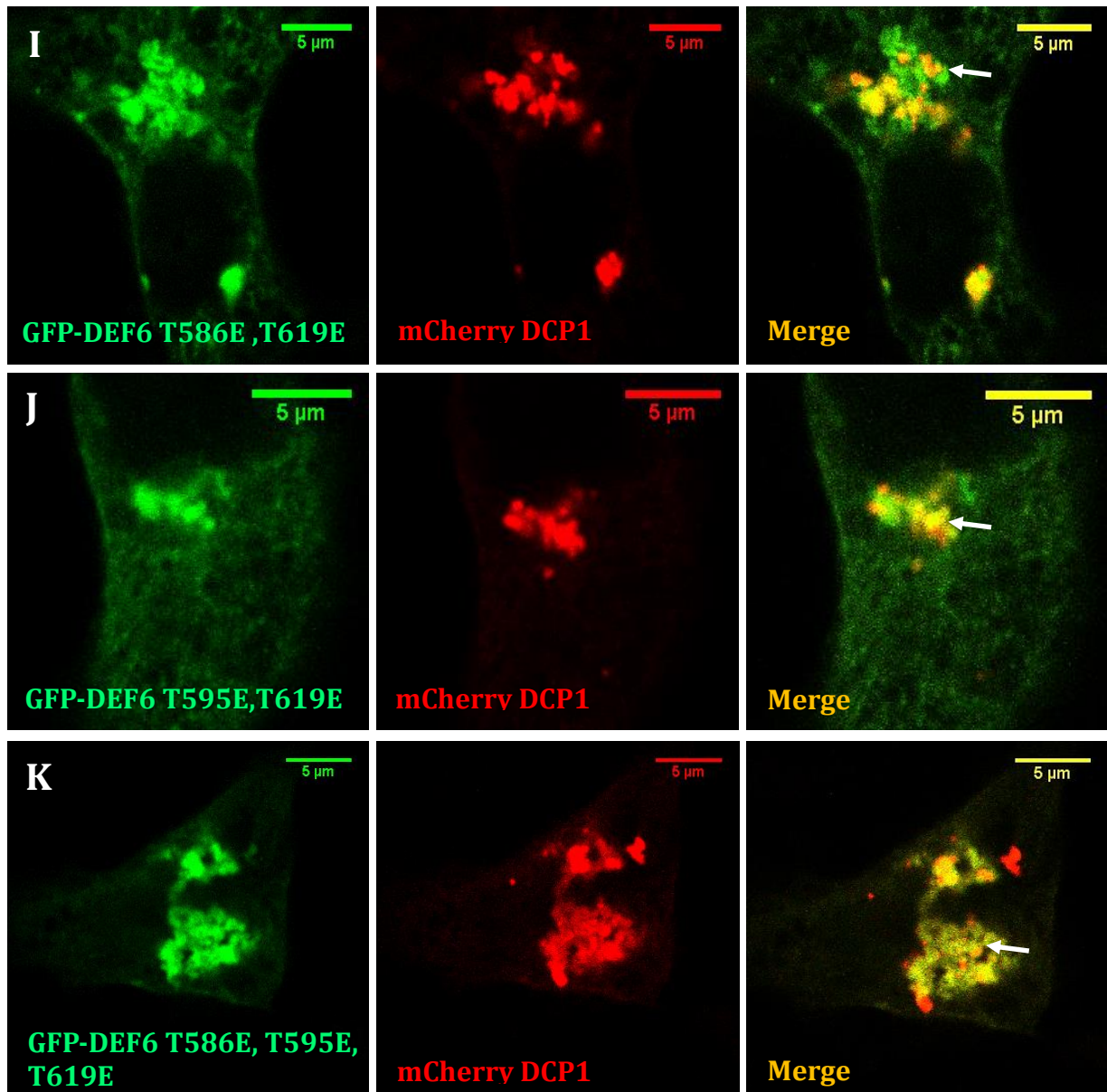


**Figure 3.2.2: Cotransfection of GFP-tagged DEF6 Serine to Glutamic acid GFP tagged mutants with P-body marker (DCP1)**

Co-transfected COS7 cells with GFP-DEF6 Serine mutant and mCherry- tagged DCP1 for 24h. **(A)** Wild type GFP- tagged DEF6 and Wild type mCherry DCP1. **(B)** GFP-tagged S580E, S581E, S590E and S597E DEF6. **(C)** GFP-tagged S580E, S581E and S597E-DEF6. **(D)** GFP tagged S580E, S581E, S590E, S597E and S606E DEF6. White arrows indicate aggregates trapped DCP1 (merge images).

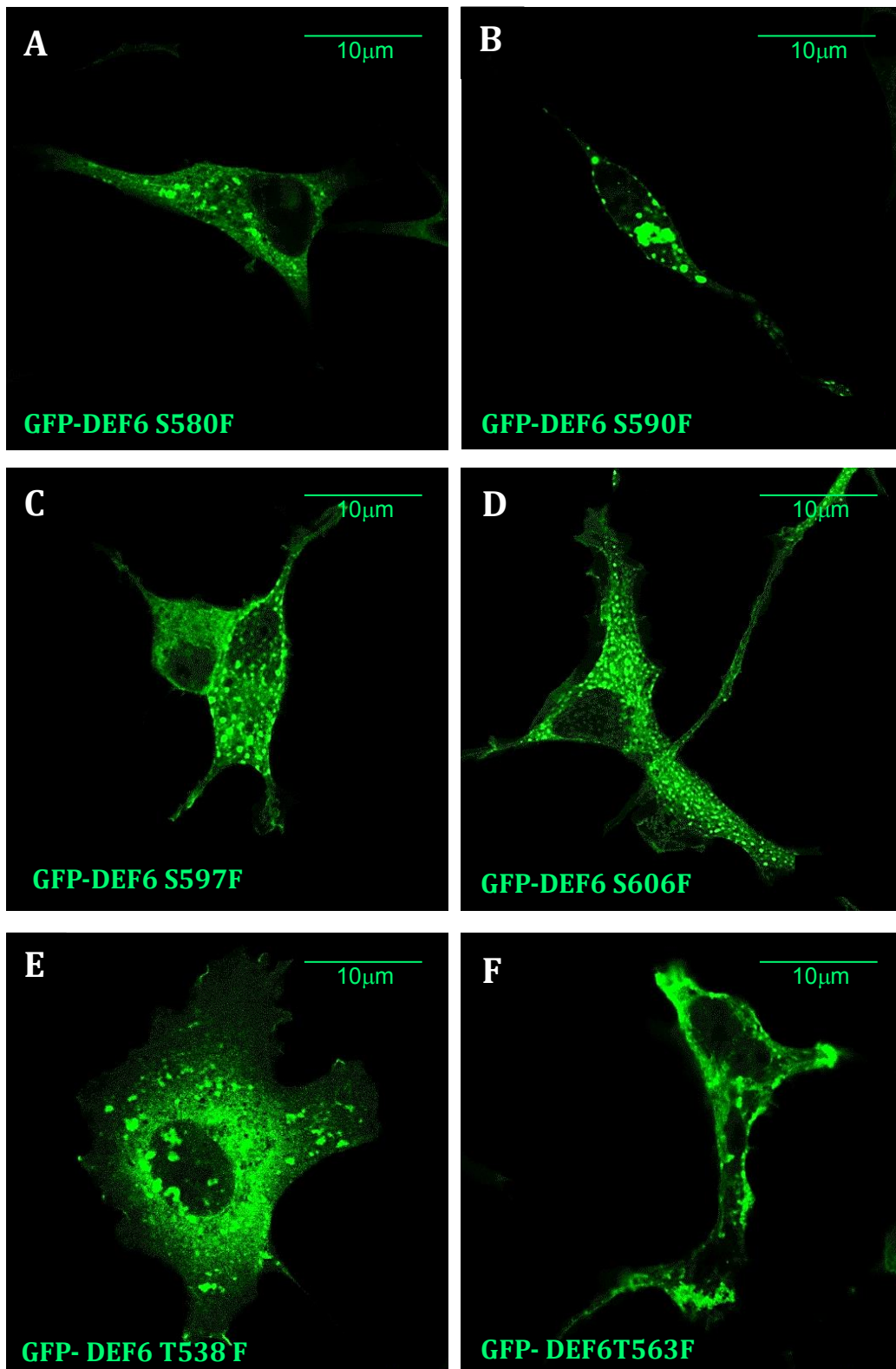
Images were taken using a Zeiss LSM710 confocal microscope at a 63x magnification and 2x zoom. n = 3 replicates. Scale bars: 5 $\mu$ m





**Figure 3.2.3: Cotransfected DEF6 Threonine to Glutamic acid GFP-tagged mutants either occurring singly or in combination with P-body marker (DCP1)**

Cotransfected COS7 cells with GFP-DEF6 Threonine mutation with mCherry DCP1 for 24h. (E) GFP-tagged T586E DEF6. (F) GFP-tagged T595E DEF6. (G) GFP-tagged T619E DEF6. (H) GFP-tagged T586E & T595E DEF6. (I) GFP-tagged T586E & T619E DEF6. (J) GFP-tagged T595E&T619E DEF6. (K) GFP-tagged T586E, T595E & T619E DEF6. White arrow indicates aggregates trapped/overlap with DCP1. Images were taken using a Zeiss LSM710 confocal microscope at a 63x magnification and 2x zoom. n = 3 replicates. Scale bars: 5μm



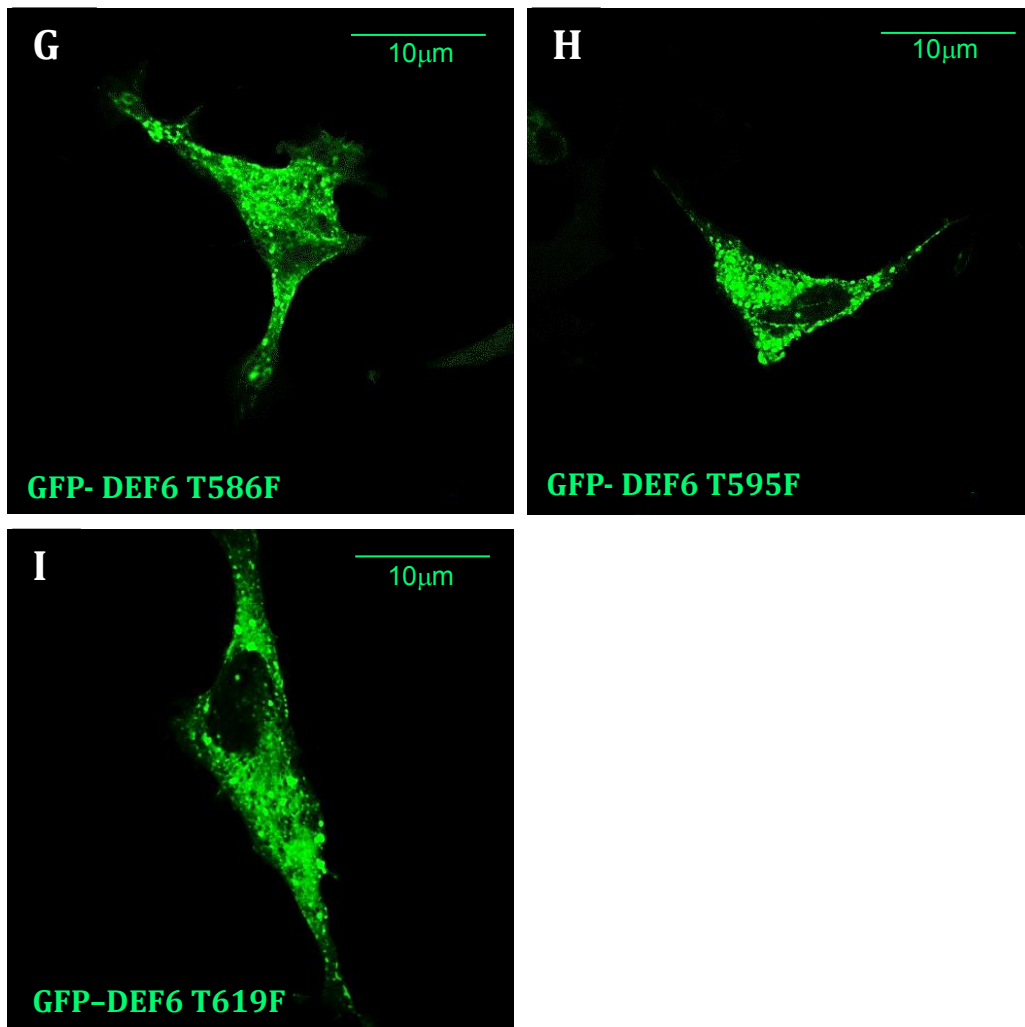


**Figure 3.2.4: Localisation of DEF6 Serine or Threonine to Phenylalanine Mutants**

Transfected COS7 cells for 24h expressing cytoplasmic foci (A) GFP-tagged S580F mutant of DEF6 (B) GFP-tagged S590F mutant of DEF6 (C) GFP-tagged S597F mutant of DEF6 and (D) GFP-tagged S606F mutant of DEF6. (E) GFP-tagged T538F mutant of DEF6 (F) GFP-tagged T563F mutant of DEF6 (G) GFP-tagged T586F mutant of DEF6 (H) GFP-tagged T595F mutant of DEF6 and (I) GFP-tagged T619F DEF6. Images were taken using a Zeiss LSM710 confocal microscope at a 63x magnification. n = 3 replicates. Scale bars: 10µm

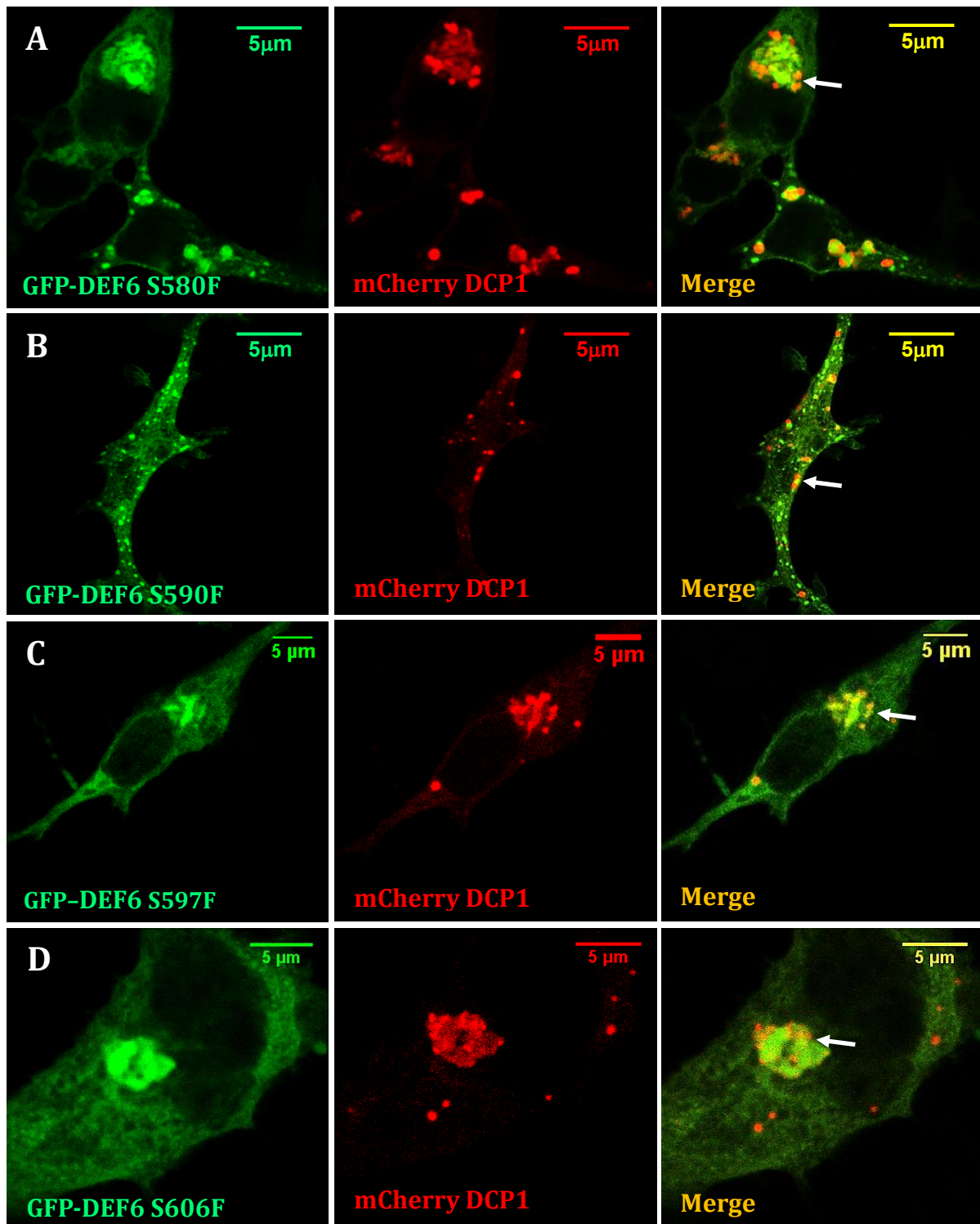


**Figure 3.2.5: Cotransfected of DEF6 Serine mutants to Phenylalanine with P-body marker (DCP1)**

Cotransfected COS7 cells with GFP-DEF6 Serine mutation with mCherry DCP1 for 24h (A) GFP-tagged S580F DEF6. (B) GFP-tagged S590F DEF6. (C) GFP-tagged S597F DEF6. (D) GFP-tagged S606F DEF6. White arrow indicates aggregates trapped DCP1(merge image). Images were taken using a Zeiss LSM710 confocal microscope at a 63x magnification and 2x zoom. n = 3 replicates and scale bars: 5μm

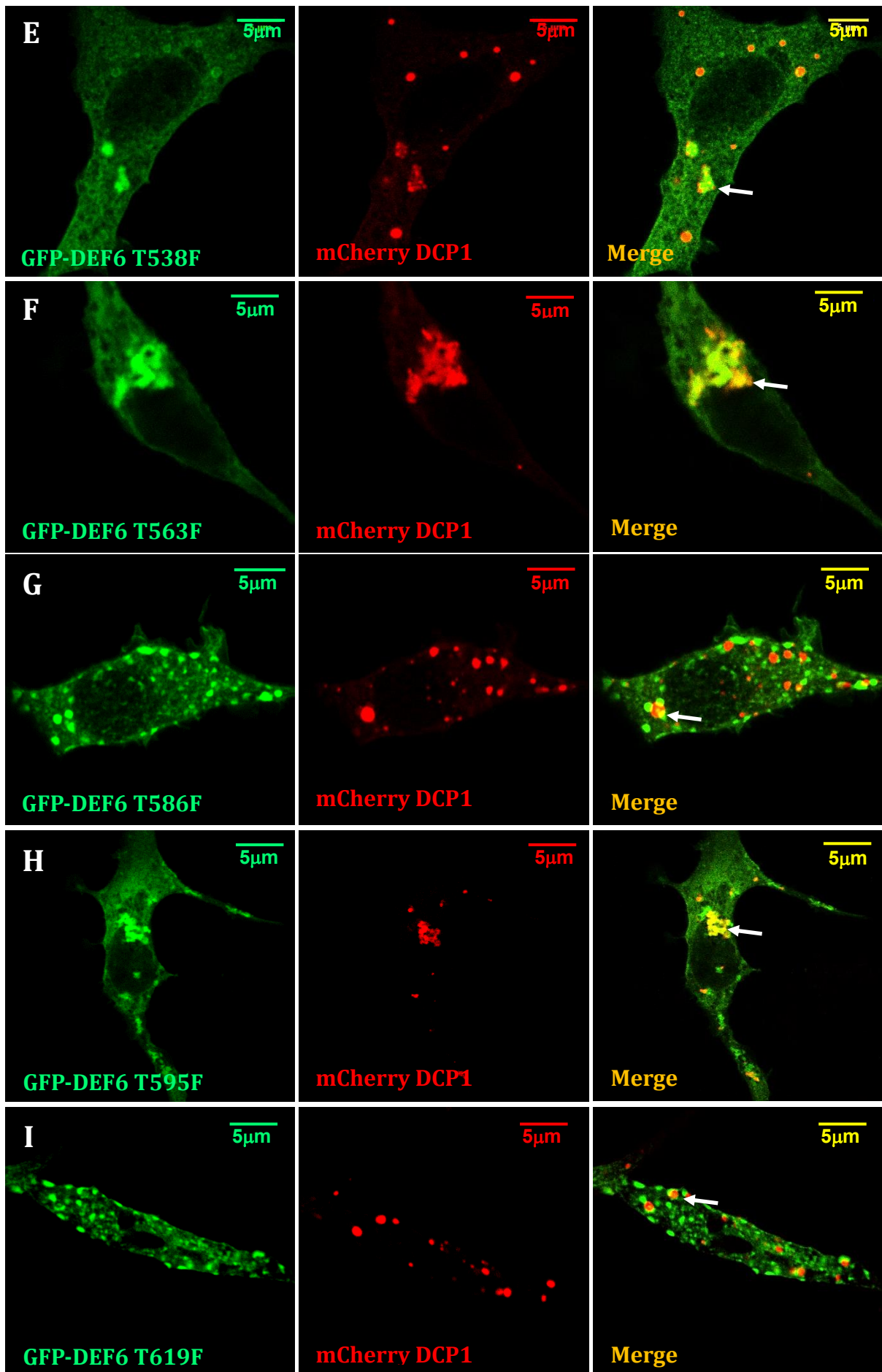


**Figure 3.2.6: Cotransfected of DEF6 Threonine mutants to Phenylalanine with P-body marker (DCP1)**

Cotransfected COS7 cells with GFP-DEF6 Serine mutation with mCherry DCP1 for 24h. (E) GFP-tagged T538F DEF6. (F) GFP-tagged T563F DEF6. (G) GFP tagged T586F DEF6. (H) GFP-tagged T595F DEF6. (I) GFP-tagged T619F DEF6. White arrow indicates aggregates trapped/overlap with DCP1 (merge image). Experiments were performed three independent times. Images were taken using a Zeiss LSM710 confocal microscope at a 63x magnification and 2x zoom and scale bars: 5 $\mu$ m

Serine/Threonine mutant DEF6	Diffuse (D), Granules (G), Aggregates (A)	Association with DCP1	Figure
S580E, S581E, S590E, S597E	A	Trapped	3.2.2 B
S580E, S581E, S597E	A	Trapped	3.2.2 C
S580E, S581E, S590E, S597E, S606E	A	Trapped	3.2.2 D
T586E	A	Trapped	3.2.3 E
T595E	A	Trapped	3.2.3 F
T619E	D/G	Some Trapped	3.2.3 G
T586E, T595E	D/G	No overlap	3.2.3 H
T586E, T619E	A	Trapped	3.2.3 I
T595E, T619E	A	Some Overlap	3.2.3 J
T586E, T595E, T619E	D/A	Trapped	3.2.3 K
S580F	D/G/A	Trapped	3.2.5 A
S590F	D/G	Trapped	3.2.5 B
S597F	D/G	Trapped	3.2.5 C
S606F	D/G/A	Trapped	3.2.5 D
T538F	D/G	Some Trapped	3.2.6 E
T563F	A	Trapped	3.2.6 F
T586F	D/G	Some overlap	3.2.6 G
T595F	D/G	Overlap	3.2.6 H
T619F	D/G	Some Trapped	3.2.6 I

**Table 3: Summary of behaviour and localisation of Serine/Threonine mutant DEF6 proteins ectopically expressed in COS7 cells.** Mutant DEF6 proteins were coexpressed with mCherry-tagged DCP1 as shown in the figures above and behaviour and cellular localisation of the mutant proteins were

analysed. Phosphomimic DEF6 mutants, replacing Serine/Threonine residues with Glutamic acid (E), formed large aggregates that trapped DCP1 but did not overlapped with it (see figure 3.2.2.B for example). In contrast, mutant DEF6 proteins with phenylalanine (F) replacing Serine/Threonine residues exhibited diffuse localisation with some granules formation that trapped or partially overlapped with DCP1 (for example merged image in figure 3.2.6.G).

### **3.3 Endogenous DEF6 is highly expressed in Jurkat T cells but absent in other cell lines**

Endogenous DEF6 expression was investigated in the following cell lines: Jurkat T, Raji B, COS7, HEK293 and HeLa cells. Protein lysates from these cells were prepared and analysed by western blotting using a rabbit monoclonal antibody specific for human DEF6 (Method 2.10.1). As shown in Figure 3.3 A, DEF6 protein was readily detectable in Jurkat T cells with a protein size of approximately 74 kDa as predicted (Gupta *et al.*, 2003). Raji B cells appeared to express some DEF6, but the loading control using antibodies recognising  $\beta$ -actin (Method 2.10.5) indicated that much more lysate was loaded compared to Jurkat T cells. DEF6 protein was undetectable in COS7, HEK293 and HeLa cells (Fig. 3.3 A). Even though the DEF6 antibody used here is specific for human DEF6, lack of DEF6 in COS7 cells was confirmed using a cross-reactive poly clonal rabbit anti DEF6 anti sera (Hey *et al.*, 2012).

To test efficiency of transfection with GFP-tagged DEF6 vector, protein lysates from Jurkat and COS7 cells were prepared 24 hrs after transfection and analysed by western blotting as above (Fig. 3.3. B and C). Other than the replaced codons to create the mutant proteins, the plasmid vector and DEF6 cDNA was identical in all experiments (see Appendix Fig 6.1). Exogenous GFP-DEF6 expression was readily detectable in both, Jurkat and COS7 cells with protein size of approximately 104 kDa, indicating that the transfection efficiency was high in both cases. It is worth mentioning that the endogenous expression of DEF6 seemed to be reduced in Jurkat cells over-expressing GFP-DEF6 (a repeatedly observed phenomenon) which might suggest that the total amount of DEF6 protein is limited and enforced

expression of GFP-DEF6 somehow results in reduction of endogenous DEF6 protein.

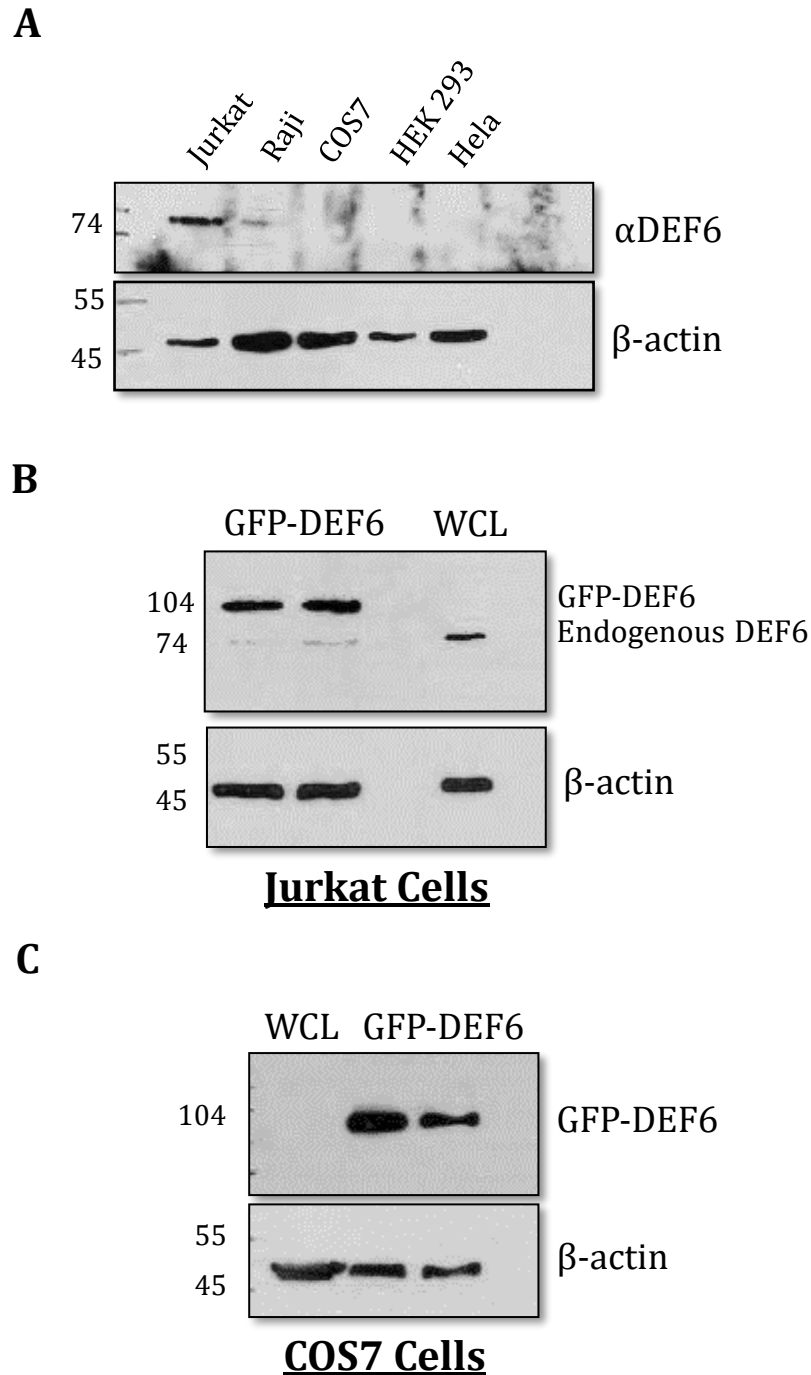


**Figure 3.3: Western blot analysis of DEF6 expression**

(A) Endogenous DEF6 is highly expressed in Jurkat T cells, barely detectable in Raji B cells and absent in COS 7, HEK 293 and HeLa cells. (B) Over-expression of GFP-tagged DEF6 in Jurkat cells. GFP-DEF6: 104 kDa; endogenous DEF6 74 kDa as indicated. (C) Over-expression of GFP-tagged DEF6 (104 kDa) in COS 7 cells. Whole Cell lysate (WCL) of untransfected Jurkat and COS 7 cells was analysed as control. The same western blots were re-probed with an anti  $\beta$ -actin antibody as loading control (lower panels in A-C). n=3 replicates.

### 3.4 DEF6 colocalises with sites of translational initiation

As shown in Fig. 1.3.3 DEF6 is associated with polysomes in resting Jurkat cells suggesting a role for DEF6 in protein translation. To test whether DEF6 might be involved in initiation of mRNA translation, fluorescently-tagged L-azidohomoalanine (AHA) was employed. AHA is an amino acid analogue of methionine containing an azide moiety that can be applied to cultured cells and is readily incorporated with newly synthesized proteins during active protein synthesis (Zhang *et al.*, 2017).

Jurkat cells were starved in methionine-free medium to synchronise translation. Subsequently the cells were either treated with 100mg/ml Cycloheximide (CHX) for 30 mins to inhibit mRNA translation or they were left untreated. AHA labelled with Alexa fluor 488 (green) was then added to both CHX treated and non-CHX treated cells and incubated for 30 mins. DEF6 antibody was added and was fluorescently tagged with Alexa fluor 568 (red) secondary antibody. As shown in Fig. 3.4, endogenous DEF6 and AHA clearly colocalised in non-CHX treated Jurkat cells. However, colocalisation was not complete suggesting that (i) DEF6 is associated with a subset of translational initiation complexes and (ii) not all DEF6 protein is engaged in translation initiation.

No clear overlap was observed in cells treated with CHX. Since translation is stalled in the CHX treated cells AHA fluorescence was much less intense and very diffuse as expected. In addition, CHX treatment might have affected cell morphology as a consequence of translation inhibition and indeed approximately 39% of the cells did not survive the treatment (data not shown).

Taken together, these results show that some DEF6 is associated with a subset of translation initiation complexes further suggesting a role for DEF6 in the control of mRNA translation

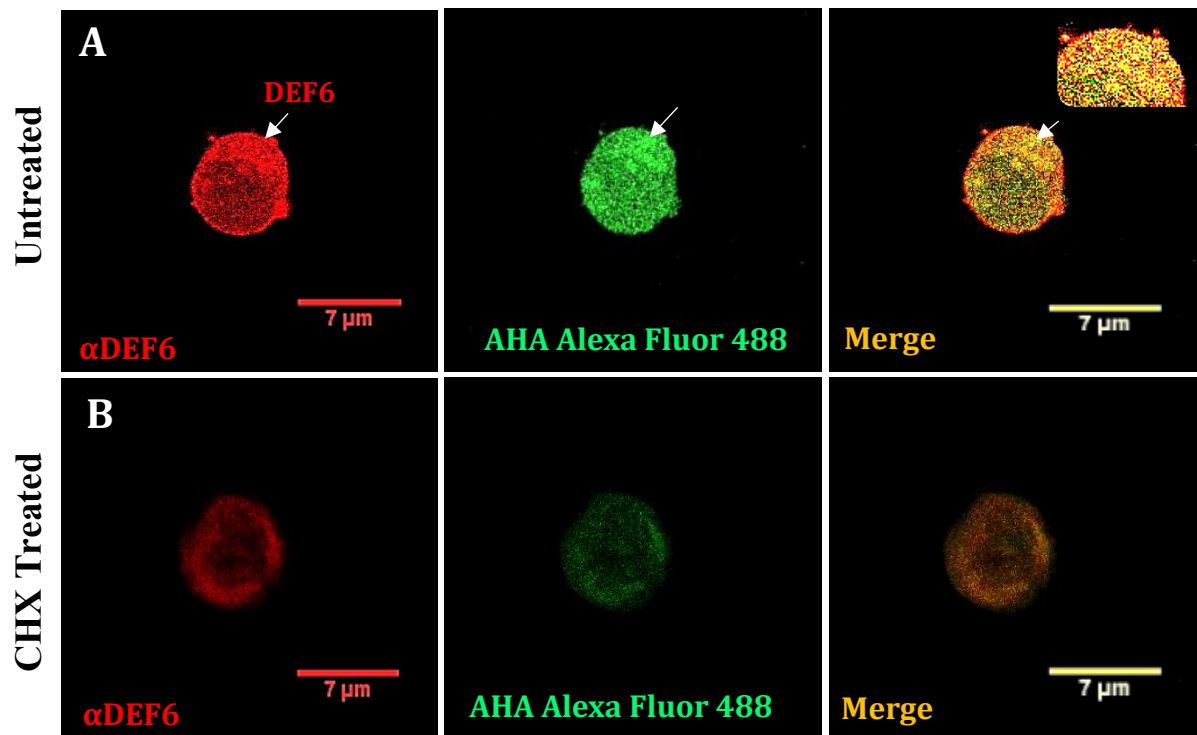


**Figure 3.4: DEF6 is associated with initiation of mRNA translation in resting Jurkat T cells**

Confocal microscopy illustrating localisation of endogenous DEF6 labelled with anti DEF6 antibody and Alexa fluor 568 secondary antibody (red) and AHA (L-azidohomoalanine) conjugated with Alexa fluor 488 (green) in Jurkat cells. **(A)**  $2 \times 10^6$  Cells/ml were either treated with AHA alone for 30min in full RPMI medium or **(B)** pre-treated with 100mg/ml Cycloheximide (CHX) for 30 min to block translation in the absence of methionine prior to AHA treatment. In non CHX treated cells, DEF6 and AHA clearly colocalised (yellow in the merged images on the right). However, colocalisation was not complete as green and red staining is still observable in the merged images. CHX treated cells exhibited much less AHA staining as expected and DEF6 staining was diffuse with no clear overlap of the two (merged image bottom row). Data are representative of four independent experiments. Images were taken using a Zeiss LSM710 confocal microscope at a 63x magnification and 2x zoom. Scale bar: 7  $\mu$ m



### 3.4.2 DEF6 colocalises with translational initiation factors eIF4E and 4E-transporter

eIF4E is a translational initiation factor that binds to the 5'-7'-methyl-guanosine cap where it recruits ribosomes to the cap (Kentsis *et al.* 2004). During mRNA decay, eIF4E is associated with P-bodies (Andrei *et al.*, 2005; Ferraiuolo *et al.*, 2005). Given that both eIF4E and DEF6 are associated with translational initiation and can colocalise with P-bodies, it was likely that these two proteins are in close proximity to each other and potentially interact with each other. In fact, a fellow PhD student Kerry Remon had demonstrated that the former is indeed the case. Using a proximity ligation assay (Sigma #DUO92101; Soderberg *et al.*, 2006), she established that both proteins are within 40 nm distance to each other (Remon, PhD 2016). Analysis using immunocytochemistry and confocal microscopy revealed that DEF6 and eIF4E indeed colocalised in resting Jurkat cells (Fig. 3.4.2 A-D). In line with the data shown above, colocalisation was not complete reemphasising that a fraction of DEF6 is engaged with eIF4E and that not all eIF4E is associated with DEF6. Interestingly, colocalisation of both proteins was observed in the cytoplasm surrounding the nucleus but neither in the periphery of the cells nor the nucleus.

The translation initiation factor 4E transporter (4E-T) is known to interact physically with eIF4E and plays a role in associating eIF4E with P-bodies (Kamenska *et al.*, 2014) and Remon had shown that 4E-T and DEF6 are in proximity in Jurkat cells (Remon, PhD 2016). Therefore, colocalisation of 4E-T and DEF6 was tested using immunocytochemistry and confocal microscopy as before. As shown in Fig. 3.4.2 D-G) both proteins also partially overlapped. However, the merged images

revealed, that colocalisation of DEF6 with 4E-T was much less frequent compared to colocalisation of DEF6 with eIF4E. It is not known whether DEF6 colocalises with both eIF4E and 4E-T but the data suggest that DEF6 might be able to interact with either eIF4E or 4E-T or both proteins.

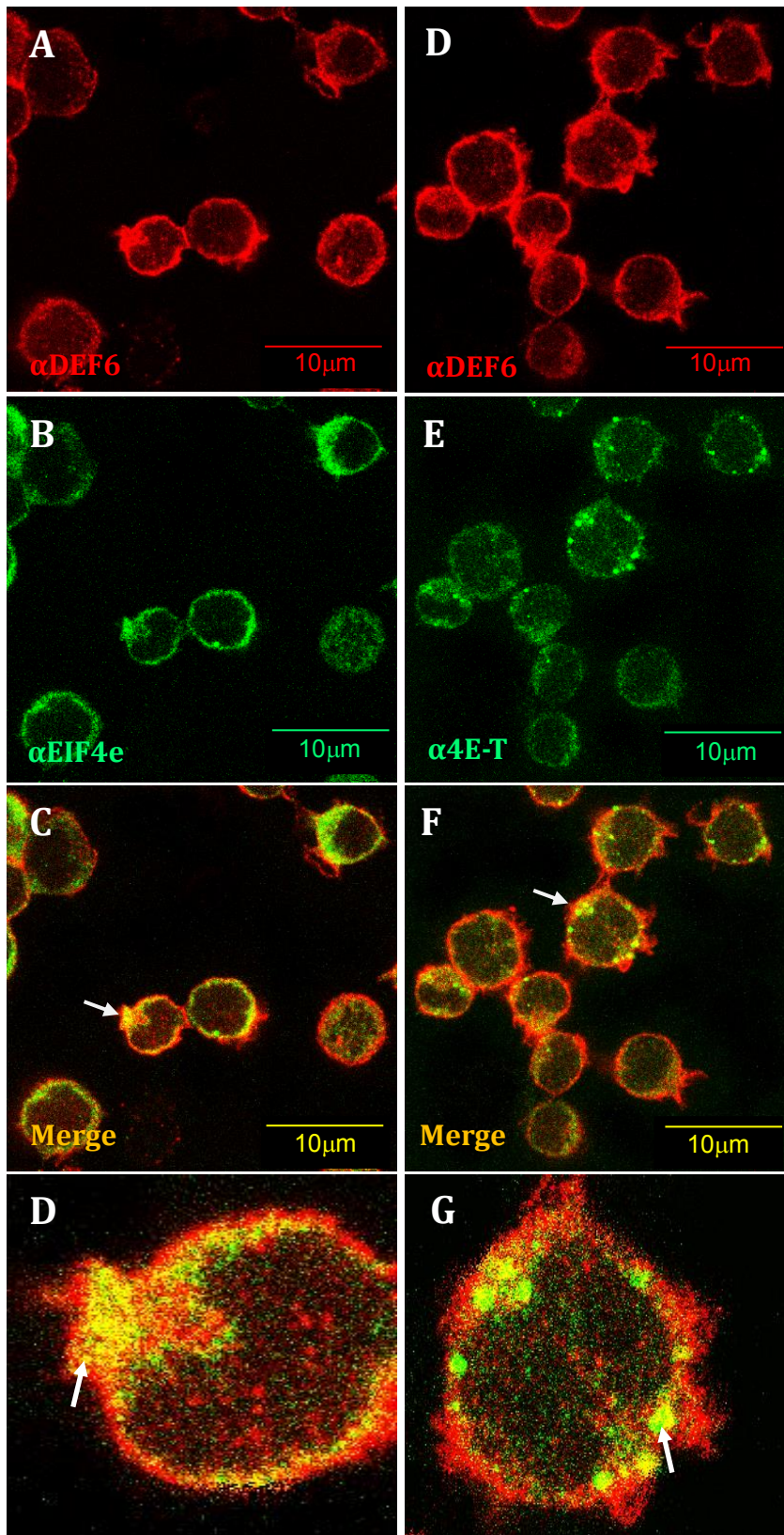


**Figure 3.4.2: Partial colocalisation of DEF6 with eIF4E and 4E-T in Jurkat cells** Double immunocytochemistry and confocal analysis revealed partial colocalisation of DEF6 with eIF4E (A-D) as well as 4E-T (D-G). Jurkat cells were stained with rabbit anti-DEF6 primary antibody followed by anti-rabbit Alexa fluor 568 (red) fluorescent secondary antibody. Incubation with mouse anti-eIF4E (left

column) and mouse anti-4E-T (right column) was followed by staining with Alexa fluor 488 fluorescent secondary antibody (green). White arrows in merged images highlight colocalisation. Images were taken by a Zeiss LSM710 confocal microscopy at 63x magnification and 2x zoom. Data are representative of four independent experiments. The scale bar: 10 $\mu$ m. D and G enlarged images from C and F, respectively.

### **3.4.3 DEF6 also colocalises with PABP and ARP2/3 albeit to a much lesser extent than observed for eIF4E and 4E-T**

Poly (A)-binding protein (PABP) interacts with eIF4E and this interaction is crucial for mRNA translation (Kahvejian *et al.*, 2001). It was shown by Remon (PhD 2016), that a minor fraction of DEF6 was in close proximity to PABP. Therefore, double immunocytochemistry and confocal microscopy was employed to test whether both proteins colocalise in Jurkat cells. As illustrated in Fig. 3.4.3, approximately 1.5% of the protein foci appeared yellow in the merged image indicating colocalisation of DEF6 and PABP confirming Remon's results (PhD 2016).

ARP2/3 is an actin binding protein, which is involved in promoting actin polymerisation and has a role in TCR engagement and IS formation (Kumari *et al.*, 2014 & van der Merwe, 2002). Despite its similar role to DEF6, less than 1% of ARP2/3 protein foci colocalised with DEF6 in resting Jurkat cells (Fig. 3.4.3).

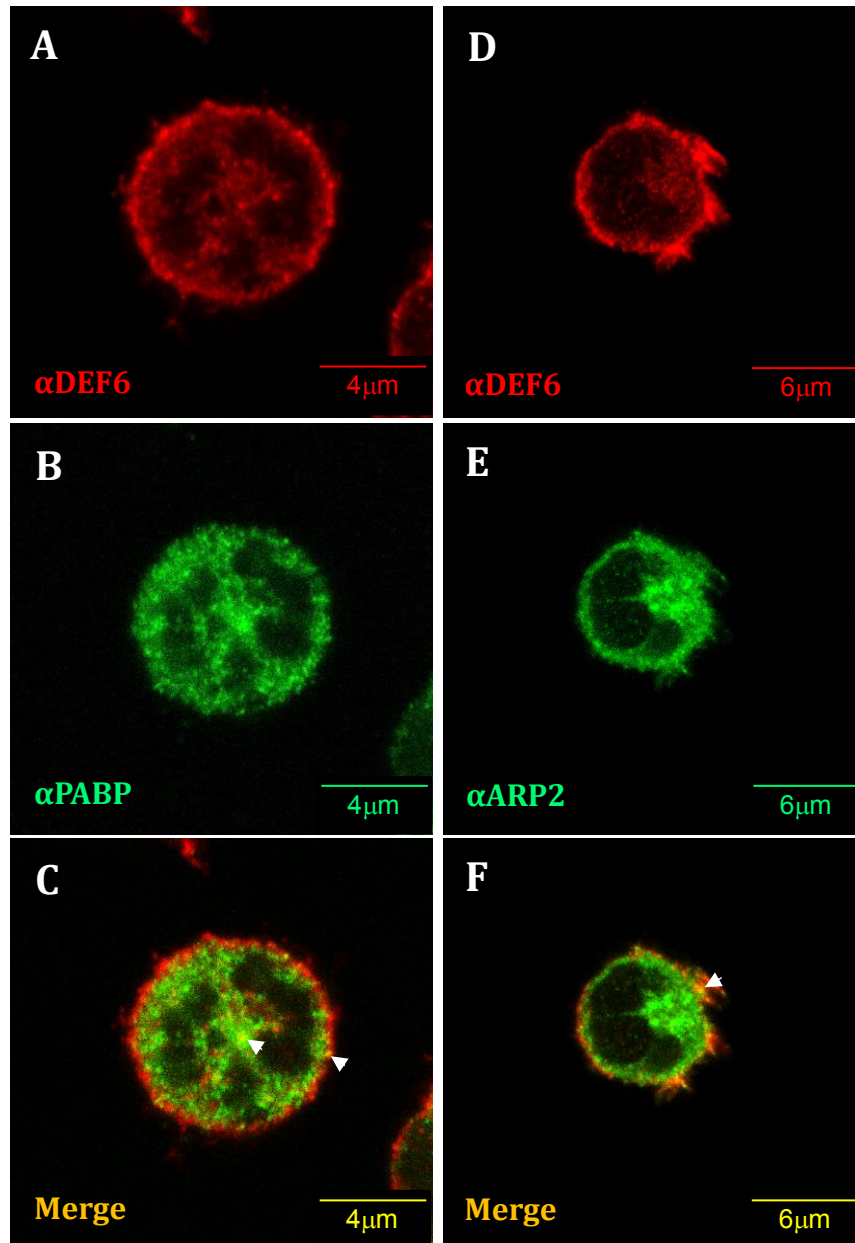


**Figure 3.4.3: Only a minor fraction of DEF6 colocalise with PABP and Arp2/3**  
 DEF6 primary rabbit antibody tagged with secondary antibody Alexa fluor 568 (red; A, C, D, F). PABP stained with mouse anti-PABP tagged with secondary antibody Alexa fluor 488 (green; B, C). Arp2/3 stained with antibody -Alexa fluor 488 (green; E, F). Merged images (C, F) exhibit some yellow stain but most DEF6 is not overlapping with neither PABP nor Arp2/3. White arrowheads indicate colocalisation. Images were taken by confocal microscopy at 63x magnification and 2x zoom. Data are representative of three independent experiments. The scale bar is 4μm and 6μm.

### **3.4.4 DEF6 physically interacts with eIF4E and 4E-T but not with PABP**

Given that DEF6 partially colocalised with eIF4E, 4E-T and to a much lesser extent PABP as shown in Figure 3.4.3, coimmunoprecipitation experiments were performed to test whether these proteins interact with each other. Protein G beads and DEF6 antibody were mixed together to immobilise DEF6 antibody on the beads. Protein lysate from untransfected (WCL) or transfected Jurkat cells with GFP-tagged DEF6 (GFP-DEF6) was then added to the beads and the mixture incubated for 30 mins at room temperature. After denaturing the protein lysates by boiling at 95°C for 5 min, they were loaded onto SDS-PAGE gel and analysed by western blotting as described before. As shown in Fig. 3.4.4, both eIF4E (A) and 4E-T (B) were readily detectable in WCL and GFP-DEF6 samples indicating that these proteins were co-immunoprecipitated with anti DEF6 antibodies. While 4E-T shows 2 bands in western blot (see figure 3.5.2. B), it seems only one of them was co-immunoprecipitated. In contrast, PABP was not co-immunoprecipitated (Fig. 3.4.4 B). Protein (G) beads did not show any bands as expected, and input lysates exhibited bands of appropriate sizes.

These results suggest that DEF6 binds to eIF4E in the mRNA translational initiation complex resulting in colocalisation with PABP that also binds eIF4E. Binding of DEF6 to 4E-T on the other hand might occur in P-bodies. Together with the fact that DEF6 was copurified with ribosomes and polysomes, these data reveal a potential role for DEF6 in initiation of mRNA translation, elongation of mRNA translation and degradation of mRNAs.

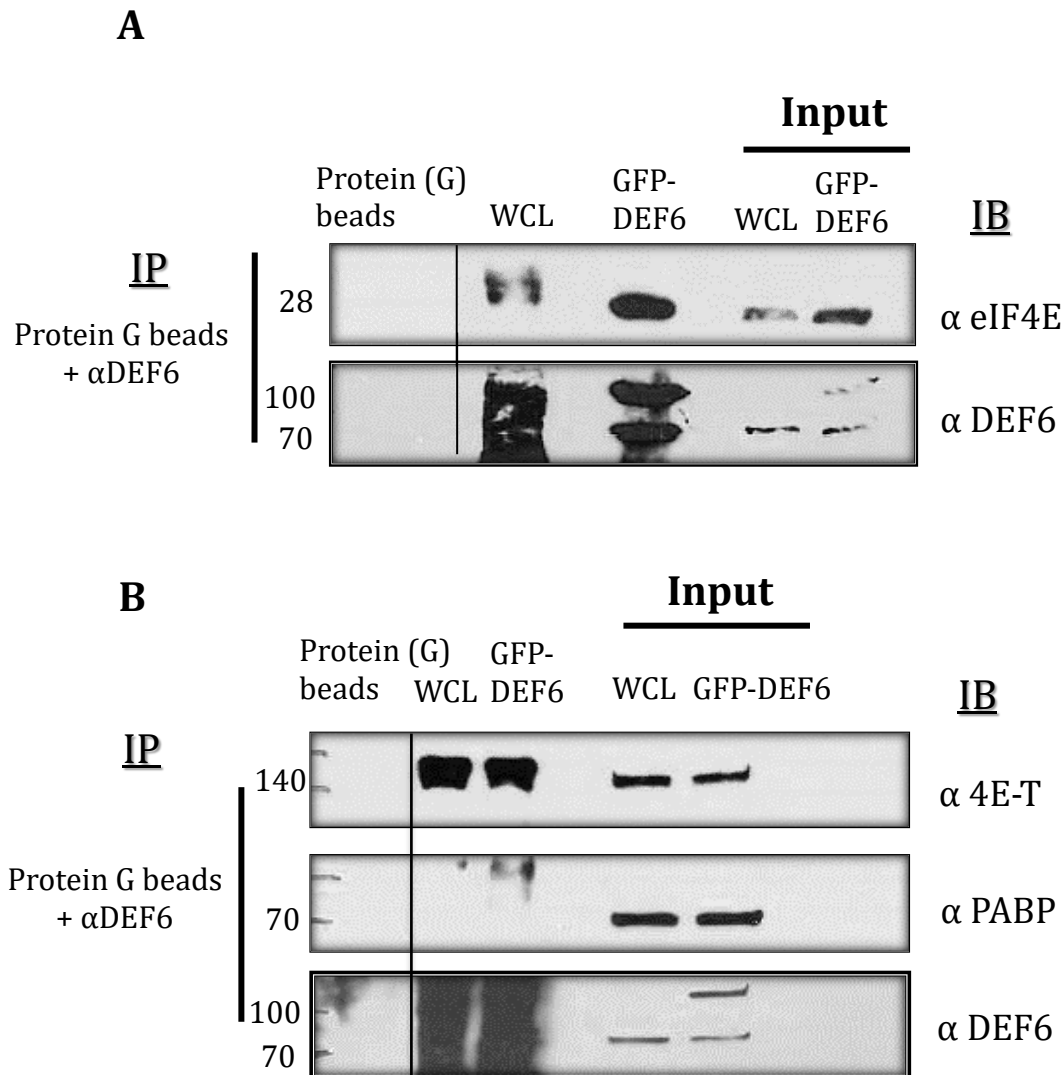


**Figure 3.4.4: DEF6 interacts with eIF4E and 4E-T but not with PABP**

Co-immunoprecipitation analysis of DEF6 and eIF4E 28kDa (A), 4E-T 140kDa and PABP 70kDa (B) untransfected (WCL) and GFP-tagged DEF6 overexpressing Jurkat cells (GFP-DEF6). The corresponding input lanes and beads-only control lanes are as indicated. The same membrane in B was first incubated with the eIF4E antibody and after stripping incubate with the PABP antibody. These two blots later were stripped and thereafter redeveloped with DEF6 antibody. Data are representative of three independent experiments.

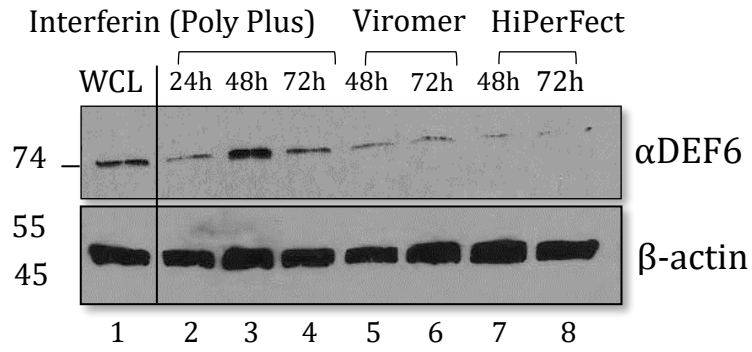
### **3.5 siRNA-mediated knockdown of DEF6 expression in Jurkat T cells.**

siRNA-mediated knockdown of DEF6 expression in Jurkat cells proved to be challenging. Initially, transfection efficiency with siRNAs was low and DEF6 protein expression unaltered (data not shown). The siRNA-mediated knockdown of DEF6 expression in Jurkat T cells was achieved using several siRNA and transfection reagents. Using the same siRNAs, the percent relative expression of DEF6 normalised to  $\beta$ -actin for the Polyplus reagent demonstrating the reduction at 24 hours. This value is approximately 0.1%. Furthermore, the Viromer reagent demonstrated the efficient of knockdown at 72, rather than 48 hours (~0.06%). In addition, the Hiperfect reagent demonstrated the great efficiency ratio for knockdown at 72 hours; the result showed that there was 16 fold reduction (~0.03%) in the expression of DEF6 protein. A graphical representation of these values is provided in Figure 3.5 A. An additional assessment of the DEF6 knockdown pattern of expression revealed that knockdown using HiPerFect for siRNA transfection results in the diminished production of the DEF6 protein even after 48 hours, which is represented in Figure 3.5 B.

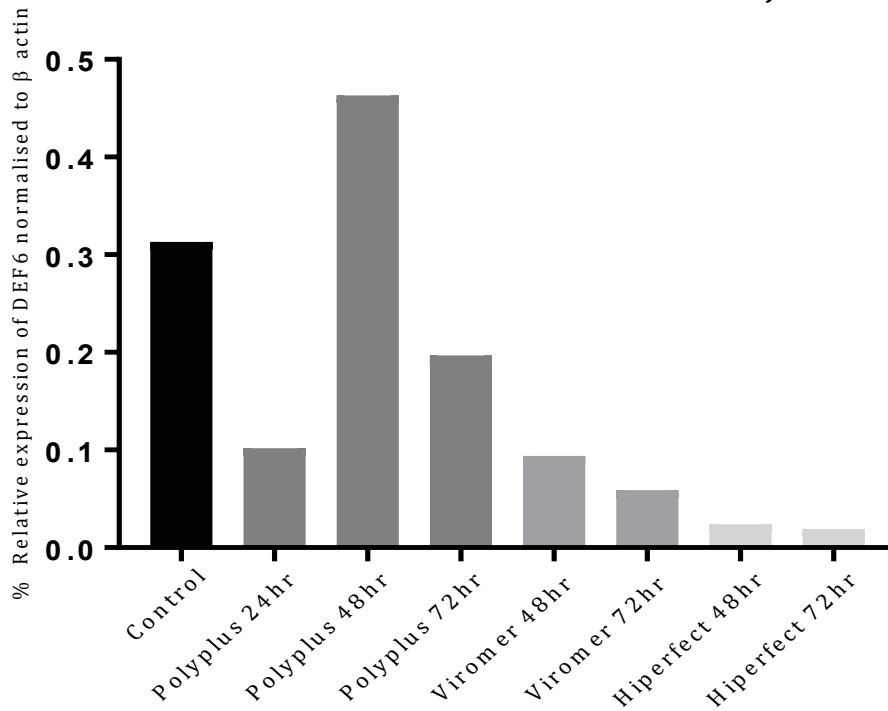
The monoclonal rabbit DEF6 antibody was shown to be able to detect DEF6 in cells using Flow cytometry (abcam). Therefore, siRNA-mediated knockdown of DEF6 was also analysed using Flow cytometry (Fig. 3.5.C-F). Jurkat cells were transfected with DEF6 siRNA as described above and after washing and fixing, cells were stained with primary antibody in appropriate dilution for 1 hr in the dark. Anti-rabbit Alexa Fluor 488-conjugated secondary antibody was added for 45 mins. Cells were resuspended in PBS and stored in the dark at 4°C before analysis using

a Flow cytometer (Method 2.4.12). Forward and side scatter was used to exclude dead cells. Staining with the secondary antibody alone shown in Fig.3.5.C was used as negative control and the gates set accordingly. In accordance with the Western blot analysis, most resting Jurkat cells (~92%) expressed DEF6 and only a few (~7.4%) appeared negative Fig. 3.5.D). In contrast, siRNA-mediated knockdown increased the negative cell population to 16.4 % after 72 hr and 28.8% after 96 hr of transfection (Fig. 3.5.E & F). In addition, staining intensity of the DEF6-positive Jurkat cells was markedly reduced from ~500 in untransfected cells to ~200 after knockdown (Fig. 3.5.D-F). Taken together, the Flow cytometry analysis confirmed a clear reduction of DEF6 protein after siRNA-mediated knockdown but also highlighted an apparent difference in the sensitivity of the assays used; with western blotting being less sensitive than Flow cytometry.

**A**



**siRNA-mediated Knockdown of DEF6 in Jurkat cells**



**B**

**siRNA-mediated Knockdown of DEF6 in Jurkat cells**

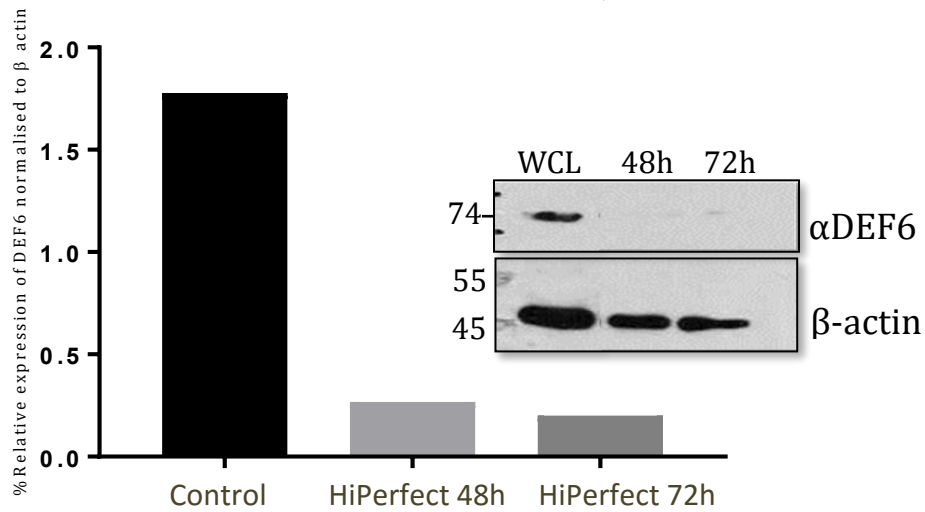
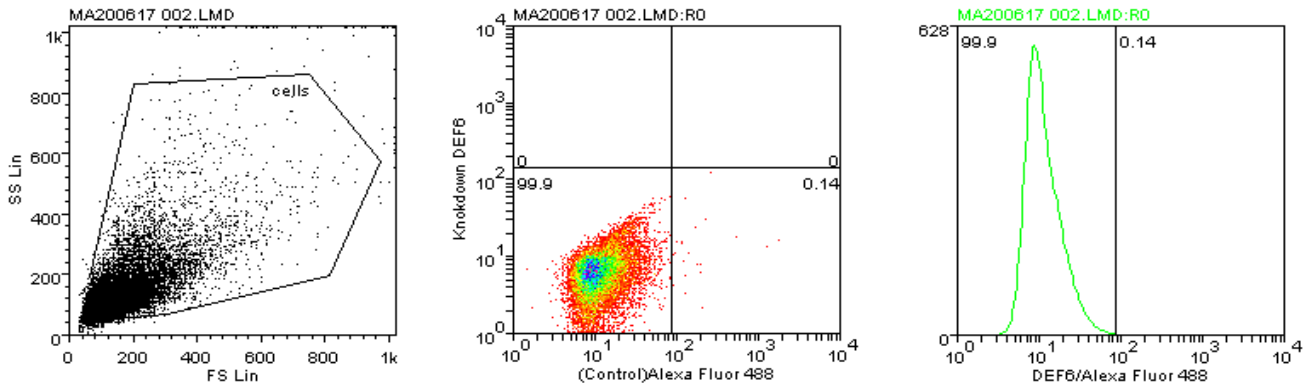


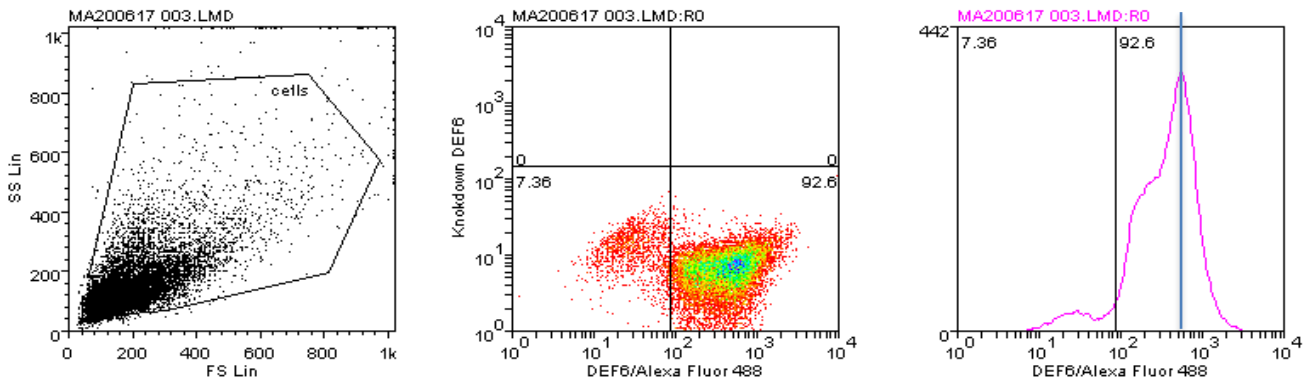
**Figure 3.5: Efficient siRNA-mediated knockdown of DEF6 expression in Jurkat T cells**

**A)** Western blot analysis of Jurkat cell lysates transfected with siRNA using various transfection reagents as reflected by the study protocol. Compared to whole cell lysate (WCL) of resting Jurkat cells, efficient siRNA-mediated knockdown of DEF6 expression was achieved with HiPerfect. Furthermore, this process was found to be less efficient in the Viromer and Interferin (Polyplus) reagents. The percent relative expression in the HiPerfect reagent were both close to zero at 48 and 72 hours. **B)** The transfection of siRNAs with HiPerfect was robust and often resulted in complete knockdown after 48 hr (anti-DEF6 at concentration 1:1000). The same Western blots were re-probed with an anti  $\beta$ -actin antibody as loading control. At 48 hours, the HiPerfect reagent reflected a 0.25% relative expression of DEF6, and the expression was 0.20% at 72 hours. Quantification of knockdown levels of DEF6 were measured using GraphPad Prism and normalised against  $\beta$ -actin. Nine replicates were performed.

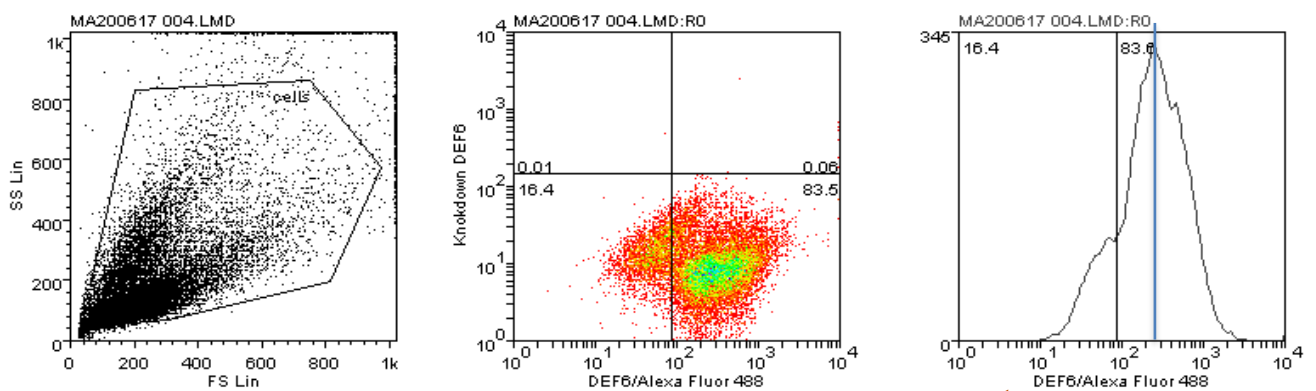
**C** Control: Jurkat cells staining with Alexa fluor



**D** Jurkat cells staining with  $\alpha$  DEF6 and Alexa fluor 488



**E** Transfected of Jurkat cells with siRNA knockdown DEF6 for 72hrs



**F** Transfected of Jurkat cells with siRNA knockdown DEF6 for 96hrs

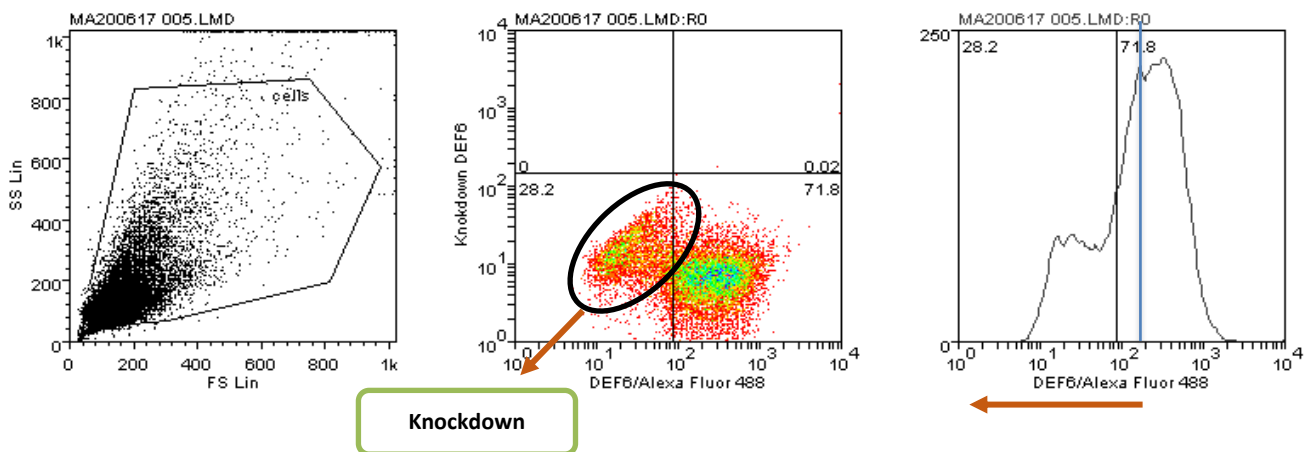


**Figure 3.5-1: Flow Cytometry analysis confirmed efficient knockdown of DEF6 expression**

Gates were set using forward and side scatter to exclude dead cells (left column) and according to the negative control staining using secondary antibody alone. (**C**; middle and right column). **D**) 92.6% of resting Jurkat cells stained for DEF6 with a peak intensity of ~ 500 (right column). siRNA-mediated knockdown of DEF6 after 72h (**E**) and 96h (**F**) resulted in a marked increase of negative cells (16.4% and 28.2 %). In addition, the peak intensity was reduced 2.5 fold to ~200 as indicated by the shift of the peaks to the left.

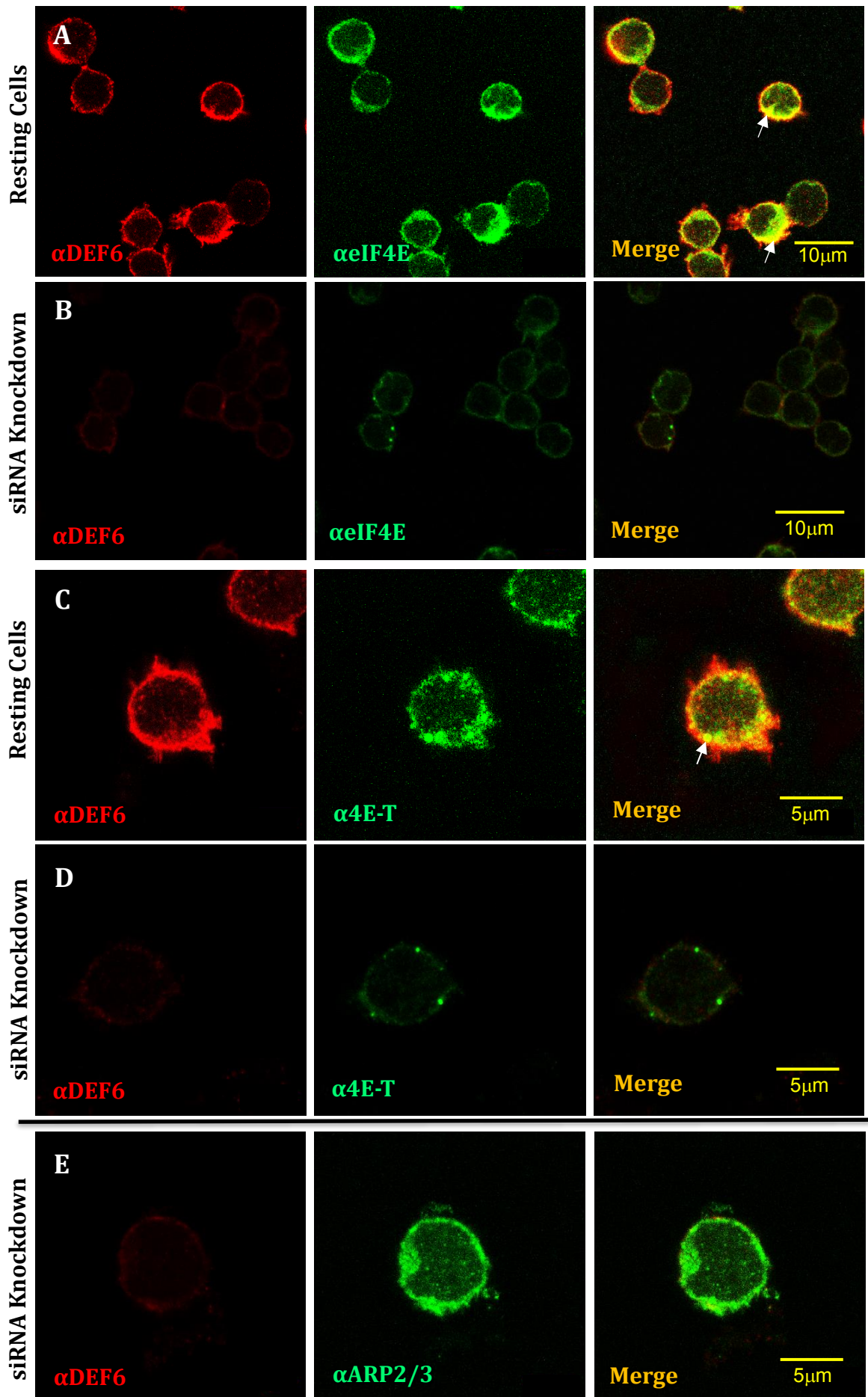
### **3.5.1 siRNA-mediated DEF6 knockdown resulted in down regulation of eIF4E, 4E-T and PABP protein expression in Jurkat cells**

The results described so far suggest a role for DEF6 in mRNA metabolism that might be mediated through eIF4E and/or 4E-T. To test whether knockdown of DEF6 had any consequences on localisation of eIF4E or 4E-T immunocytochemistry was performed on Jurkat cells that had been transfected with siRNA targeting DEF6 using the condition established as described earlier in section 3.5. Seventy-two hours after transfection, Jurkat cells were applied to Poly-L-Lysine coated coverslips, fixed and double stained with rabbit anti-DEF6 and mouse anti-eIF4E or mouse anti-4E-T. As untreated control, resting Jurkat cells were incubated with the above antibodies. In line with the data described above in Fig 3.4.2 A-D, DEF6 colocalised with eIF4E and 4E-T in untransfected Jurkat cells. Surprisingly, knockdown of DEF6 expression had a profound effect on the expression of both eIF4E and 4E-T. As shown in Fig. 3.5.1 B and D, DEF6 expression was almost completely abolished in siRNA transfected cells and expression of eIF4E and 4E-T was also much reduced compared to Jurkat cells that were not subject to transfection. In contrast, knockdown of DEF6 expression had no obvious effect on the expression level of Arp2/3; a protein regulating actin cytoskeleton (Kumari *et al.*, 2014) (Fig. 3.5.1.E).

To confirm the results obtained with immunocytochemistry and confocal microscopy, a western blot analysis was carried out. After 48,72 and 96 hours of transfection, the cells were collected, and protein was extracted from either Jurkat cells transfected with DEF6 siRNAs or from non-transfected cells, and the western

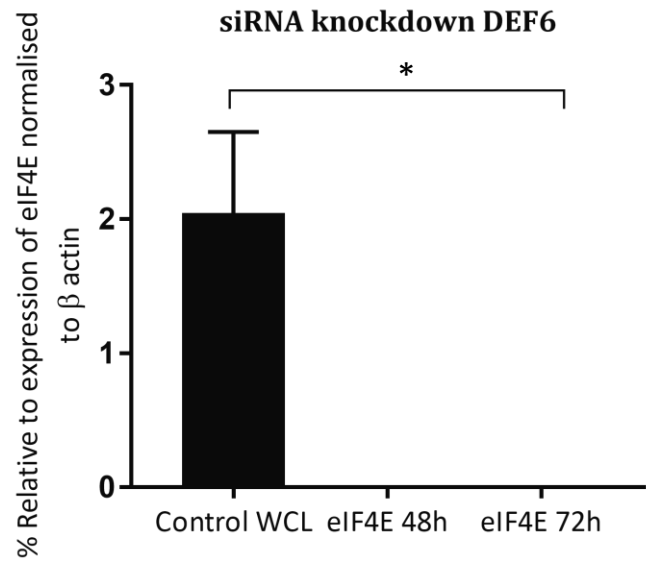
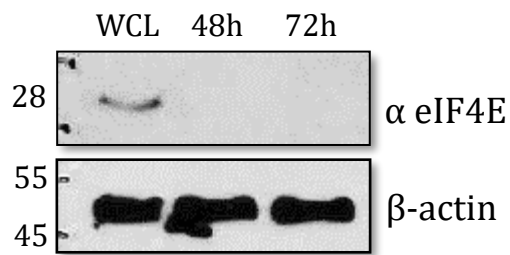
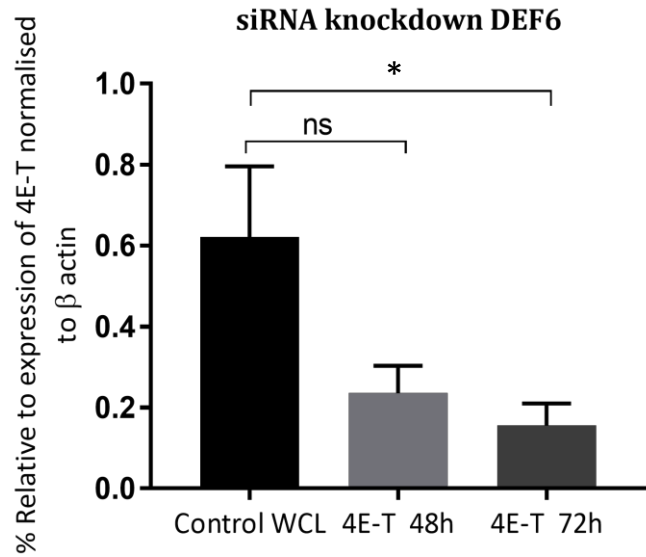
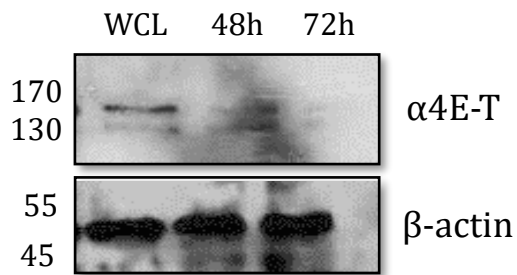
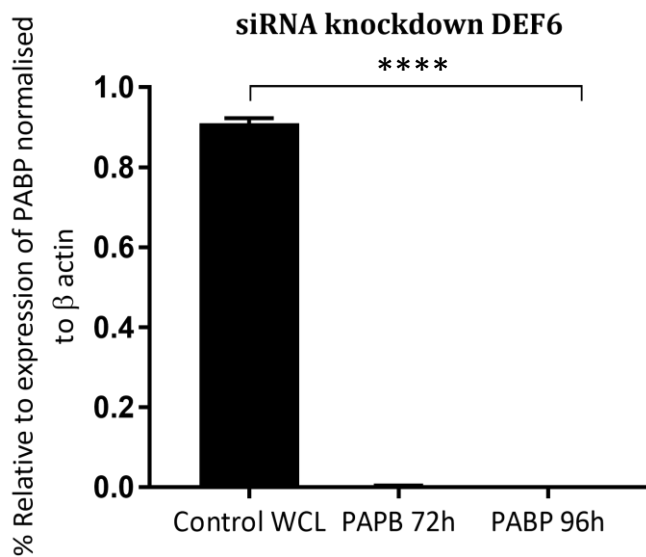
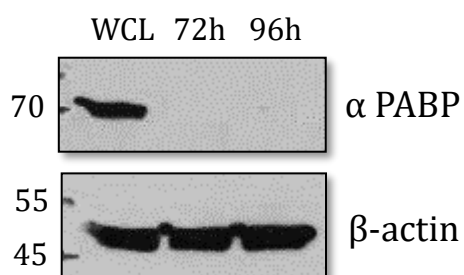
blots were probed with antibodies recognising DEF6, eIF4E, 4E-T, PABP or ARP2/3. In all these experiments  $\beta$ -actin was used as the loading control. In Figures 3.5.1-1 F and H, the western blot results illustrate that the knockdown of DEF6 led to a decrease in the expression of eIF4E and PABP. These western blot images, from three independent experiments, were quantified using GraphPad Prism software; the data showed that there was a significant decrease in eIF4E and PABP (\*  $P < 0.05$  and \*\*\*\* $P < 0.0001$  respectively). The expression of the 4E-T protein was reduced after 48 hr and barely detectable after 72 hr (Figure 3.5.1-1 G). In contrast, the expression of Arp2/3 was not altered (Figure 3.5.1-1 I).

Taken together these data clearly establish a striking correlation between DEF6 expression and protein expression of eIF4E, 4E-T and PABP in Jurkat cells suggesting that DEF6 is regulating expression of proteins involved in mRNA translation and metabolism but not proteins like ARP2/3 that are involved in F-actin organisation.



**Figure 3.5.1: DEF6 regulates expression of eIF4E, 4E-T and PABP proteins in Jurkat T cells**

**A-E:** Confocal microscopy analysis as described before of non-transfected, resting Jurkat cells (**A** and **C**) and  $2 \times 10^5$  cells/ml Jurkat cells transfected with DEF6-specific siRNAs 72 hr after transfection (**B**, **D** and **E**) stained with anti DEF6 antibody (red; left column) and antibodies specific for either eIF4E (**A** and **B**), 4E-T (**C** and **D**) or Arp2/3 (**E**; green; middle column). Merged images are shown on the right. siRNA-mediated knockdown of DEF6 almost completely abolished DEF6 expression (**B**, **D** and **E**) and largely reduced expression of eIF4E (**B**) and 4E-T (**D**). In contrast, ARP2/3 expression was unaltered (**E**). Images were taken using a Zeiss LSM710 confocal microscope at a 63x magnification and 2x zoom. Data are representative of three independent experiments. The scale bar is 10 $\mu$ m and 5 $\mu$ m.

**F****G****H**

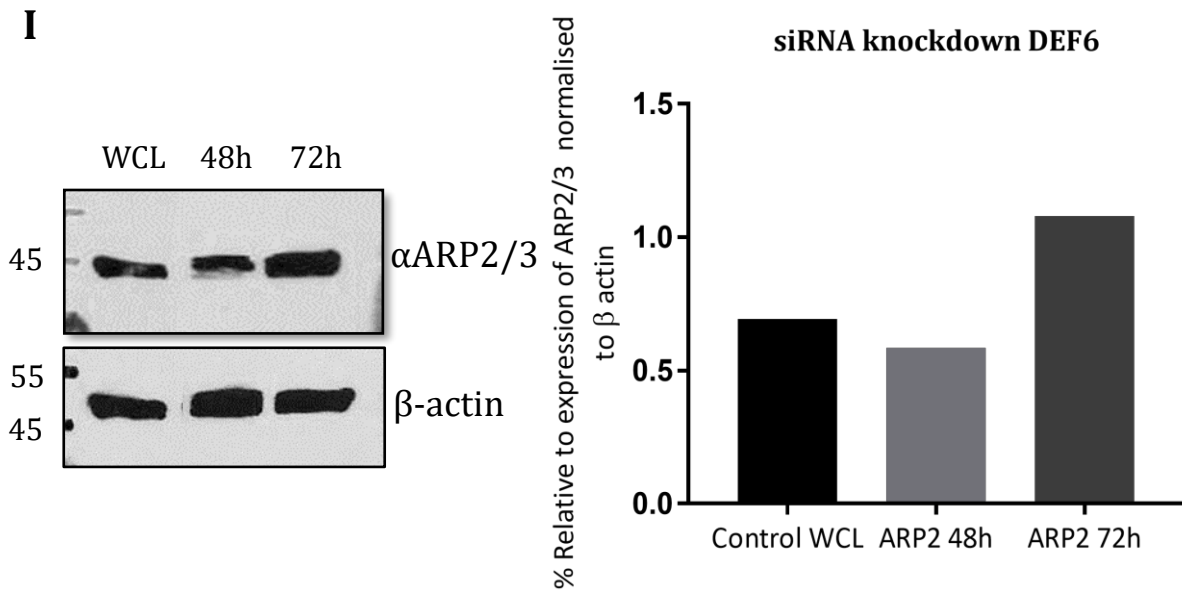


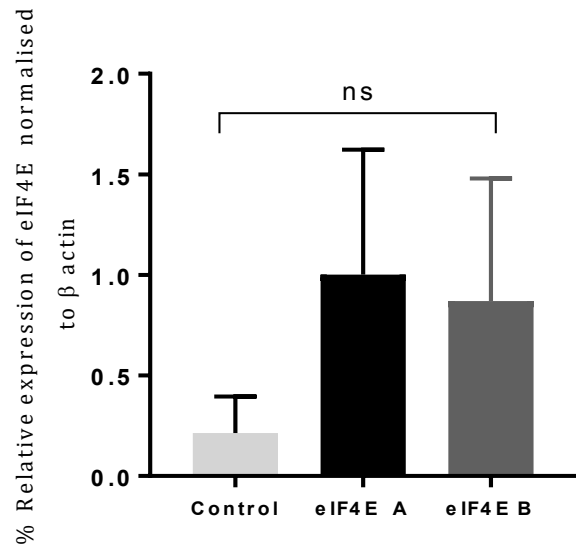
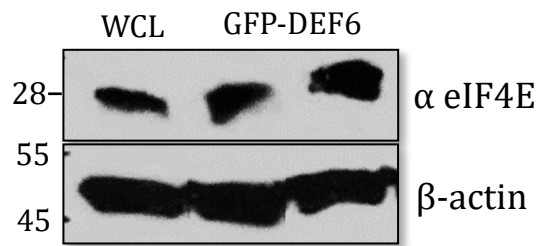
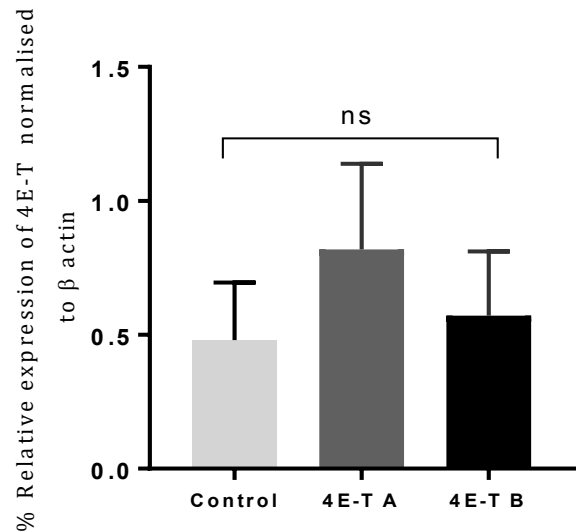
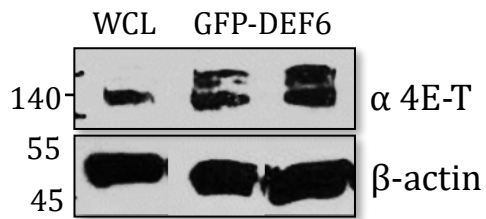
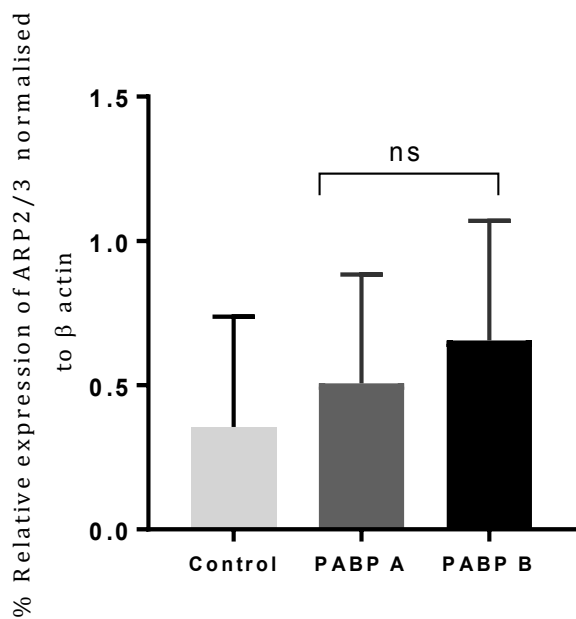
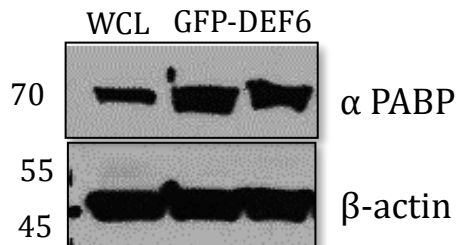
**Figure 3.5.1-1: DEF6 is regulate expression of mRNA translation proteins**

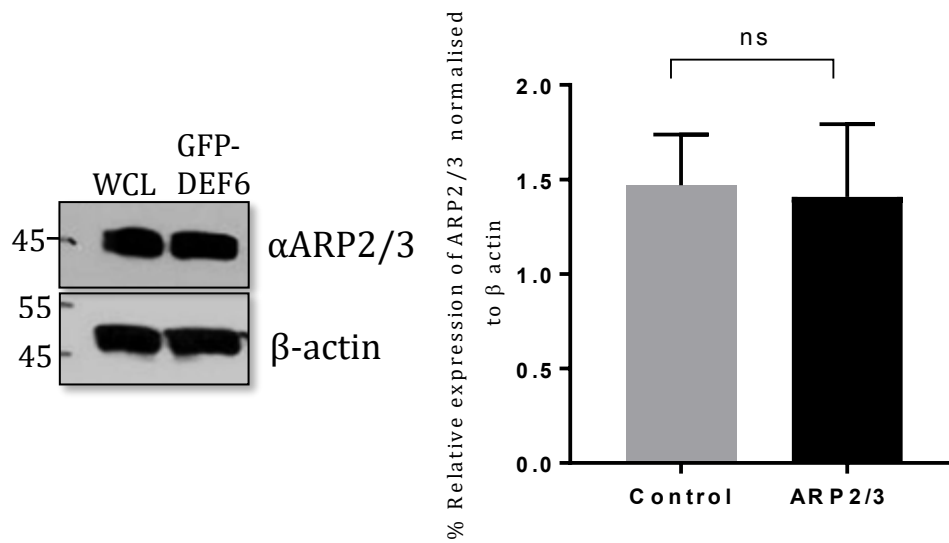
(F-I) Western blot in left panel analysis as described before of protein lysates isolated from non-transfected, resting Jurkat cells (WCL) and Jurkat cells transfected with DEF6-specific siRNAs 48, 72 and 96 hr after transfection as indicated. The quantified results are shown in the right panel using a one-way ANOVA and a multiple comparison. siRNA-mediated knockdown of DEF6 completely abolished eIF4E (F) and PABP (H) expression and almost complete 4E-T expression (G) while ARP2/3 expression was unaltered (I). All membranes subsequently were re-probe with  $\beta$ -actin antibody as a loading control. Densitometry data shown for each protein, eIF4E \*  $P < 0.05$ , 4E-T\*  $P < 0.05$  and PABP \*\*\*\* $P < 0.0001$ , Significant different. The results are expressed as the mean  $\pm$  SEM. Error bars show the standard deviation from a three independent experiments. ns: is not Significant different

### **3.5.2 Increase of eIF4E, 4E-T and PABP protein expression upon DEF6 overexpression in Jurkat cells**

Having established a striking correlation between DEF6, eIF4E, 4E-T and PABP protein expression, Jurkat cells were transfected with GFP-tagged DEF6 to establish whether overexpression of DEF6 would have any effect on the expression of eIF4E, 4E-T and PABP. Twenty-four hours after transfection protein lysates were isolated and analysed by western blotting as described in method 2.10.1. As shown in Figure 3.5.2, the overexpression of DEF6 resulted in the increased expression of eIF4E, 4E-T and PABP. This was evident from the more intense bands in the DEF6-GFP lanes compared to the WCL lanes (Figures 3.5.2 A, B and C), but the ARP2/3 expression was unaltered (Figure 3.5.2 D). In each instance, a greater quantity of protein was yielded than in the control. The western blots were quantified, and the results showed that the difference between eIF4E, 4E-T, PABP and the control was not statistically significant.

Together these data suggest that the expression level of a subset of proteins involved in mRNA translation and metabolism is positively correlated to the level of DEF6 protein. As described before in section 3.3, the overexpression of DEF6 reduced endogenous DEF6 protein expression (Fig. 3.5.2.A) which might suggest that DEF6 negatively regulates its own protein expression. Expression of 4E-T protein results in one or two bands which might be due to phosphorylation or other post-translational modifications (Dostie *et al.*, 2000).

**A****B****C**

**D**

**Figure 3.5.2: DEF6 overexpression increases expression of eIF4E, 4E-T and PABP but not Arp2/3**

Western blots showing the elevated expression of eIF4E and 4E-T proteins in a DEF6 overexpressed background. **A)** Blot showing DEF6 overexpression in Jurkat cells. **B)** eIF4E and **C)** 4E-T blots, the two bands shown here it might be because of GFP-DEF6 or the phosphorylation. **D)** PABP, along with loading control  $\beta$ -actin. **E)** Arp2/3 expression unchanged in a DEF6 overexpressed state. Quantification of overexpression levels of each protein were calculated and compared to control using a one-way ANOVA and normalised against  $\beta$ -actin. Error bars show the standard deviation from a three replicates ns: is not Significant different

### 3.5.3 Neither overexpression nor knockdown of DEF6 affect gene expression of eIF4E, 4E-T or PABP

As shown 3.5.2, protein expression of eIF4E, 4E-T and PABP correlated with the level of DEF6 protein expression. To examine whether this caused by the altered expression of the corresponding genes, RT-PCR was performed using gradient PCR (Takara PCR thermo cycler).

The RNA was isolated from Jurkat T cells, cDNA was synthesised and RT-PCR was performed. Using gene-specific forward and reverse primers (see appendix table 8), cDNAs for DEF6, eIF4E, 4E-T, PABP, ARP2/3 and eEF1A1 were amplified, and the PCR products were analysed by agarose gel electrophoresis. Three types of cDNA samples were analysed: (i) untransfected resting Jurkat cells; (ii) Jurkat cells in which GFP-DEF6 was overexpressed and (iii) Jurkat cells transfected with DEF6 siRNAs. The PCR product showed that the overexpression of GFP-DEF6 increased the overall *DEF6* expression (Figure 3.5.3 A; compare lanes 1 and 2), whereas the knockdown of DEF6 clearly reduced the amount of endogenous *DEF6* gene expression (Figure 3.5.3 A; compare lanes 1 and 3). The gene expression of *Arp2/3* and *eEf1A1* (Figures 3.5.3 E and F, lanes 1-3) which served as positive controls, did not change regardless of DEF6 overexpression or knockdown. *eIF4E* gene expression in the control (lane 1) and the DEF6 knockdown treatment was more intense than in the GFP-DEF6 treatment (Figure. 3.5.3 B, lane 2) despite the elevated protein expression observed in eIF4E (Figure 3.5.2). The gene expression of *4E-T* was similar among all the samples (Figure 3.5.3 C, lanes 1-3) and the expression of the *PABP* gene appeared elevated in both the GFP-DEF6 overexpression and

knockdown treatments compared to untransfected Jurkat cells (Figure 3.5.3 D, lanes 1-3). These preliminary data suggest that the lack of eIF4E, 4E-T and PABP proteins observed in DEF6 knockdown and the elevated expression of these proteins in GFP-DEF6 overexpressing Jurkat cells is due not to transcriptional regulation, but possibly translational regulation instead.

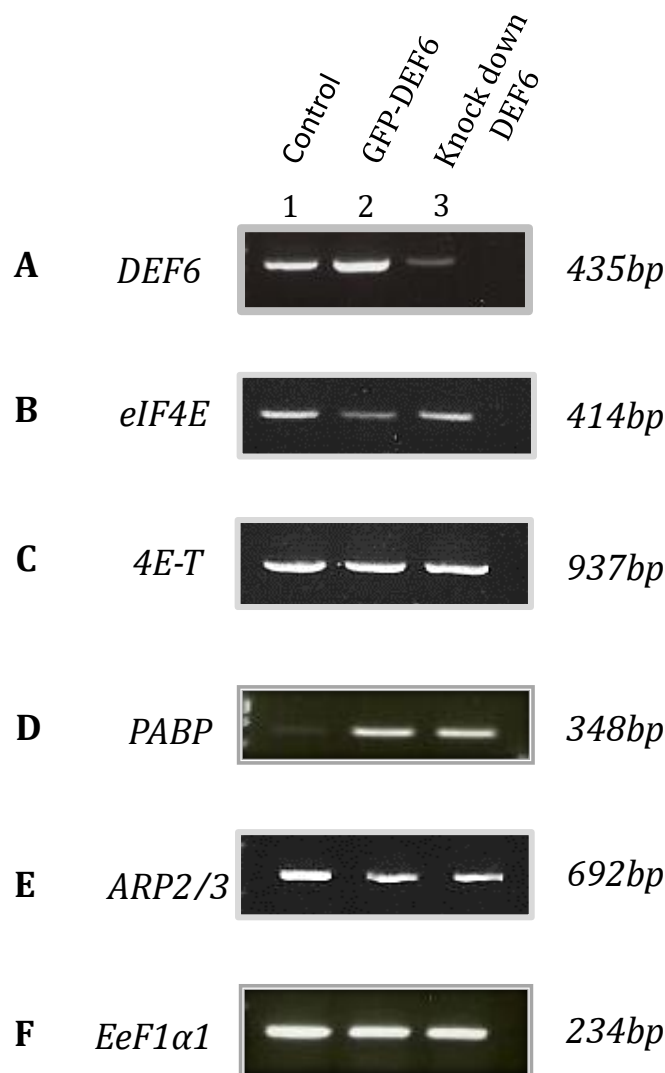


**Figure 3.5.3: RT-PCR analysis of gene expression**

cDNA samples of untransfected resting Jurkat cells, Jurkat cells overexpressing GFP-DEF6 and Jurkat cells transfected with DEF6 siRNA were amplified with gene-specific primers for A) DEF6, B) eIF4E, C) 4E-T, D) PABP, E) ARP2/3 and F) EeF1α1 as positive control.

### **3.5.4 DEF6 siRNA-mediated downregulation of eIF4E does not seem to be due to protein degradation via autophagy or ubiquitination pathways**

As shown in 3.5.3, lack of eIF4E in DEF6 siRNA-treated Jurkat cells was not a consequence of transcriptional downregulation suggesting that DEF6 is regulating abundance of eIF4E on the protein level. While the results described so far are compatible with the notion that DEF6 is regulating mRNA translation of eIF4E, they did not exclude the possibility that downregulation of eIF4E was due to selective protein degradation. Two major pathways result in protein degradation: the ubiquitin proteasome pathway and autophagy (Ge *et al.*, 2009). To investigate whether eIF4E protein reduction was due to proteasome-mediated degradation or by autophagy, Jurkat cells were either left untransfected or were transfected with siRNA targeting DEF6 for 72 hr and subsequently treated for 16hr or 24hr with either 10 or 50  $\mu$ M MG132, which prevents the proteolytic activity of the 26S proteasome (Lee & Goldberg 1998), or with 20 nM of bafilomycin A1 inhibitor, which prohibits the maturation of autophagy vacuoles by blocking the fusion of autophagosomes with lysosomes (Zhang *et al.*, 2014). Resting Jurkat cells and two samples of transfected cells were left untreated as controls. Western blot analysis shown in Fig. 3.5.4, demonstrate that neither treatment with MG132 or bafilomycin A1 inhibitor resulted in the rescue of eIF4E protein expression in DEF6 siRNA transfected Jurkat cells. This result suggests that DEF6 is not involved in the regulation of protein degradation and further supports a role for DEF6 in mRNA translation controlling expression of a subset of proteins such as eIF4E.

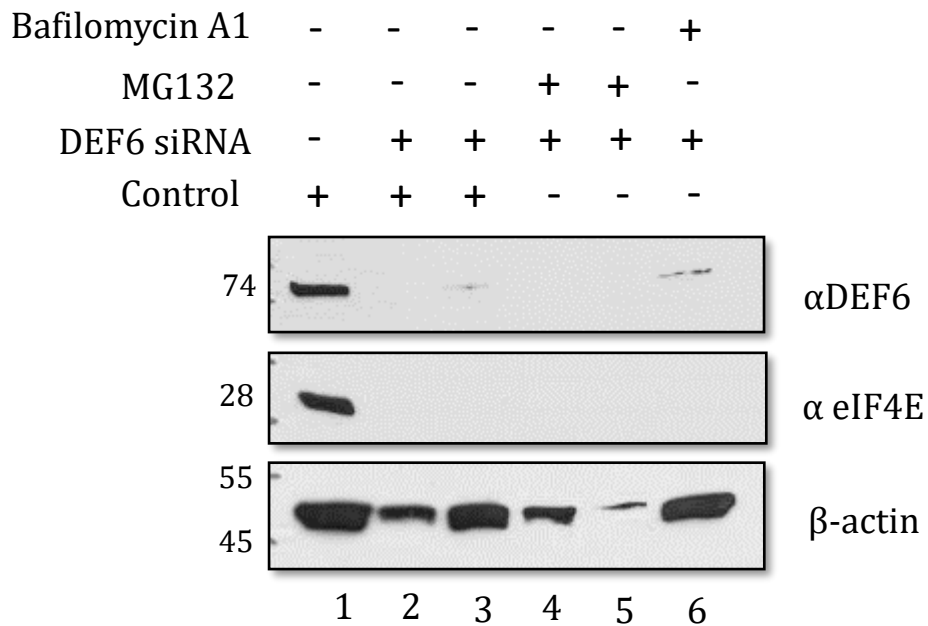


**Figure 3.5.4: Inhibition of protein degradation does not rescue eIF4E protein expression in DEF6 siRNA-treated Jurkat T cells**

Western blot analysis of Jurkat cells either untransfected (1) or transfected with DEF6-specific siRNAs for 72 hr (2, 3). After transfection, cells were treated with either 10  $\mu$ M (4) or 50  $\mu$ M (5) of MG13 or with 20 nM of Bafilomycin A1 (6) for 24hr. n: two separate experiments

## **3.6 DEF6 colocalises with eIF4E and PABP at the Immune synapse (IS)**

### **3.6.1 Presence of DEF6 at the IS**

TCR-mediated activation results in IS formation and recruitment of DEF6 to the IS which might be regulated through phosphorylation of DEF6 by LCK (Gupta *et. al.* 2003a; Bécart *et. al.*, 2008a).

To verify this, calcein blue labelled Raji cells in the presence of *Staphylococcus aureus* enterotoxin A and B superantigen were mixed at a 1:1 ratio with Jurkat to promote formation of immunological synapses at their interface. Cells were applied to Poly-L-Lysine coated coverslips and then immunostained with anti-DEF6 antibody followed by addition of fluorescent labelled secondary antibody. Antifade Mountant was applied to cells to prolong the fluorescent signal (see method 2.4.9).

Calcein blue was used to stain Raji B cells (Fig 3.6.1B) to easily distinguish Jurkat cells from Raji cells. As shown in Fig. 3.6.1 C&D, DEF6 was detected almost exclusively in the IS (red fluorescent signal at the junction of the cells).

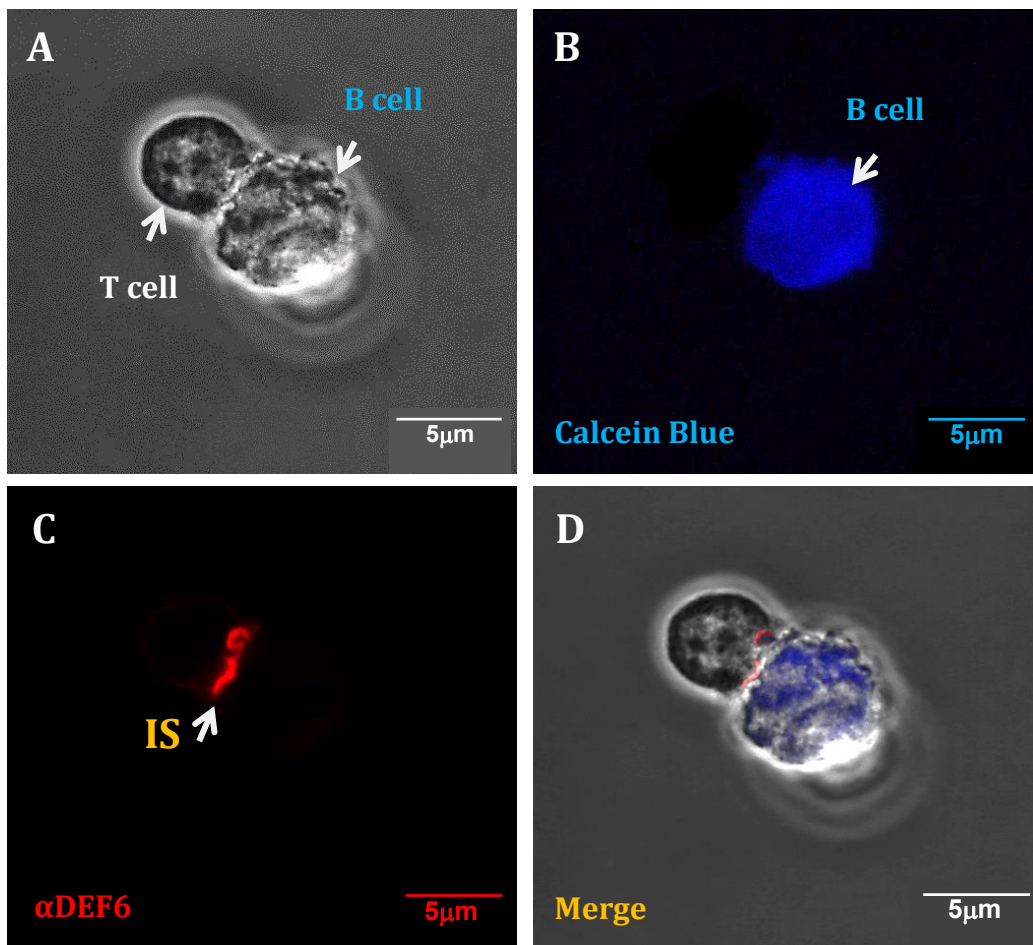


**Figure 3.6.1: DEF6 recruitment to the Immune synapse in Jurkat cells upon antigen presentation by Raji B cells**

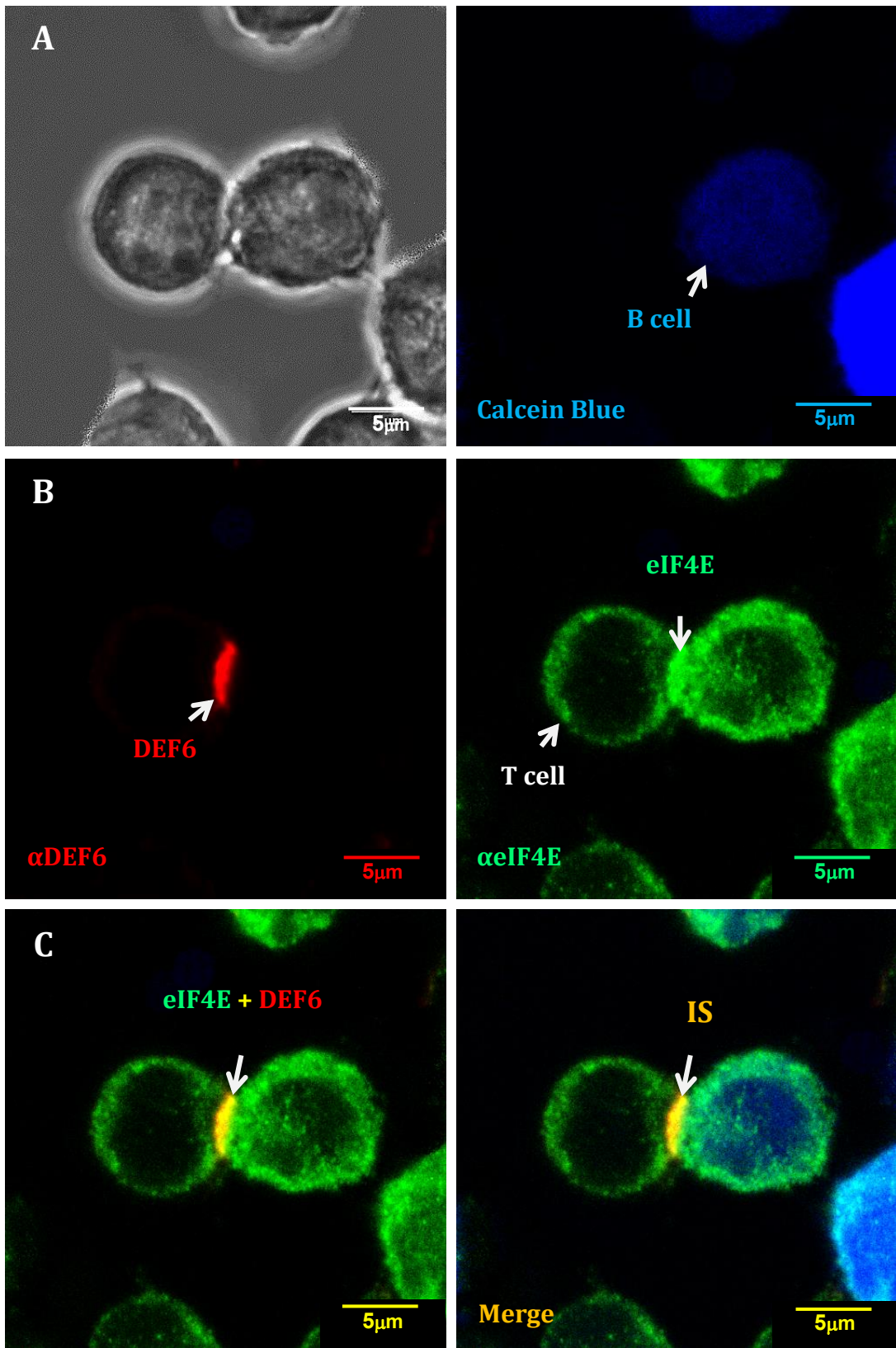
**(A)** Phase contrast image showing the B and T cells. **(B)** Calcein blue staining of the B cell. **(C)** Anti-DEF6 antibody showing DEF6 localisation at the IS (red) **(D)** Merged picture of A, B and C showing IS formed at the junction of B and T cells with DEF6 localising at the IS. Images were taken using a Zeiss LSM710 confocal microscope at a 63x magnification and 2x zoom. Data are representative of three independent experiments. Scale bar: 5µm

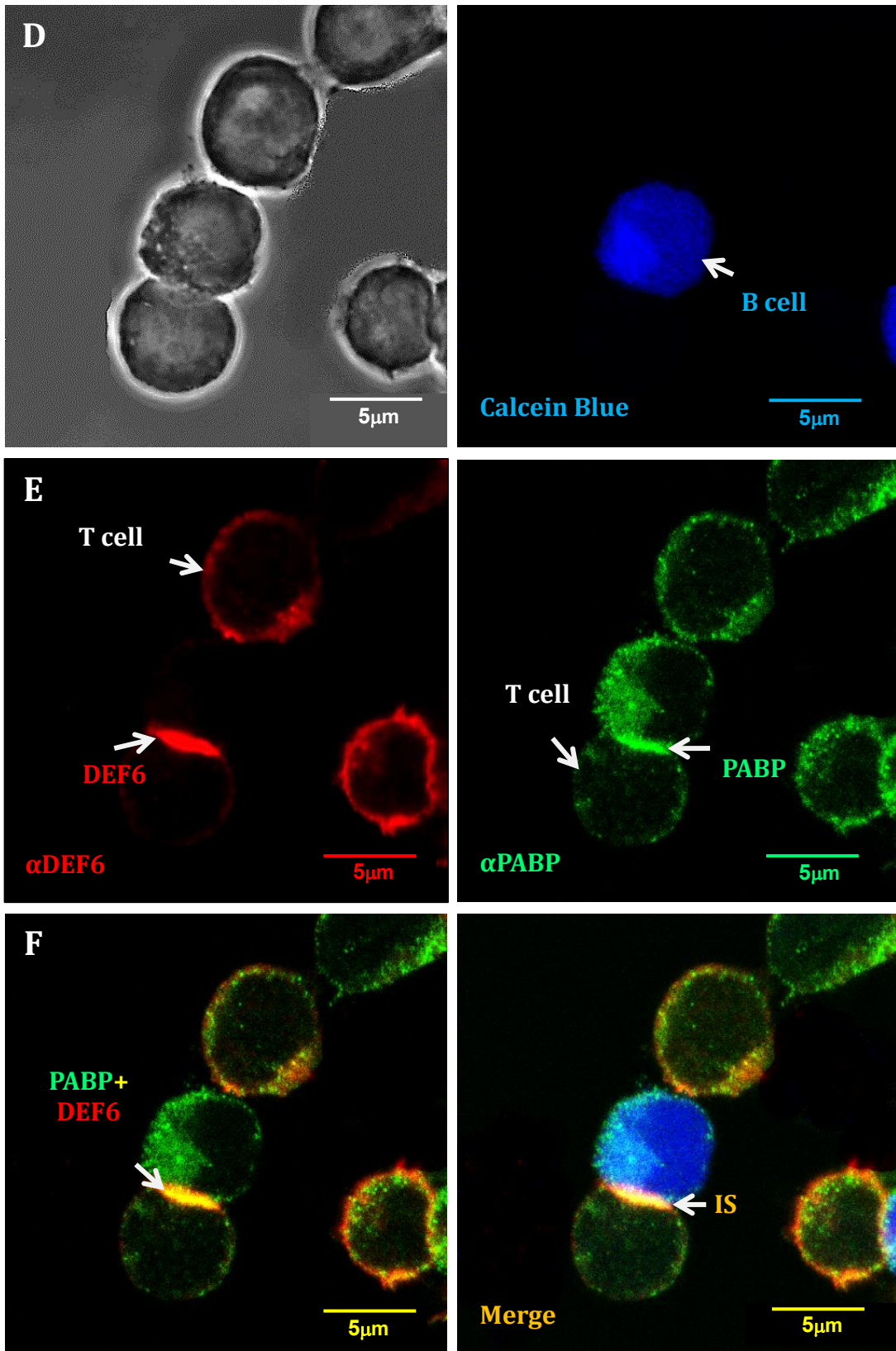
### 3.6.2 DEF6 colocalises with translational initiation complex during IS formation

As described above, DEF6 partially colocalised and interacted with proteins of the mRNA translation initiation complex comprising of eIF4E, 4E-T transporter protein and PABP in resting Jurkat cells. To test whether DEF6 and proteins of the mRNA initiation complex were also present in the IS, immunohistochemistry was performed after Raji B cell-mediated IS formation in Jurkat cells. Monoclonal rabbit DEF6 antibody was used in combination with either mouse anti-eIF4E, mouse anti-4E-T or mouse anti-PABP and subsequently anti-rabbit Alexa flour 568 (red) in combination with anti-mouse Alexa flour 488 (green) secondary antibodies were used.

Strikingly, eIF4E colocalised with DEF6 in the IS (Fig 3.6.2 A-C) as indicated by the yellow colour in the merged image (Fig 3.6.2 C right panel, white arrow). Similarly, PABP that did barely colocalise with DEF6 in resting Jurkat cells and did not bind DEF6 *in vitro*, also showed colocalisation with DEF6 in the IS (Fig 3.6.2 D-F). As shown in Fig.3.6.2 F, merged images clearly indicate colocalisation (yellow) of DEF6 and PABP in the IS. In contrast, 4E-T transporter that partially colocalised with DEF6 in resting Jurkat cells did not show any colocalisation with DEF6 in the IS (Fig 3.6.2 G-I).

Together these results suggest that DEF6 interaction with proteins of the mRNA translation initiation complex is dynamic, changing between resting and TCR-mediated activation. In addition, these data provide the first evidence that DEF6 might control mRNA translation in the IS.





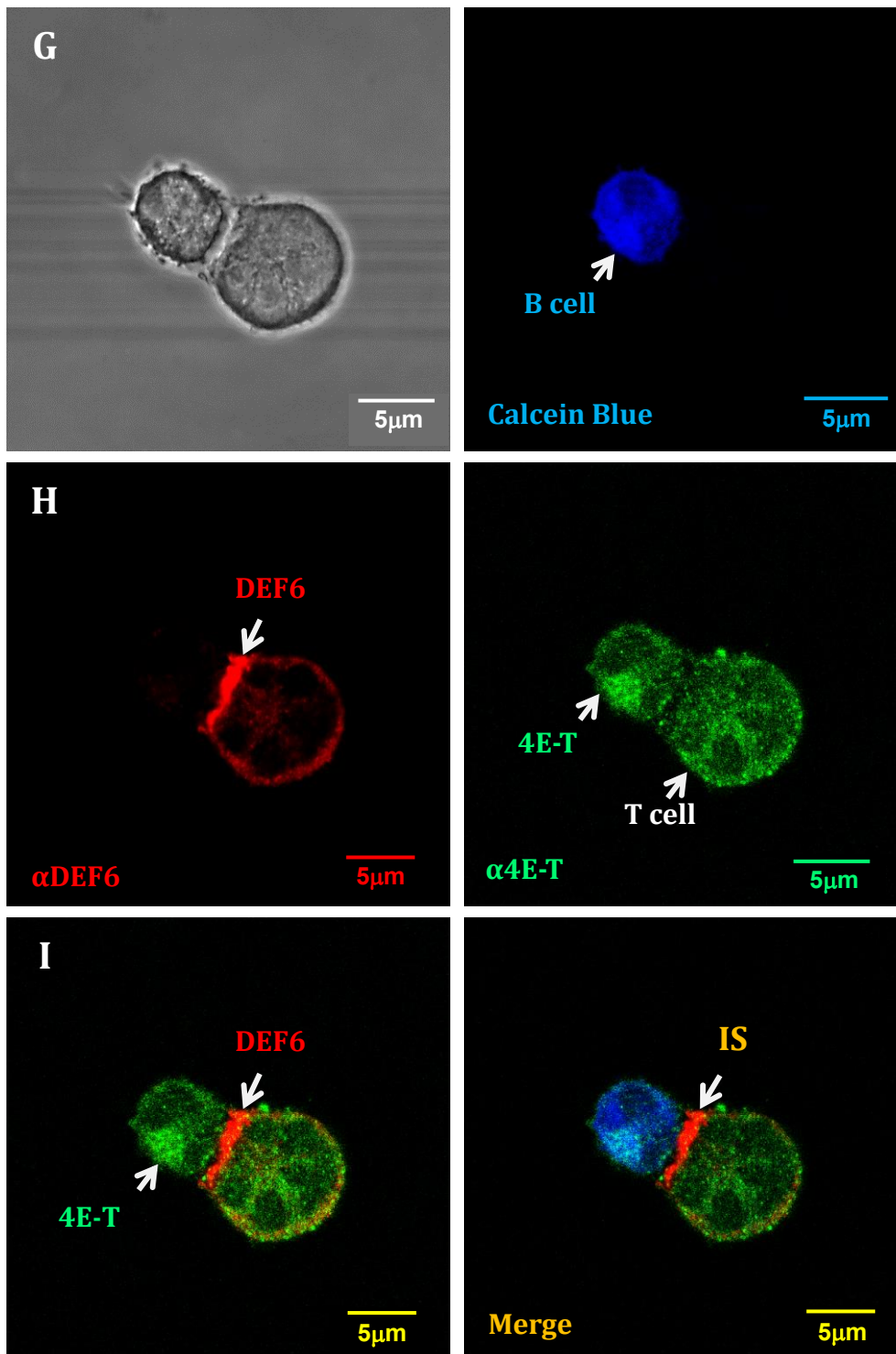


**Figure 3.6.2: DEF6 colocalisation with proteins of the mRNA initiation complex in the IS**

**A, D, G)** Left panels: phase contrast image of the participating B and T cells. Right panels: Calcein blue staining of Raji B cells. **B)** DEF6 (red; Alexa 568) and eIF4E (green, Alexa 488). **C)** Merged images of B (left panel) and A and B (right panel). **E)** DEF6 (red; Alexa 568) and PABP (green, Alexa 488). **F)** Merged images of E (left panel) and D and E (right panel). **H)** DEF6 (red; Alexa 568) and 4E-T (green, Alexa 488). **I)** Merged images of H (left panel) and G and H (right panel). White arrows indicate T and B cells as well as the IS. Images were taken using a Zeiss

LSM710 confocal microscope at a 63x magnification and 2x zoom. Data are representative of three independent experiments. Scale bar: 5 $\mu$ m.

## Summary of major findings

- Deletion of the coiled coil domain results in spontaneous colocalisation of DEF6 N-terminal mutants with P-body marker DCP1 and serine and/or threonine phosphorylation in the C-terminal end of DEF6 results in aggregates that trap DCP1
- DEF6 colocalises with nascent translational and with translational initiation factor eIF4E and the eIF4E-binding protein 4E-T in resting Jurkat T cells
- DEF6 physically interacts with eIF4E and 4E-T but not with PABP
- Protein expression of eIF4E, 4E-T and PABP in Jurkat T cells is positively correlated with DEF6 expression
- Neither overexpression nor knockdown of DEF6 affect gene expression of eIF4E, 4E-T or PABP and DEF6 siRNA-mediated downregulation of eIF4E does not seem to be due to protein degradation via autophagy or ubiquitin proteasome pathways
- DEF6 colocalises with eIF4E and PABP, but not 4E-T at the Immune synapse

## **Chapter 4 Discussion**

## 4.1 Structure-function analysis of DEF6

### 4.1.1 The coiled coil domain constrains the N-terminal end of DEF6 to target P-bodies

The DEF6 domain structure is shared by its only homologue SWAP70 and is highly conserved from human to *tricoplax adhaerens* (Shuen, MRes 2010). The two N-terminal EF hands bind  $\text{Ca}^{2+}$  (Bécart *et al.*, 2008; Fos *et al.*, 2014), the immunoreceptor tyrosine-based activation motif (ITAM) is target for LCK phosphorylation (Bécart *et al.*, 2008a; Hey *et al.*, 2012), the central pleckstrine-homology domain (PH) binds PIP3 (Mavrakis *et al.* 2004, Tanaka *et al.*, 2003) and the C-terminal end acts like a dbl-homology domain (DH-like) that contains a coiled coil domain and facilitates GEF activity (Mavrakis *et al.*, 2004, Hey *et al.*, 2012; Cheng, PhD 2017). However, several analyses have shown that DEF6 can adopt different functions upon posttranslational modification and postulated conformational change including colocalisation with P-bodies (Hey *et al.*, 2012) and coiled coil-mediated aggregation (Cheng, PhD 2017). Initially, Mollett had demonstrated that the first 108 amino acids of DEF6 fused to GFP were sufficient to colocalise with P-bodies, whereas the GFP-tagged DHL domain (amino acids 312-590) was associated with P-bodies but did not overlap with them (Mollett, PhD 2014). Fellow postgraduate Huaitao Cheng established that indeed the first 45 amino acids including one EF hand were sufficient to target P-bodies but the first 35 amino acids were not (Cheng, PhD 2017). To establish which domains(s) in the wild type DEF6 protein conformation is restraining its ability to localise with P-bodies by masking the N-terminal end, mutant GFP-tagged N216 (containing EF hands and ITAM domains) and N312 (containing EF hands, ITAM and Ph domains but lacking

the DHL domain) were expressed in COS7 cells in conjunction with the P-body marker DCP1. Both mutant proteins spontaneously colocalised with DCP1 indicating that it is the coiled coil domain that constrains the N-terminal end in the native conformation. The protein structure of DEF6 is unknown but modelling using I-Tasser (<https://zhanglab.ccmb.med.umich.edu/I-TASSER/>; Roy *et al.*, 2010; Zhang, 2008 and 2009) predicted a conserved structure for DEF6 and SWAP70 orthologues that resembled a 'donut' with the C-terminal end contacting the N-terminal end (Shuen, MRes 2010). This predicted conformation of unmodified wild type DEF6 is certainly in line with the results obtained here and would suggest that some type of posttranslational modifications such as phosphorylation are required to release the constrain mediated through the coiled coil domain. Together, these results correct the initial interpretation by Hey *et al.* (2012) who proposed that phosphorylation of the residues Y210 and Y222 by ITK would release the coiled coil domain of DEF6 resulting in granule formation and P-body colocalisation. As shown here, the coiled coil domain is not essential for P-body colocalisation but instead phosphorylation of DEF6 renders the conformation releasing the coiled coil-mediated constrain.

#### **4.1.2 Serine/threonine phosphorylation in the C-terminal end of DEF6 results in coiled coil-mediated aggregation that trap DCP1**

Several proteomic studies have identified serine and threonine residues in DEF6 that are phosphorylated in T cells (Mayya *et al.*, 2009; Navarro *et al.*, 2011; Ruperez *et al.*, 2012). In particular, the C-terminal end of DEF6 (amino acids S537 to S618) contains 9 serine and 4 threonine residues that have been

shown to be phosphorylated many of which in human and mouse T cells (<https://www.phosphosite.org/proteinAction.action?id=21147&showAllSites=true>).

However, until recently, it was not known what functional and structural consequences serine/threonine phosphorylation of DEF6 would have. To test this, selected phosphomimic (S/T to E) and phosphosilent (S/T to F) mutant DEF6 proteins were established and GFP-tagged versions of these expressed in COS7 cells. As listed in table 3, most phosphomimic mutants tested formed large aggregates that trapped DCP1 altering its normal cytoplasmic distribution. Phosphosilent mutants on the other hand were less prone to aggregation but were more diffuse with some granule formation that often overlapped with DCP1. It seems therefore that the observed serine/threonine phosphorylation in T cells would result in conformational change of DEF6 that facilitates aggregation. More detailed structure-function analysis by Cheng (PhD 2017), revealed that aggregation of DEF6 is mediated through an uncontrolled interaction of the coiled coil domain resulting in formation of large cytoplasmic structures. These structures, as shown here for some phosphomimic mutants, trapped DCP1 presumably through interaction of the coiled coil domain of DEF6 with coiled coil domains frequently found in proteins within P-bodies (Fiumara *et al.*, 2010). However, it remains to be seen whether DEF6 aggregates trap entire P-bodies or just the coexpressed mCherry-tagged DCP1.

Recently, Joshi *et al.* (2017) showed that residues T595 and S597 of DEF6 are phosphorylated upon TCR-mediated activation in conventional T cells (Tcons) from human and that suppression of Tcons by regulatory T cells (Tregs) results in dephosphorylation of these residues. Furthermore,

phosphosilent (S/T to A) mutants repeal the interaction of DEF6 with the IP3 receptor and affected NFAT activation and cytokine transcription (Joshi *et al.*, 2017). While neither T595A/S597A nor T595E/S597E mutants were tested here, mutant T595E formed aggregates and T595F was diffuse with some granule formation. T595E in conjunction with other phosphomimic mutations also formed aggregates. S597E on its own was not tested here, but in conjunction with other phosphomimic mutations also formed aggregates whereas S597F on its own was diffuse with some granule formation. So, it remains to be seen how phosphorylation of T595 and S597 alters the conformation of DEF6 allowing interaction with IP3 receptor as proposed by Joshi *et al.*, (2017).

## **4.2 DEF6 function in mRNA translation**

### **4.2.1 DEF6 is associated with the nascent mRNA translation**

As discussed earlier, DEF6 had been copurified with ribosomes and polysomes (Fig.1.3.3) from resting Jurkat T cells and as shown in figure 3.4.1, a subset of DEF6 is associated with a subset of translational initiation complexes in resting Jurkat T cells. Together, these results establish a novel role for DEF6 in the regulation of translation at both initiation and elongation stages of selected mRNAs.

### **4.2.2 DEF6 is associated with the translational initiation complex binding eIF4E**

Previous analysis by fellow graduate student Kerry Remon demonstrated that DEF6 is in proximity to initiation factor eIF4E and the result shown here confirmed colocalisation of DEF6 with eIF4E (Remon, PhD 2016). Moreover, DEF6 and eIF4E interact *in vitro* suggesting that DEF6 is directly contacting eIF4E in the translational initiation complex rather than the 5' cap of the mRNA which DEF6 did not bind to. Furthermore, while DEF6 also colocalised with PABP, it did not bind PABP *in vitro* suggesting that close proximity to and colocalisation of DEF6 with PABP is due to the interaction of PABP with eIF4E (Jackson *et al.*, 2010, de Melo Neto *et al.*, 2015)

Together these data firmly establish that DEF6 in unstimulated resting Jurkat T cells is part of a subset of translation initiation complexes as well as translational elongation in polysomes.

### 4.2.3 DEF6 binds eIF4E-binding protein 4E-T

The transporter of eIF4E, known as 4E-T, is a P-body marker that is expressed in many different species such as mice, rats, yeast and *Drosophila* (Ferraiuolo *et al.*, 2005; Dostie *et al.*, 2000). Initial observations by Remon (PhD 2016) showed that some DEF6 and 4E-T colocalised in resting Jurkat cells (which was confirmed here) and that cellular stress through treatment with sodium arsenate increased colocalisation significantly. This data is in line with the findings by Hey *et al.*, (2012) that showed that arsenate treatment resulted in wild type DEF6 colocalising with P-bodies and that ITK phosphomimic mutant Y210E/Y222E spontaneously colocalised with P-bodies. Proteomics data summarised in BioGrid (<https://thebiogrid.org/119099/summary/homo-sapiens/def6.html>) suggested that DEF6 interacts with 4E-T (here called EIF4ENIF1). Coimmunoprecipitation of 4E-T with DEF6 *in vitro* confirmed this interaction. It is not known how DEF6 associated with P-bodies, but it might well be through interaction with 4E-T. If so, then the N-terminal 45 amino acids of DEF6 should interact with 4E-T but this has not been tested. On the other hand, recruitment to P-bodies mediated through the N-terminal end could be independent from interaction with other proteins including 4E-T within P-bodies. Nevertheless, DEF6 seems to play a role not only in mRNA translational initiation and elongation but also in storage and/or degradation of mRNAs in P-bodies.

### 4.2.5 DEF6 controls protein expression of eIF4E, PABP and 4E-T

To further elucidate the functional role of DEF6 in mRNA translation and metabolism, cellular localisation of eIF4E, PABP and 4E-T were analysed in

siRNA-mediated knockdown of DEF6 expression in Jurkat cells. Immunocytochemistry analysis revealed that knockdown of DEF6 had a profound effect on the expression level of eIF4E and 4E-T rather than their cellular localisation. Western blot analysis demonstrated that in the absence of DEF6, expression of eIF4E, PABP and 4E-T was abolished. Moreover, ectopic overexpression of GFP-tagged DEF6 in Jurkat cells resulted in elevated expression of these proteins. RT-PCR analyses suggested that expression of the corresponding genes was similar comparing wild type and siRNA-mediated DEF6 knockdown or GFP-tagged DEF6 overexpressing Jurkat cells eliminating transcriptional regulation and hinting towards translational regulation.

In any case, at this point the data established a clear positive correlation between DEF6 expression and expression of eIF4E, PABP and 4E-T.

#### **4.2.6 DEF6 controls translation of eIF4E**

While all the evidence so far suggested that DEF6 is regulating mRNA translation of a subset of mRNAs including those encoding eIF4E, PABP and 4E-T, it was also possible that in the absence of DEF6 protein degradation is enhanced resulting in rapid loss of eIF4E, PABP and 4E-T proteins while other proteins such as ARP2/3 would not be affected. Two main pathways regulate protein degradation: the ubiquitin proteasome pathway and autophagy (Ge *et al.*, 2009). Both pathways can be blocked through the established inhibitors MG132 (ubiquitin proteasome pathway; Lee & Goldberg 1998) or bafilomycin A1 (autophagy pathway; Zhang *et al.*, 2014). However, neither treatment of Jurkat cells that had been transfected with DEF6 siRNAs resulted in a rescue of eIF4E expression (Fig.3.5.4) suggesting that the absence of eIF4E in DEF6

knockdown Jurkat cells is not due to protein degradation through either of these two pathways. Due to time constraints it was not tested whether this is also the case for PABP and 4E-T. Nevertheless, these preliminary data are in line with the overall interpretation that DEF6 plays a crucial role in the translational control of eIF4E, PABP and 4E-T.

Indeed, recently it was shown that DEF6-deficient T cells had elevated BCL6 expression and that this was due to enhanced activation of the mTORC1-4E-BP-eIF4E axis, secondary to the aberrant assembly of a raptor-p62-TRAF6 complex (Yi *et al.*, 2017). DEF6 was shown to interact with TRAF6 and p62 preventing the assembly of the raptor-p62-TRAF6 complex inhibiting activation of mTORC1. Proteomics analysis of nuclear extracts from DEF6-deficient T cells identified 20 proteins whose expression was upregulated and 18 whose expression was downregulated (Yi *et al.*, 2017). While eIF4E was not among those proteins that were down regulated presumably because nuclear extracts had been analysed, eIF4E was shown to control protein expression of BCL6 in diffuse large B cell lymphomas (Culjkovic-Kraljacic *et al.*, 2016). In addition, eIF4E enhances translation of a specific subset of mRNAs during cellular stress and knockdown of eIF4E selectively affects these transcripts without a global decrease in protein levels (Yanagiya *et al.*, 2012; Bhat *et al.*, 2015). Furthermore, during the T cell activation, eIF4E translation is induced which in turn led to the translation of cell cycle related mRNAs and proliferation (Bjur *et al.*, 2013; Piccirillo *et al.*, 2014). It is plausible therefore that upon TCR-mediated activation DEF6 is enhancing eIF4E protein translation, but this needs to be established. Nevertheless, together these data clearly establish that DEF6 controls protein synthesis in addition to its known roles in

cytoskeletal organisation, immunological synapse function,  $\text{Ca}^{2+}$  homeostasis and transcription factor activity (Mavrakis *et al.*, 2004, Bécart *et al.*, 2009; Biswas *et al.*, 2010).

### 4.3 Translational control in the immunological synapse

It is now well established that mRNAs are transported to various cellular localisations and are translated on site and the translation initiation factor eIF4E acts as a major node for this regulation (Besse and Ephrussi, 2008; Jung *et al.*, 2014; Piccirillo *et al.*, 2014). The mTORC1 pathway has been shown to play a central role in the regulation of translation. mTORC1 is a kinase phosphorylating eIF4E-binding proteins (4E-BPs) that as a result dissociate from eIF4E, thereby enabling assembly of the translational initiation complex. The mTORC1–4E-BP–eIF4E axis influences the translation of many mRNAs that encode proteins with central roles in immunology, such as the transcription factors IRF7 (Colina *et al.*, 2008) and GATA-3 (Cook *et al.*, 2010), the cytokine interleukin 4 (IL-4; Gigoux *et al.*, 2014) and, as discussed above, is inhibited by DEF6 (Yi *et al.*, 2017). It is not known whether mRNA translation is occurring in the IS but local translation in axons and neurological synapses have long been known regulating axon pathfinding, mitochondrial function and synapse-specific plasticity (Korsak *et al.*, 2016). The finding that DEF6 colocalises with eIF4E as well as PABP, but not with 4E-T in the IS would suggest that DEF6-mediated mRNA translational control is not restricted to resting T cells but might also occur in the IS. If so, target mRNAs need to be identified perhaps through crosslinking DEF6/eIF4E and the mRNA and subsequent sequencing of the mRNAs.

#### 4.4 DEF6: a multifunctional signalling hub in T cells

DEF6 function in T cells is remarkably diverse linking TCR-mediated signalling, cytoskeletal organisation,  $\text{Ca}^{2+}$  homeostasis, transcription factor activity and control of mRNA translation. Its versatile functions are likely dependent upon conformational change, some of which can be triggered through tyrosine or serine/threonine phosphorylation and possibly other posttranslational modifications. In addition, it seems that association with itself and/or other proteins might also influence conformation and function. While the N-terminal end targets DEF6 to P-bodies, the coiled coil domain facilitates oligomerisation under controlled conditions resulting in GEF activity, but it mediates the formation of aggregates that form a large cytoplasmic structure when unleashed (Cheng, PhD 2017). While phosphorylation of tyrosine residues 210 and 222 by ITK results in P-body localisation (Hey *et al.*, 2012), it is not known what modification and domains of DEF6 are required to bind eIF4E, PABP or 4E-T nor is it clear how DEF6 is associated with polysomes. Given that the results described here clearly indicate that only a subset of DEF6 is engaged in any of the above functions it is plausible that DEF6 molecules adopt different conformations and functions at any given time but that needs to be established. How DEF6 is actually regulating the expression of proteins such as eIF4E, PABP and 4E-T is also not known but might be connected to the mTORC1–4E-BP–eIF4E axis (Yi *et al.*, 2017).

## **Conclusion**

DEF6 is involved in active mRNA translation in resting and activated Jurkat T cells controlling expression of components of the translational initiation complex as well as P-bodies.

## References

- Aitken, C.E. & Lorsch, J.R (2012). "A mechanistic overview of translation initiation in eukaryotes." *Nature Structural & Molecular Biology* 19: pp. 568–576.
- Altman, A. & Bécart, S (2009). "Does Def6 deficiency cause autoimmunity?" *Immunity* 31(1): 1-2; author reply 2-3.
- Alarcón, B., Mestre, D, Martínez-Martín, N (2011). "The immunological synapse: a cause or consequence of T-cell receptor triggering?" *Immunology* 133(4): 420-425.
- Anderson, P. & Kedersha, N (2002). "Visibly stressed: the role of eIF2, TIA-1, and stress granules in protein translation." *Cell Stress & Chaperones*, 7, 213-221.
- Anderson, P. & Kedersha, N (2006). "RNA granules". *Journal of Cell Biology*, 172, 803-808.
- Andrei, M. A., Ingelfinger, D., Heintzmann, R., Achsel, T., Rivera-Pomar, R. & Luhrmann, R (2005). "A role for eIF4E and eIF4E-transporter in targeting mRNPs to mammalian processing bodies." *Rna-a Publication of the Rna Society*, 11, 717-727.
- Bashkirov, V. I., Scherthan, H., Solinger, J. A., Buerstedde, J. M. & Heyer, W. D. (1997). "A mouse cytoplasmic exoribonuclease (mXRN1p) with preference for G4 tetraplex substrates." *Journal of Cell Biology*, 136, 761-773.
- Bachmann, M. F., Mckall-Faienza, K., Schmits, R., Bouchard, D., Beach, J., Speiser, D.E., Mak, T.W., Ohashi, P.S (1997). "Distinct roles for LFA-1 and CD28 during activation of naive T cells: adhesion versus costimulation." *Immunity*, 7, 549-57.
- Besse, F., López de Quinto, S., Marchand, V., Trucco, A., Ephrussi, A., (2009). "Drosophila PTB promotes formation of high-order RNP particles and represses oskar translation." *Genes Dev* 23(2): 195-207.
- Besse, F, Ephrussi, A. (2008) " Translational control of localized mRNAs: restricting protein synthesis in space and time" *Nat Rev Mol Cell Biol.* (12):971-80

- Bécart, S., Charvet, C., Canonigo Balancio, A. J., De Trez, C., Tanaka, Y., Duan, W., Ware, C., Croft, M., Altman, A. (2007). "SLAT regulates Th1 and Th2 inflammatory responses by controlling Ca<sup>2+</sup>/NFAT signaling." *J Clin Invest* 117(8): 2164-2175.
- Bécart, S. & Altman, A (2009). "SWAP-70-like adapter of T cells: a novel Lck-regulated guanine nucleotide exchange factor coordinating actin cytoskeleton reorganization and Ca<sup>2+</sup> signaling in T cells." *Immunol Rev* 232(1): 319-333.
- Bécart, S., Balancio, A.J., Charvet, C., Feau, S., Sedwick, C.E, Altman, A (2008a). "Tyrosine-phosphorylation-dependent translocation of the SLAT protein to the immunological synapse is required for NFAT transcription factor activation." *Immunity* 29(5): 704-719.
- Beal, A. M., Anikeeva, N., Varma, R., Cameron, T.O, Vasiliver-Shamis, G., Norris, P.J., Dustin, M.L., Sykulev, Y (2009). "Kinetics of early T cell receptor signaling regulate the pathway of lytic granule delivery to the secretory domain." *Immunity* 31(4): 632-642.
- Biswas, S.K, Mantovani, A (2010) " Macrophage plasticity and interaction with lymphocyte subsets: cancer as a paradigm" *Nat Immunol.* (10):889-96
- Billadeau, D. D., Nolz, J.C., & GOMEZ, T.S (2007). "Regulation of T-cell activation by the cytoskeleton." *Nat Rev Immunol*, 7, 131-43.
- Biswas, P. S., Gupta, S., Stirzaker, R. A., Kumar, V., Jessberger, R., Lu, T. T., Bhagat G., Pernis A. B (2012). "Dual regulation of IRF4 function in T and B cells is required for the coordination of T-B cell interactions and the prevention of autoimmunity." *J Exp Med* 209(3): 581-596.
- Binder N, Miller C, Yoshida M, Inoue K, Nakano S, Hu X, Ivashkiv LB, Schett G, Pernis A, Goldring SR, Ross FP, Zhao B. (2017). "Def6 Restrains Osteoclastogenesis and Inflammatory Bone Resorption." *J Immunol.*; 198(9):3436-3447.
- Bhat, M, Robichaud, N, Hulea, L, Sonenberg, N, Pelletier, J, Topisirovic, I (2015) " Targeting the translation machinery in cancer" *Nat Rev Drug Discov.* (4):261-78

- Bjur, E, Larsson, O, Yurchenko, E, Zheng, L, Gandin, V, Topisirovic, I, Li, S, Wagner, C.R, Sonenberg, N, Piccirillo, C.A (2013) "Distinct translational control in CD4+ T cell subsets" *PLoS Genet.* (5): e1003494
- Blower, M. D. (2013). "Molecular insights into intracellular RNA localization." *Int Rev Cell Mol Biol* 302: 1-39.
- Borggreffe, T., Wabl, M., Akhmedov A. T., Jessberger, R. (1998). "A B-cell-specific DNA recombination complex." *J Biol Chem* 273(27): 17025-17035.
- Borggreffe, T., Masat, L., Wabl, M., Riwar, B., Cattoretti, G., Jessberger R. (1999)." Cellular, intracellular, and developmental expression patterns of murine SWAP-70." *Eur J Immunol.* 29(6):1812-22
- Buchan, J.R & Parker, R (2009). "Eukaryotic stress granules: The ins and outs of translation." *Mol Cell* 36: pp. 932–941.
- Canonigo-Balancio, A. J., Fos, C., Prod'homme, T., Bécart S., Altman, A. (2009). "SLAT/Def6 plays a critical role in the development of Th17 cell-mediated experimental autoimmune encephalomyelitis." *J Immunol* 183(11): 7259-7267.
- Chen, Q., Yang, W., Gupta, S., Biswas, P., Smith, P., Bhagat, G., Pernis A. B (2008). "IRF-4-binding protein inhibits interleukin-17 and interleukin-21 production by controlling the activity of IRF-4 transcription factor." *Immunity* 29(6): 899-911.
- Cheng, H. (2017). Structure-Fuction Relationship of DEF6.
- Côte M, Fos C, Canonigo-Balancio AJ, Ley K, Bécart S, Altman A (2015)."SLAT promotes TCR-mediated, Rap1-dependent LFA-1 activation and adhesion through interaction of its PH domain with Rap1." *J Cell Sci.*; pp. 128(23):4341-52.
- Colina, R, Costa-Mattioli, M, Dowling, R.J, Jaramillo, M, Tai, L.H, Breitbach, C.J, Martineau, Y, Larsson, O, Rong, L, Svitkin, Y.V, Makrigiannis, A.P, Bell, J.C, Sonenberg, N. (2008) " Translational control of the innate immune response through IRF-7" *Nature.* 452(7185):323-8
- Cook, K.D., Miller, J (2010). "TCR-dependent translational control of GATA-3 enhances Th2 differentiation." *J Immunol,* 185(6):3209-16.

- Crotty, S. (2011). "Follicular helper CD4 T cells (TFH)." *Annu Rev Immunol* 29: 621-663.
- Culjkovic-Kraljacic, B, Fernando, T.M, Marullo, R, Calvo-Vidal, N, Verma, A, Yang S, Tabbò, F, Gaudio, M, Zahreddine, H, Goldstein R.L, Patel J, Taldone T, Chiosis G, Ladetto M, Ghione P, Machiorlatti R, Elemento O, Inghirami G, Melnick A, Borden KL, Cerchietti L (2016) "Combinatorial targeting of nuclear export and translation of RNA inhibits aggressive B-cell lymphomas" *Blood*. 127(7):858-68
- Davis, D. M. & Dustin, M. L (2004). "What is the importance of the immunological synapse?" *Trends Immunol* 25(6): 323-327.
- Daniels, R. H. & Bokoch, G. M (1999). "P21-activated protein kinase: a crucial component of morphological signaling?" *Trends Biochem Sci* 24(9): 350-355.
- Delon, J. (2000). "The immunological synapse." *Curr Biol* 10(6): R214.
- Decker, C. J. & Parker, R (2012). "P-Bodies and Stress Granules: Possible Roles in the Control of Translation and mRNA Degradation". *Cold Spring Harbor Perspectives in Biology*, 4, a012286.
- De Melo Neto O.P., da Costa Lima, T.D., Xavier, C.C., Nascimento, L.M., Romão, T.P., Assis, L.A., Pereira, M.M., Reis, C.R., Papadopoulou, B. (2015) "The unique Leishmania EIF4E4 N-terminus is a target for multiple phosphorylation events and participates in critical interactions required for translation initiation" *RNA Biol*.12 (11):1209-21
- Dostie, J., Ferraiuolo, M., Pause, A., Adam, S.A., Sonenberg, N. (2000) "A novel shuttling protein, 4E-T, mediates the nuclear import of the mRNA 5' cap-binding protein, eIF4E." *EMBO J*.19(12):3142-56.
- Dustin, M.L., Olszowy, M.W., Holdorf, A.D., Li, J., Bromley, S., Desai, N., Widder, P., Rosenberger, F., van der Merwe, P.A, Allen, P.M., Shaw, A.S (1998). "A novel adaptor protein orchestrates receptor patterning and cytoskeletal polarity in T-cell contacts." *Cell*. 94:667–677.
- Dustin, M. L. & Chan, A. C (2000). "Signaling takes shape in the immune system." *Cell* 103(2): 283-294.

- Dustin, M. L. (2008). "T-cell activation through immunological synapses and kinapses." *Immunol Rev* 221: 77-89.
- Dustin, M. L., Chakraborty, A. K., Shaw, A. S (2010). "Understanding the structure and function of the immunological synapse." *Cold Spring Harb Perspect Biol* 2(10): a002311.
- Eulalio, A., Behm-Ansmant, I., Izaurralde, E (2007a). "P bodies: at the crossroads of post-transcriptional pathways." *Nat Rev Mol Cell Biol* 8(1): 9-22.
- Eulalio, A., Behm-Ansment, I., Schweizer, D., Izaurralde, E (2007b)." P-body formation is a consequence, not the cause, of RNA-mediated gene silencing." *Molecular and Cellular Biology*, 27, 3970-3981.
- Eulalio, A., Helms, S., Fritsch, C., Fauser, M., Izaurralde, E (2009). "A C-terminal silencing domain in GW182 is essential for miRNA function." *RNA*, 15, 1067-77.
- Fanzo, J. C., Yang, W., Jang, S. Y., Gupta, S., Chen, Q., Siddiq, A., Greenberg, S., Pernis, A. B (2006). "Loss of IRF-4-binding protein leads to the spontaneous development of systemic autoimmunity." *J Clin Invest* 116(3): 703-714.
- Ferraiuolo, M. A., Basak, S., Dostie, J., Murray, E. L., Schoenberg, D. R., Sonenberg, N (2005). "A role for the eIF4E-binding protein 4E-T in P-body formation and mRNA decay." *J Cell Biol*, 170, 913-24.
- Feau, S., Schoenberger, S. P., Altman, A., Bécart, S. (2013). "SLAT regulates CD8+ T cell clonal expansion in a Cdc42- and NFAT1-dependent manner." *J Immunol* 190(1): 174-183.
- Friedl, P. & Gunzer, M (2001)." Interaction of T cells with APCs: the serial encounter model". *Trends Immunol* 22(4):187-91.
- Frischmeyer, P.A, van Hoof, A., O'Donnell, K., Guerrerio, A.L., Parker, R., Dietz, H.C (2002)." An mRNA surveillance mechanism that eliminates transcripts lacking termination codons." *Science* 295: pp. 2258–2261.
- Franks, T.M & Lykke-Andersen, J. (2008)."The control of mRNA decapping and P body formation." *Mol Cell* 32: pp. 605–615.

- Fiumara, F., Fioriti, L., Kandel, E.R., Hendrickson, W.A (2012). Essential role of coiled-coils for aggregation and activity of Q/N- rich prions and polyQ proteins, *Cell*. 143 (7), 1121–1135
- Fos, C., Becart, S., Canonigo Balancio, A.J., Boehning, D., Altman, A (2014).” Association of the EF-hand and PH domains of the guanine nucleotide exchange factor SLAT with IP<sub>3</sub> receptor 1 promotes Ca<sup>2+</sup> signaling in T cells”. *Sci Signal*. 7 (345): ra93.
- Furic, L., Rong. L, Larsson O, Koumakpayi I.H, Yoshida. K, Brueschke. A, Petroulakis. E, Robichaud. N, Pollak .M, Gaboury. L.A, Pandolfi. P.P, Saad. F., Sonenberg. N (2010).” eIF4E phosphorylation promotes tumorigenesis and is associated with prostate cancer progression.” *Proc Natl Acad Sci U S A*. 10; 107(32): 14134–14139.
- Garneau, N.L, Wilusz, J., Wilusz, C.J. (2007).” The highways and byways of mRNA decay.”*Nature reviews Mol Cell Biol* 8 (2):113-26
- Ge, P.F., Zhang, J.Z., Wang, X.F., Meng, F.K., Li, W.C., Luan, Y.X., Ling, F., Luo, Y.N (2009).” Inhibition of autophagy induced by proteasome inhibition increases cell death in human SHG-44 glioma cells” *Acta Pharmacol Sin*. 30 (7):1046-52
- Gingras AC., Raught B., Sonenberg N. (1999)” eIF4 initiation factors: effectors of mRNA recruitment to ribosomes and regulators of translation.” *Annu Rev Biochem* 68:913-63.
- Gigoux, M, Lovato, A, Leconte, J, Leung, J, Sonenberg, N, Suh, W.K (2014) “ Inducible costimulator facilitates T-dependent B cell activation by augmenting IL-4 translation” *Mol Immunol*. 59(1):46-54.
- Guhaniyogi, J. & Brewer, G (2001) Regulation of mRNA stability in mammalian cells. *Gene*, 265(1-2): pp. 11–23.
- Gupta, S., Fanzo, J. C., Hu, C., Cox, D., Jang, S. Y., Lee, A. E., Greenberg S., Pernis, A. B (2003). "T cell receptor engagement leads to the recruitment of IBP, a novel guanine nucleotide exchange factor, to the immunological synapse." *J Biol Chem* 278(44): 43541-43549.

- Gupta, S., Lee, A., Hu, C., Fanzo, J., Goldberg, I., Cattoretti, G., Pernis, A. B (2003) "Molecular cloning of IBP, a SWAP-70 homologous GEF, which is highly expressed in the immune system" *Human Immunology*. 64(4):389-401.
- Hall, A. (1998). "Rho GTPases and the actin cytoskeleton." *Science* 279(5350): 509-514.
- Hey, F., Czyzewicz, N., Jones, P., Sablitzky, F (2012). "DEF6, a novel substrate for the Tec kinase ITK, contains a glutamine-rich aggregation-prone region and forms cytoplasmic granules that co-localize with P-bodies." *J Biol Chem* 287(37): 31073-31084.
- Hotfilder, M., Baxendale, S., Cross, M. A., Sablitzky, F (1999). "Def-2, -3, -6 and -8, novel mouse genes differentially expressed in the haemopoietic system." *Br J Haematol* 106(2): 335-344.
- Huppa, J. B. & Davis, M. M. (2003). "T-cell-antigen recognition and the immunological synapse." *Nat Rev Immunol* 3(12): 973-983.
- Huber, M., Brüstle, A., Reinhard, K., Guralnik, A., Walter, G., Mahiny, A., von Löw, E., Lohoff, M (2008). "IRF4 is essential for IL-21-mediated induction, amplification, and stabilization of the Th17 phenotype." *Proc Natl Acad Sci USA* 105(52): 20846-20851.
- Ingelfinger, D., Arndt-Jovin, D. J., Luhrmann, R., Achsel, T (2002). "The human LSm1-7 proteins colocalize with the mRNA-degrading enzymes Dcp1/2 and Xrn1 in distinct cytoplasmic foci." *RNA*, 8, 1489-501.
- Jackson, R. J., Hellen, C. U. T., Pestova, T. V (2010). "The mechanism of eukaryotic translation initiation and principles of its regulation." *Nat Rev Mol Cell Biol*, 11, 113-127.
- Joshi, R. N., Binai, N. A., Marabita, F., Sui, Z., Altman, A., Heck, A. J. R., Tegnér, J., Schmidt, A (2017). "Phosphoproteomics Reveals Regulatory T Cell-Mediated DEF6 Dephosphorylation That Affects Cytokine Expression in Human Conventional T Cells". *Front Immunol*, 8:1163
- Jung, H., Gkogkas, C.G., Sonenberg, N., Holt, C.E (2014). "Remote control of gene function by local translation." *Cell*, 157(1):26-40

- Kawakami, A., Tian, Q., Duan, X., Streuli, M., Schlossman, S. F., Anderson, P (1992). "Identification and functional characterization of a TIA-1-related nucleolysin". *Proc Natl Acad Sci U S A*, 89, 8681-5.
- Kahvejian, A., Roy, G., Sonenberg, N. (2001). "The mRNA closed-loop model: the function of PABP and PABP-interacting proteins in mRNA translation." *Cold Spring Harb Symp Quant Biol*, 66, 293-300.
- Kaizuka, Y., Douglass, A.D., Varma, R., Dustin, M.L., Vale, R.D (2007). "Mechanisms for segregating T cell receptor and adhesion molecules during immunological synapse formation in Jurkat T cells." *Proc Natl Acad Sci U S A*, 104, 20296-301.
- Kamenska, A., Lu WT, Kubacka, D., Broomhead, H., Minshall, N., Bushell, M., Standart, N (2014). "Human 4E-T represses translation of bound mRNAs and enhances microRNA-mediated silencing." *Nucleic Acids Res.* (5): pp. 3298-313.
- Kedersha, N., Stoecklin, G., Ayodele, M., Yacono, P., Lykke-Andersen, J., Fritzler, M. J., Scheuner, D., Kaufman, R. J., Golan, D. E., Anderson, P. (2005). "Stress granules and processing bodies are dynamically linked sites of mRNP remodeling." *J Cell Biol* 169(6): 871-884.
- Kentsis, A., Topisirovic, I., Culjkovic, B., Shao, L., Borden, K.L. (2004). "Ribavirin suppresses eIF4E-mediated oncogenic transformation by physical mimicry of the 7-methyl guanosine mRNA cap." *Proc Natl Acad Sci U S A*.101(52):18105-10.
- Kentsis, A., Volpon, L., Topisirovic, I., Soll, C.E., Culjkovic, B., Shao, L., Borden, K.L (2005) " Further evidence that ribavirin interacts with eIF4E". *RNA*. 11(12):1762-6
- Kim, S. T., Shin, Y., Brazin, K., Mallis, R.J., Sun, Z.Y., Wagner, G., Lang, M.J., Reinherz, E.L. (2012). " TCR Mechanobiology: Torques and Tunable Structures Linked to Early T cell Signaling." *Front Immunol*, 3, 76.
- Klein, U., S. Casola, G. Cattoretti, Q. Shen, M. Lia, T. Mo, T. Ludwig, K. Rajewsky and R. Dalla-Favera (2006). "Transcription factor IRF4 controls plasma cell differentiation and class-switch recombination." *Nat Immunol* 7(7): 773-782.

- Korn, T., Oukka, M., Kuchroo, V., Bettelli, E (2007). "Th17 cells: effector T cells with inflammatory properties." *Semin Immunol* 19(6): 362-371.
- Kohler, A. & Hurt, E (2007) Exporting RNA from the nucleus to the cytoplasm. *Nature reviews. Molecular cell biology*, 8(10): pp. 761–73.
- Korsak, L.I., Mitchell, M.E., Shepard, K.A., Akins, M.R (2016). " Regulation of neuronal gene expression by local axonal translation." *Curr Genet Med Rep*, (1):16-25
- Kuhn, J. R. & Poenie, M (2002). "Dynamic polarization of the microtubule cytoskeleton during CTL-mediated killing." *Immunity* 16(1): 111-121.
- Kumari, S., Curado, S., Mayya, V., Dustin, M. L. (2014). "T cell antigen receptor activation and actin cytoskeleton remodeling." *Biochim Biophys Acta* 1838(2): 546-556.
- Lee, D.H., Goldberg, A.L (1998)." Proteasome inhibitors: valuable new tools for cell biologists" *Trends Cell Biol.* 8(10):397- 403.
- Lee, K. H., Holdorf, A. D., Dustin, M. L., Chan, A. C., Allen, P. M., Shaw, A. S (2002). "T cell receptor signaling precedes immunological synapse formation." *Science* 295(5559): 1539-1542.
- Lewis, R. S. (2001). "Calcium signaling mechanisms in T lymphocytes." *Annu Rev Immunol* 19: 497-521.
- Linares, J.F., Duran, A., Reina-Campos, M., Aza-Blanc, P., Campos, A., Moscat, J., Diaz-Meco, M.T (2015) " Amino Acid Activation of mTORC1 by a PB1-Domain-Driven Kinase Complex Cascade" *Cell Rep.* 12(8):1339-52
- Masat, L., Caldwell, J., Armstrong, R., Khoshnevisan, H., Jessberger, R., Herndier, B., Wabl, M., Ferrick, D (2000)." Association of SWAP-70 with the B cell antigen receptor complex." *PNAS*, 97(5): 2180–2184.
- Mamane, Y., Petroulakis, E., Rong, L., Yoshida, K., Ler, L.W., Sonenberg, N (2004)."eIF4E-from translation to transformation." *Oncogene* 23(18): 3172-3179.

- Mavrakis, K. J., McKinlay, K. J., Jones, P., Sablitzky, F (2004). "DEF6, a novel PH-DH-like domain protein, is an upstream activator of the Rho GTPases Rac1, Cdc42, and RhoA." *Exp Cell Res* 294(2): 335-344.
- Martin, K. C. & Ephrussi, A (2009). "mRNA localization: gene expression in the spatial dimension." *Cell* 136(4): 719-730.
- Mayya, V., Lundgren, D. H., Hwang, S. I., Rezaul, K., Wu, L., Eng, J. K., Rodionov, V., and Han, D. K. (2009). "Quantitative phosphoproteomic analysis of T cell receptor signaling reveals system-wide modulation of protein-protein interactions". *Sci. Signal.* 2, ra46
- Marangoni, F., Murooka, T. T., Manzo, T., Kim, E. Y., Carrizosa, E., Elpek, N. M., Mempel, T. R. (2013). "The transcription factor NFAT exhibits signal memory during serial T cell interactions with antigen-presenting cells." *Immunity* 38(2): 237-249.
- Manni, M., Gupta, S., Nixon, B.G, Weaver, C.T., Jessberger, R., Pernis, A.B (2015). IRF4-Dependent and IRF4-Independent Pathways Contribute to DC Dysfunction in Lupus. *PLoS One*; 10(11): e0141927.
- Manni, M., Ricker, E., Pernis, A.B (2017) "Regulation of systemic autoimmunity and CD11c<sup>+</sup> Tbet<sup>+</sup> B cells by SWEF proteins" *Cell Immunol.* pii: S0008-8749(17)30103-X.
- Monks, C. R., Freiberg, B. A., Kupfer, H., Sciaky, N., Kupfer, A (1998). "Three-dimensional segregation of supramolecular activation clusters in T cells." *Nature* 395(6697): 82-86.
- Mollett, E. (2014). A study of DEF6 granule formation using biophysical and cellular methods.
- Muramatsu, M., Sankaranand, V. S., Anant, S., Sugai, M., Kinoshita, K., Davidson, N.O., Honjo, T (1999). "Specific expression of activation-induced cytidine deaminase (AID), a novel member of the RNA-editing deaminase family in germinal center B cells." *J Biol Chem* 274(26): 18470-18476.

- Nakayama, T. & Yamashita, M (2010). "The TCR-mediated signaling pathways that control the direction of helper T cell differentiation." *Semin Immunol* 22(5): 303-309.
- Navarro, M. N., Goebel, J., Feijoo-Carnero, C., Morrice, N., and Cantrell, D. A. (2011) "Phosphoproteomic analysis reveals an intrinsic pathway for the regulation of histone deacetylase 7 that controls the function of cytotoxic T lymphocytes". *Nat. Immunol.* 12, 352–361
- Nobes, C. D. & Hall, A (1995). "Rho, Rac, and cdc42 GTPases regulate the assembly of multimolecular focal complexes associated with actin stress fibers, lamellipodia, and filopodia." *Cell* 81(1): 53-62.
- Pernis, A.B (2009)" Rho GTPase-mediated pathways in mature CD4+ T cells". *Autoimmun Rev.* 8 (3):199-203
- Piccirillo, C.A, Bjur, E, Topisirovic, I, Sonenberg, N, Larsson, O (2014) " Translational control of immune responses: from transcripts to translomes" *Nat Immunol.* (6):503-11
- Protter, D. S., & Parker, R. (2016). Principles and properties of stress granules. *Trends in cell biology*, 26(9), 668-679)
- Ramesh, N., Antón, I. M., Hartwig, J. H., Geha, R. S (1997). "WIP, a protein associated with wiskott-aldrich syndrome protein, induces actin polymerization and redistribution in lymphoid cells." *Proc Natl Acad Sci USA* 94(26): 14671-14676.
- Remon, K.L (2016). DEF6 Aggregation is linked to Active Translation and mRNA turnover in T cells.
- Rivas, F. V., O'Keefe, J. P., Alegre, M. L., Gajewski, T. F (2004). "Actin cytoskeleton regulates calcium dynamics and NFAT nuclear duration." *Mol Cell Biol* 24(4): 1628-1639.
- Ripich, T., Chacón-Martínez, C.A., Fischer, L., Pernis, A., Kiessling, N., Garbe, A.I., Jessberger, R (2016)." SWEF Proteins Distinctly Control Maintenance and Differentiation of Hematopoietic Stem Cells." *PLoS One.* 11(8): e0161060.

- Rossman, K.L., Der, C.J., Sondek, J (2005) "GEF means go: turning on RHO GTPases with guanine nucleotide-exchange factors". *Nat Rev Mol Cell Biol*, 6 (2):167-80.
- Roy, A., Kucukural, A., Zhang, Y (2010). "I-TASSER: a unified platform for automated protein structure and function prediction" *Nat Protoc*, (4):725-38.
- Ruperez, P., Gago-Martinez, A., Burlingame, A.L., Oses-Prieto, J.A (2012). "Quantitative phosphoproteomic analysis reveals a role for serine and threonine kinases in the cytoskeletal reorganization in early T cell receptor activation in human primary T cells." *Mol Cell Proteomics*, (5):171-86.
- Samson, T., Will, C., Knoblauch, A., Sharek, L., von der Mark, K., Burridge, K., Wixler, V (2007) "Def-6, a guanine nucleotide exchange factor for Rac1, interacts with the skeletal muscle integrin chain alpha7A and influences myoblast differentiation" *J Biol Chem*. 282 (21):15730-42
- Sage, P. T., Varghese, L.M., Martinelli, R., Sciuto, T.E., Kamei, M., Dvorak, A.M., Springer, T.A., Sharpe, A.H., Carman C.V (2012). "Antigen Recognition Is Facilitated by Invadosome-like Protrusions Formed by Memory/Effector T Cells." *Journal of Immunology* 188, 3686-3699.
- Semba, C. P., & Gadek, T.R (2016). "Development of lifitegrast: a novel T-cell inhibitor for the treatment of dry eye disease. *Clinical Ophthalmology*, 10, 1083-1094.
- Schulze-Luehrmann, J., & Ghosh. S (2006). "Antigen-receptor signaling to nuclear factor kappa B." *Immunity* 25(5): 701-715.
- Shah, P., Ding, Y., Niemczyk, M., Kudla, G., Plotkin, J.B (2013). "Rate-Limiting Steps in Yeast Protein Translation." *Cell* 153: pp. 1589–1601.
- Sheth, U. & Parker, R (2003). "Decapping and decay of messenger RNA occur in cytoplasmic processing bodies." *Science*, 300, 805-808.
- Sheth, U. & Parker, R (2006). "Targeting of aberrant mRNAs to cytoplasmic processing bodies." *Cell*, 125, 1095-1109.
- Shuen, W. H. (2010) Molecular Evolution of the def6/swap70 Gene Family and Functional Analysis of swap70a in Zebrafish Embryogenesis.

- Singleton, K. L., Gosh, M., Dandekar, R. D., Au-Yeung, B. B., Ksionda, O., Tybulewicz, V. L., Altman, A., Fowell, D. J., Wülfing, C (2011). "Itk controls the spatiotemporal organization of T cell activation." *Sci Signal* 4(193): ra66.
- Stinchcombe J.C., Majorovits, E., Bossi, G., Fuller, S., Griffiths, G.M (2006). "Centrosome polarization delivers secretory granules to the immunological synapse." *Nature*. 443:462–465
- Stinchcombe, J. C., Bossi, G., Booth, S., Griffiths, G. M (2001). "The immunological synapse of CTL contains a secretory domain and membrane bridges." *Immunity* 15(5): 751-761.
- Snapper, S. B. & Rosen, F. S (1999). "The Wiskott-Aldrich syndrome protein (WASP): roles in signaling and cytoskeletal organization." *Annu Rev Immunol* 17: 905-929.
- Soderberg, O., Gullberg, M., Jarvius, M., Ridderstrale, K., Leuchowius, K. J., JARVIUS, J., Wester, K., Hydbring, P., Bahram, F., Larsson, L. G., Landegren, U. (2006). "Direct observation of individual endogenous protein complexes in situ by proximity ligation". *Nat Methods*, 3, 995-1000.
- Sprent, J. (2001). "Burnet oration. T-cell survival and the role of cytokines." *Immunol Cell Biol* 79(3): 199-206.
- Tang, D., Lahti, J.M., Grenet, J., Kidd, V.J (1999) " Cycloheximide-induced T-cell death is mediated by a Fas-associated death domain-dependent mechanism" *J Biol Chem*. 274 (11): 7245-52.
- Tanaka, Y., Bi, K., Kitamura, R., Hong, S., Altman, Y., Matsumoto, A., Tabata, H., Lebedeva, S., Bushway, P. J., Altman, A. (2003). "SWAP-70-like adapter of T cells, an adapter protein that regulates early TCR-initiated signaling in Th2 lineage cells." *Immunity* 18(3): 403-414.
- Teixeira, D., Sheth, U., Valencia-Sanchez, M.A., Brengues, M., Parker, R (2005). "Processing bodies require RNA for assembly and contain nontranslating mRNAs." *Rna-a Publication of the Rna Society*, 11, 371-382.

- Tcherkezian, J., Brittis, P.A., Thomas, F., Roux, P.P., Flanagan, J.G (2010) " Transmembrane receptor DCC associates with protein synthesis machinery and regulates translation" *Cell*. 141(4):632-44
- Tian, Q., Streuli, M., Saito, H., Schlossman, S. F., Anderson, P (1991). "A polyadenylate binding protein localized to the granules of cytolytic lymphocytes induces DNA fragmentation in target cells." *Cell*, 67, 629-39.
- Turner, M. & Billadeau, D. D (2002). "VAV proteins as signal integrators for multi-subunit immune-recognition receptors." *Nat Rev Immunol* 2(7): 476-486.
- Tybulewicz, V. L. & Henderson, R.B (2009). "Rho family GTPases and their regulators in lymphocytes". *Nat Rev Immunol*, 9, 630-44.
- Ueda, T., Watanabe-Fukunaga, R., et al. (2004). Mnk2 and Mnk1 are essential for constitutive and inducible phosphorylation of eukaryotic initiation factor 4E but not for cell growth or development. *Mol Cell Biol* 24(15): pp. 6539-6549.
- Valiunas, V. & Brink, P.R. (2015). "A comparison of two cellular delivery mechanisms for small interfering RNA". *Physiological reports*, 3(2), p.e12286.
- Van der Merwe, P. A. (2002). "Formation and function of the immunological synapse." *Curr Opin Immunol* 14(3): 293-298.
- Van Dijk, E., Cougot, N., Meyer, S., Babajko, S., Wahle, E., Seraphin, B (2002). "Human Dcp2: a catalytically active mRNA decapping enzyme located in specific cytoplasmic structures." *EMBO J*, 21, 6915-24.
- Vistica, B. P., Shi, G., Nugent, L., Tan, C., Altman, A., Gery, I (2012). "SLAT/Def6 plays a critical role in the pathogenic process of experimental autoimmune uveitis (EAU)." *Mol Vis* 18: 1858-1864.
- Waskiewicz, A. J & Flynn, A. (1997). "Mitogen-activated protein kinases activate the serine/threonine kinases Mnk1 and Mnk2." *Embo J* 16(8): pp. 1909-1920.
- Wells, S. E., Hillner, P.E., Vale, R.D., Sachs, A.B (1998). "Circularization of mRNA by eukaryotic translation initiation factors." *Mol Cell*, 2, 135-40.
- Wennerberg, K. & Der, C. J (2004). "Rho-family GTPases: it's not only Rac and Rho (and I like it)." *J Cell Sci* 117(Pt 8): 1301-1312.

- Wittrup, A. & Lieberman, J. (2015). "Knocking down disease: a progress report on siRNA therapeutics". *Nature Reviews Genetics*, 16(9), p.543.
- Wen, Y. & Meng, W.S. (2014). "Recent in vivo evidence of particle-based delivery of small-interfering RNA (siRNA) into solid tumors". *Journal of pharmaceutical innovation*, 9(2), pp.158-173.
- Yanagiya, A, Suyama, E, Adachi, H, Svitkin, Y.V, Aza-Blanc, P, Imataka, H, Mikami S, Martineau, Y, Ronai, Z.A, Sonenberg, N (2012). "Translational homeostasis via the mRNA cap-binding protein, eIF4E" *Mol Cell*. 46(6):847-58
- Yi, W., Gupta, S., Ricker, E., Manni, M., Jessberger, R., Chinenov, Y., Molina, H., Pernis, A. B (2017) "The mTORC1-4E-BP-eIF4E axis controls de novo Bcl6 protein synthesis in T cells and systemic autoimmunity" *Nat Commun*. 8 (1): 254
- Yokosuka, T., Sakata-Sogawa, K., Kobayashi, W., Hiroshima, M., Hashimoto-Tane, A., Tokunaga, M., Dustin, M. L., Saito, T (2005). "Newly generated T cell receptor microclusters initiate and sustain T cell activation by recruitment of Zap70 and SLP-76." *Nat Immunol* 6(12): 1253-1262.
- Yu, Y., Alexander, A., Smoligovets, Groves, J. T (2013). "Modulation of T cell signaling by the actin cytoskeleton." *J Cell Sci* 126(Pt 5): 1049-1058.
- Zheng, Y. (2001). "Dbl family guanine nucleotide exchange factors." *Trends Biochem Sci* 26(12):
- Zhang, Y. (2008). "I-TASSER server for protein 3D structure prediction. 724-732." *BMC Bioinformatics*, 23;9:40.
- Zhang, Y. (2008). "I-TASSER: fully automated protein structure prediction in CASP8." *Proteins*, 77 Suppl 9:100-13
- Zhang, J., Wang, J., Ng, S., Lin, Q., Shen, H.M. (2014) "Development of a novel method for quantification of autophagic protein degradation by AHA labeling" *Autophagy*. 10 (5):901-12.
- Zhang, J., Wang, J., Lee, Y.M., Lim, T.K., Lin, Q., Shen, H.M (2017) "Proteomic Profiling of De Novo Protein Synthesis in Starvation-Induced Autophagy Using Bioorthogonal Noncanonical Amino Acid Tagging". *Methods Enzymol*. 588:41-59.

# Appendix

## 6.1 Plasmid map:

### DEF6 construct

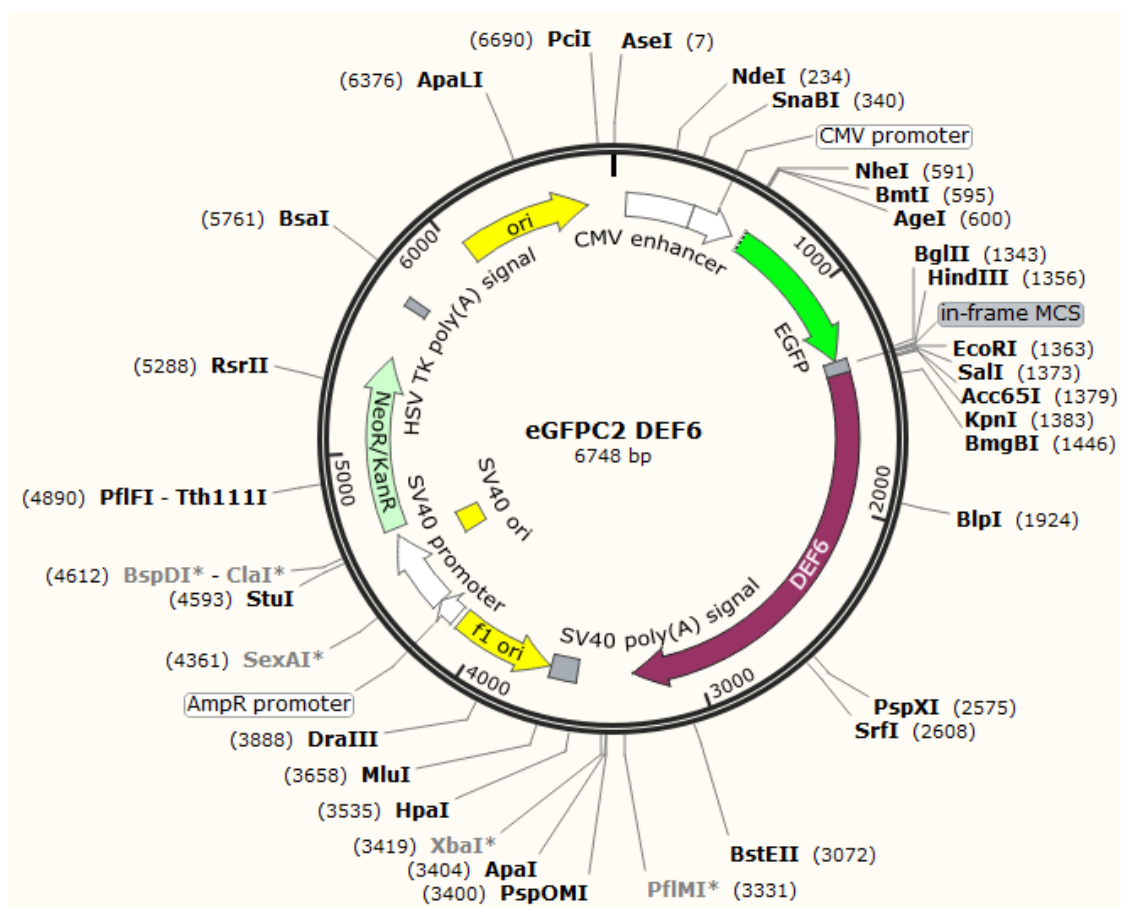


**Figure 6.1: Plasmid map of GFP-tagged DEF6.** eGFPC2 plasmid (Invitrogen) was used to clone the human-derived cDNA of DEF6 (purple) in-frame to the GFP coding sequence (green). The CMV promoter/enhancer cassette (white) allows expression of the GFP-tagged DEF6 in mammalian cells. The SV40-derived promoter facilitates expression of the neomycin gene that confers resistance in bacterial (kanamycin) as well as mammalian cells (neomycin). Origins of replications are shown in yellow. Key restriction enzyme sites are as indicated. Plasmid map was established using SnapGene Viewer 2.8.

## 6.2 Amino acid and Codons:

Amino acids and their Abbreviation			Codons
<b>A</b>	Ala	Alanine	GCA GCC GCG GCU
<b>C</b>	Cys	Cysteine	UGC UGU
<b>D</b>	Asp	Aspartic acid	GAC GAU
<b>E</b>	Glu	Glutamic acid	GAA GAG
<b>F</b>	Phe	Phenylalanine	UUC UUU
<b>G</b>	Gly	Glycine	GGA GGC GGG GGU
<b>H</b>	His	Histidine	CAC CAU
<b>I</b>	Ile	Isoleucine	AUA AUC AUU
<b>K</b>	Lys	Lysine	AAA AAG
<b>L</b>	Leu	Leucine	UUA UUG CUA CUC CUG CUU
<b>M</b>	Met	Methionine	AUG
<b>N</b>	Asn	Asparagine	AAC AAU
<b>P</b>	Pro	Proline	CCA CCC CCG CCU
<b>Q</b>	Gln	Glutamine	CAA CAG
<b>R</b>	Arg	Arginine	AGA AGG CGA CGC CGG CGU
<b>S</b>	Ser	Serine	AGC AGU UCA UCC UCG UCU
<b>T</b>	Thr	Threonine	ACA ACC ACG ACU
<b>V</b>	Val	Valine	GUA GUC GUG GUU
<b>W</b>	Trp	Tryptophan	UGG
<b>Y</b>	Tyr	Tyrosine	UAC UAU
		Stop Codon	UAA UAG UGA

**Table 4:** List of amino acids, their single and three letter abbreviations and codons.

### 6.3 Primary and Secondary Antibodies

Table 5: List of Primary antibodies used:

Antibody	Host	Isotype	Clone	Use	Dilution	MW (kDa)	Cat. Number	Supplier
<b>DEF6</b>	Rabbit	IgG	Monoclonal [EPR7492]	IF WB/IP Flow cyto	1/250 1/1000 -1/100 1/500	74kDa	ab 126792	abcam
<b>eIF4E</b>	Mouse	IgG	Monoclonal [P-2]	IF WB	1/500 1/1000	28kDa	Sc-9976	Santa Cruz
<b>eIF4E-t</b>	Rabbit	IgG	Polyclonal	WB	1/1000	140kDa	Ab55880	abcam
<b>eIF4E-t</b>	Mouse	IgG	Polyclonal	WB IF	1/1000 10 µg /ml	140kDa	Ab168098	abcam
<b>PABP</b>	Mouse	IgG	Monoclonal [10E10]	WB IF	1/1000 1/250	70kDa	Sc-32318	Santa Cruz
<b>ARP2</b>	Mouse	IgG	Monoclonal [E-2]	WB IF	1/1000 1/250	43kDa	Sc-137250	Santa Cruz
<b>β-actin</b>	Mouse	IgG2b	Monoclonal [8H10D10]	WB	1/1000	45kDa	#3700	Cell Signaling

Table 5.1 List of Secondary antibodies used:

<b>Antibody</b>	<b>Host</b>	<b>Use</b>	<b>Dilution</b>	<b>Cat. Number</b>	<b>Supplier</b>
Rabbit IgG (H+L) Alexa fluor 568	Goat	IF	1/500	A11011	Molecular probes
Mouse IgG (H+L) Alexa fluor 488	Goat	IF	1/500	A11001	Molecular probes
Rabbit IgG H+L HRP linked	Goat	WB	1/2000	#7074	Cell Signaling Technology
Mouse IgG H+L HRP linked	Horse	WB	1/2000	#7076	Cell Signaling Technology

**Table 6: Cell Stain;**

<b>Stain</b>	<b>Use</b>	<b>Dilution</b>	<b>Cat. Number</b>	<b>Supplier</b>
Calcein blue	IF	1 $\mu$ g/ml	C1429	Life technologies

**Table 7: List of Primer Sequences:**

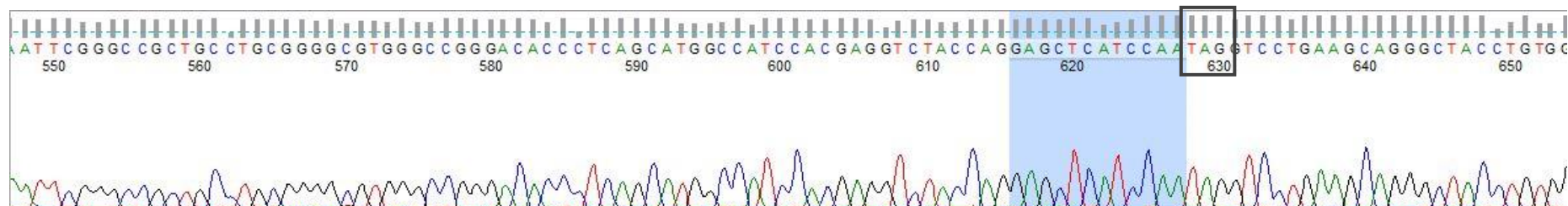
<b>Target</b>	<b>Primer</b>	<b>Primer Sequence 5'-3'</b>	<b>Application</b>
DEF6	216 Stop codon	GAGCTCATCCAA TAG GTCCTGAAGCAG	Mutagenesis
Y210E – Y222E	216E Stop codon	GAGCTCATCCAA TAG GTCCTGAAGCAG	Mutagenesis
DEF6	312 Stop codon	G ATG GCG ATC TAG CTG CAG GCC G	Mutagenesis
Y210E- Y222E	312EE Stop codon	G ATG GCG ATC TAG CTG CAG GCC G	Mutagenesis
DEF6	T586E	CTA AAG CGC CTG GAG CGC TGG GGA TCC	Mutagenesis
DEF6	T595E	GGC AAC AGG GAG CCC TCG CCC AAC AGC	Mutagenesis
DEF6	T619E	CCG GCT TCC GAG CCT CAG GAA GAT AAA	Mutagenesis
DEF6	T538F	CAG GCC AGC TTT AAC GTG AAA CAC TGG	Mutagenesis
DEF6	T563F	CGT CCG GTC TTT AGC AGC TCC TTC TCA	Mutagenesis
DEF6	T586F	CTA AAG CGC CTG TTT CGC TGG GGA TCC	Mutagenesis
DEF6	T595F	GGC AAC AGG TTT CCC TCG CCC AAC AGC	Mutagenesis
DEF6	T619F	CCG GCT TCC TTT CCT CAG GAA GAT AAA	Mutagenesis
DEF6	S580F	CAC CGT GAC TTT TCC CTA AAG CGC CTG	Mutagenesis
DEF6	S590F	CGC TGG GGA TTT CAG GGC AAC AGG	Mutagenesis
DEF6	S597F	GGC AAC AGG ACC CCC TTT CCC AAC AGC	Mutagenesis
DEF6	S606F	CAG AAG TTT CTC AAT GGT GGG GAT GAG	Mutagenesis

**Table 8: List of Reverse Transcription Polymerase Chain Reaction (RT-PCR) Primers:**

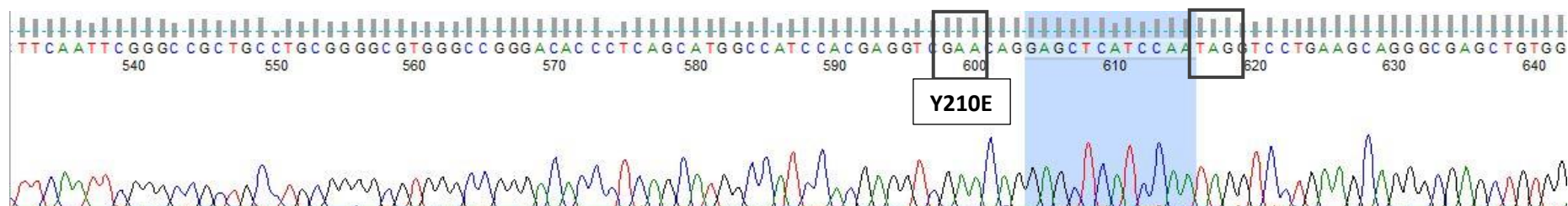
<b>Target</b>	<b>Exon</b>	<b>Primer Sequence 5'-3'</b>	<b>Application</b>
ARP2	Exon 1 Fwd.	GAAGACGCAAGAGGAAGAAGAG	RT-PCR
ARP2	Exon 6 Rev	CGTATCCTCGCAACAGAAGTAG	RT-PCR
PABP	Exon 1 Fwd.	GGACCTGCCTCAAGTGTAAG	RT-PCR
PABP	Exon 1 Rev	GCAACCACCCTCCATCATAA	RT-PCR
eIF4E	Exon 1 Fwd.	CACCCTTGTGAGGTAAGTGTATC	RT-PCR
eIF4E	Exon 1 Rev	GTGGTCATTCGTTGCCATTTC	RT-PCR
4E-T	Exon 5 Fwd.	GATTGGCAGTGGGAGGATAAT	RT-PCR
4E-T	Exon10 Rev	CAAGGTCTCTTCTAGGTGTTCTG	RT-PCR
DEF6	Exon 3 Fwd.	GGGAACAGTATGCTCTCCAATC	RT-PCR
DEF6	Exon 5 Rev	GCACTCTTCACTCCCAAAGTAG	RT-PCR
eEF1a1	Exon 2 Fwd.	GTATGCCTGGGTCTTGGATAAA	RT-PCR
eEF1a1	Exon 3 Rev	GTCTGCCCATTCCTTGGAGATAC	RT-PCR

## 6.4 Verification of DEF6 by DNA Sequencing:

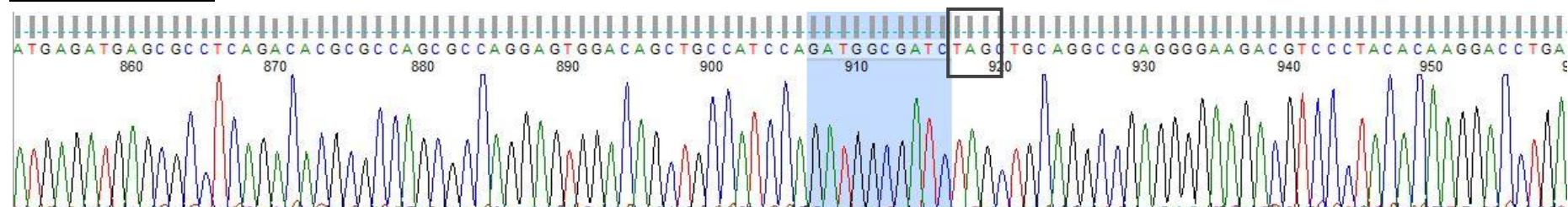
### 216 Stop Codon

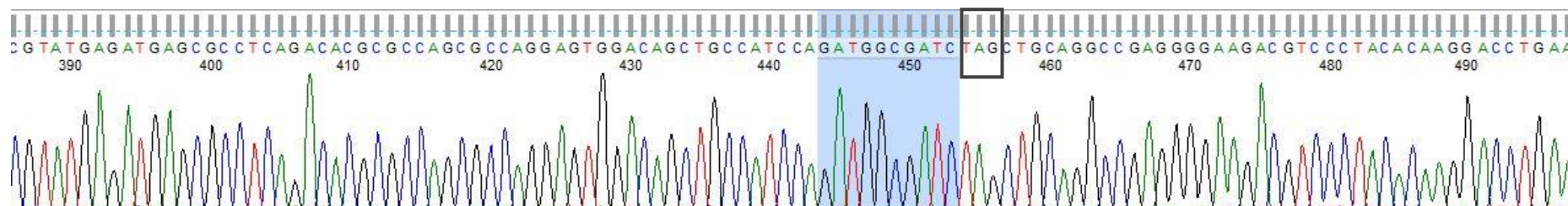
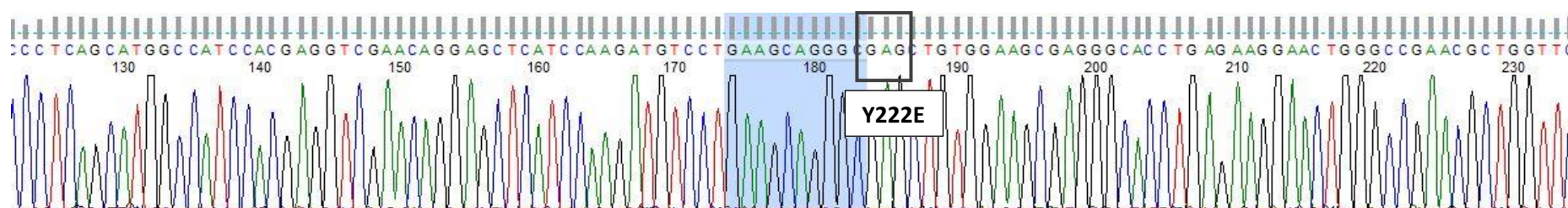
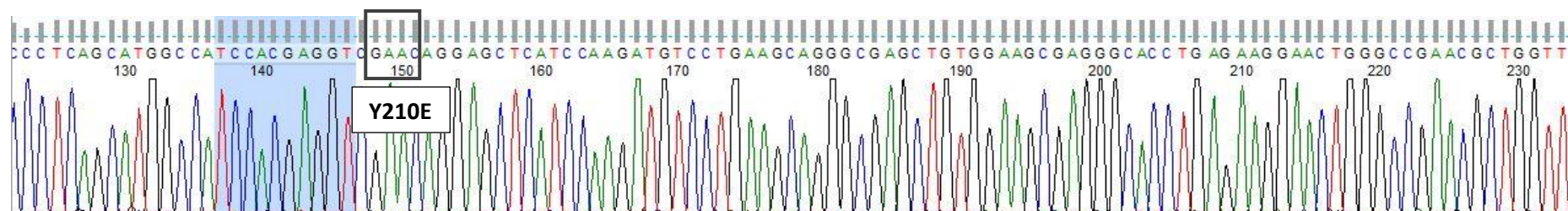


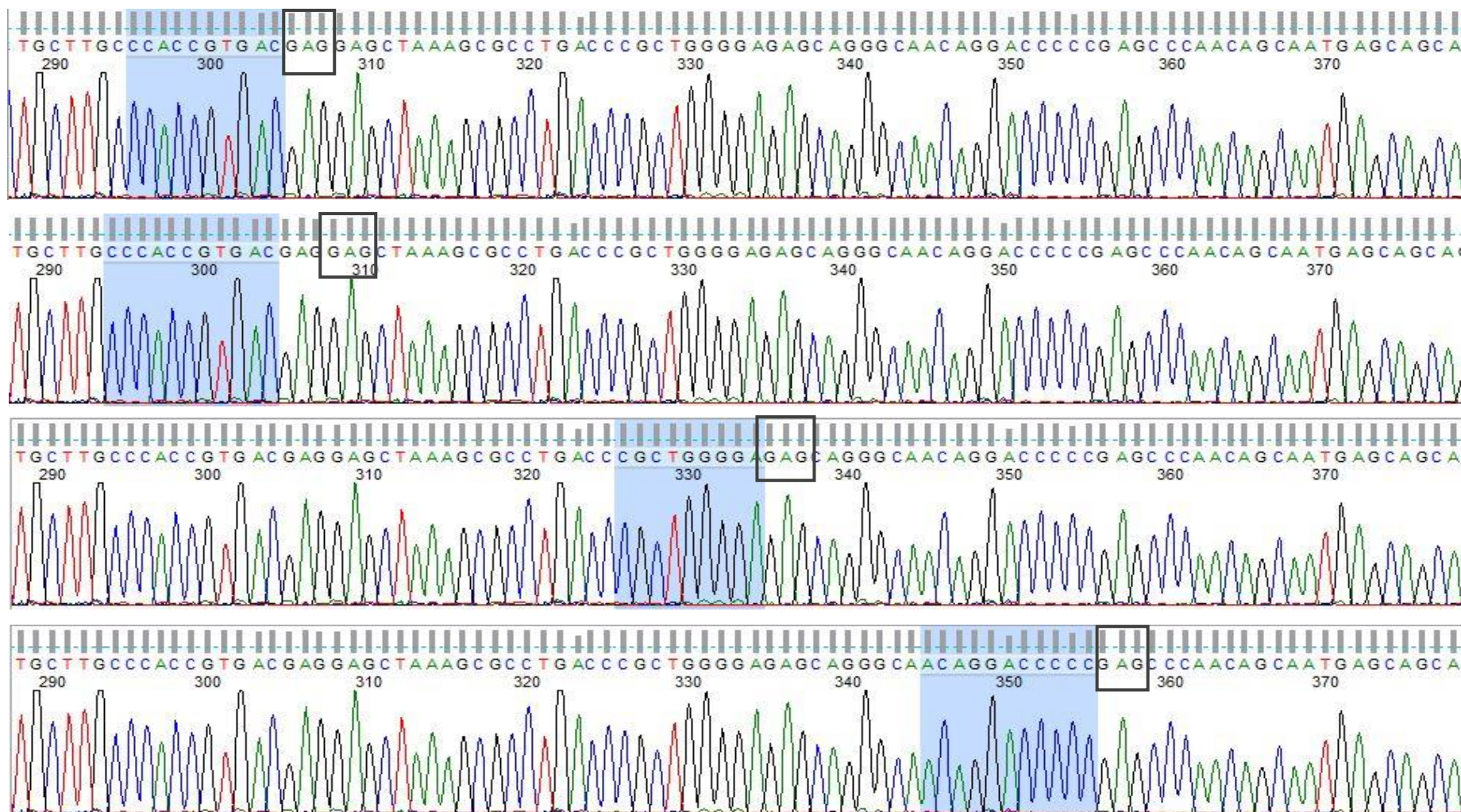
### 216E Stop codon

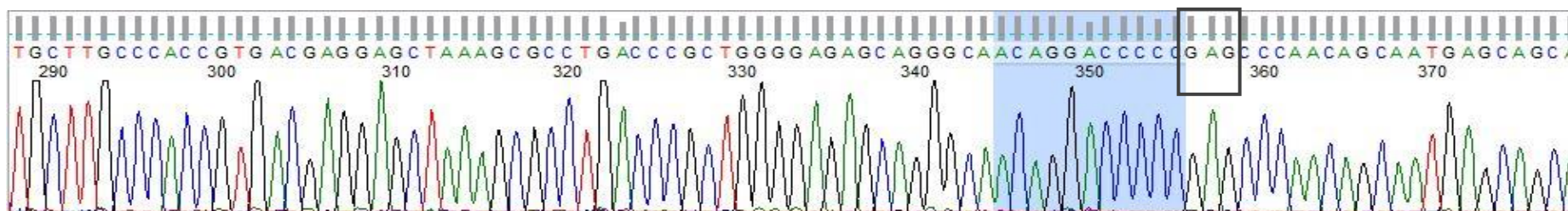
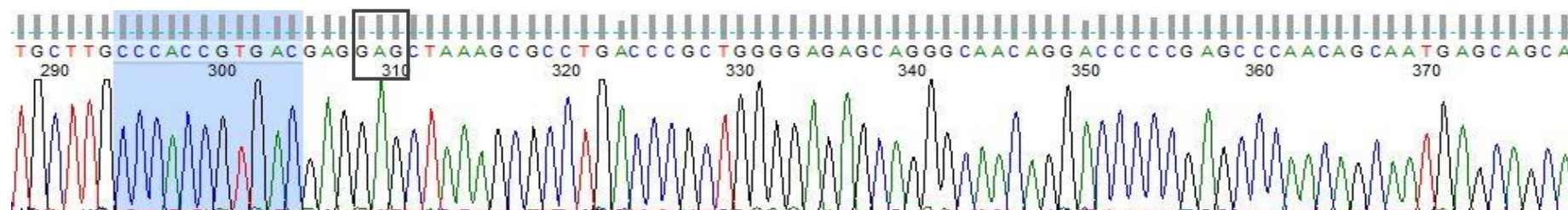
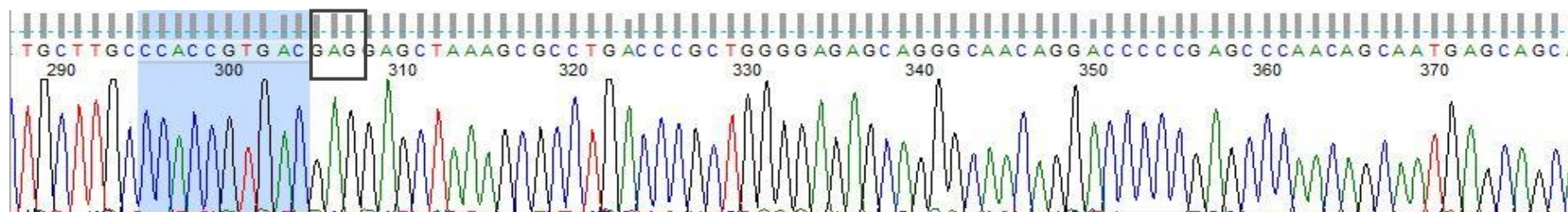


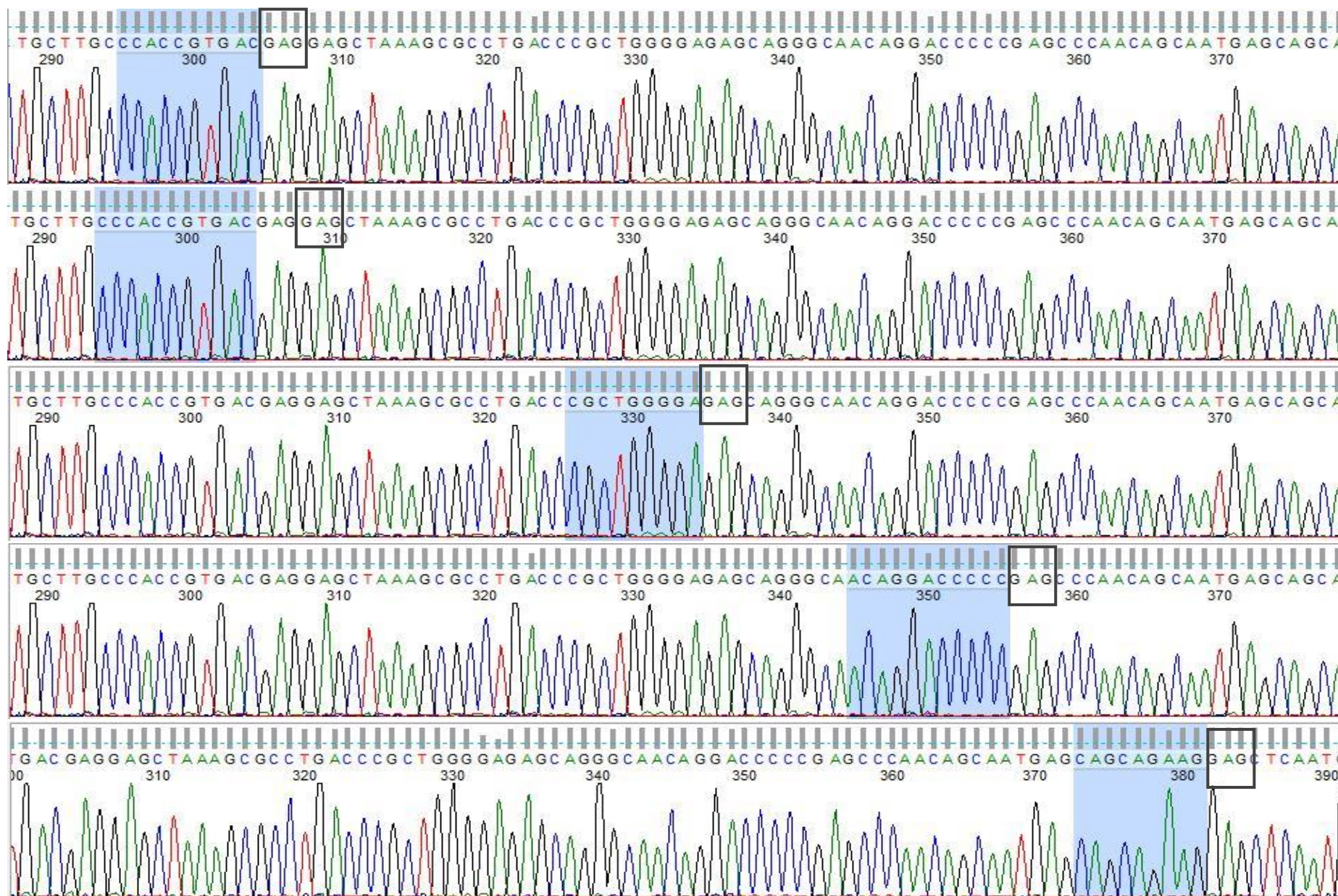
### 312 Stop Codon

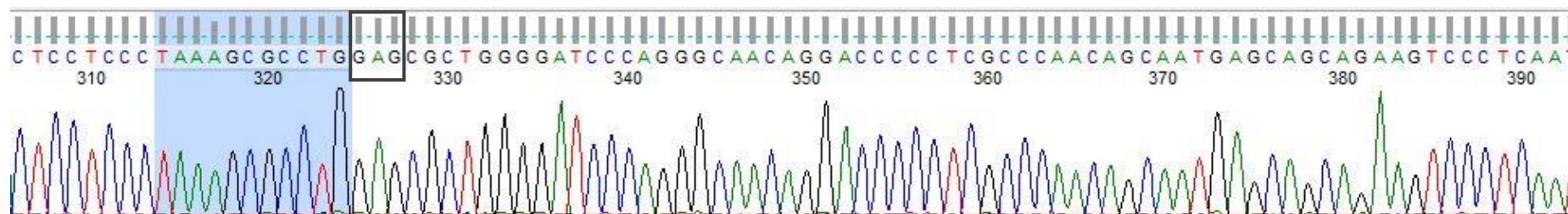
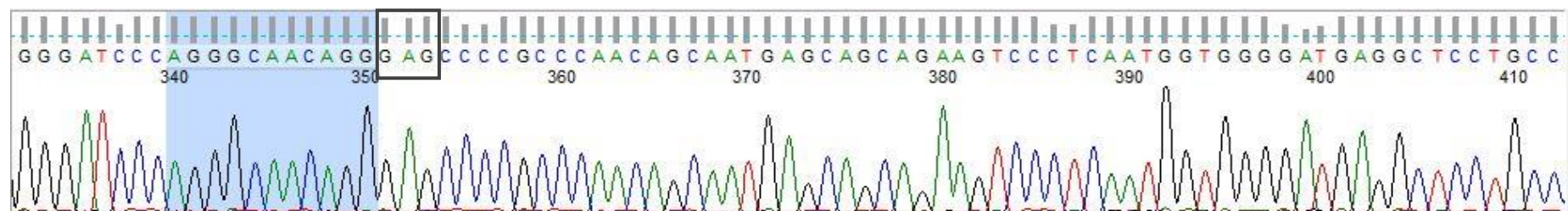
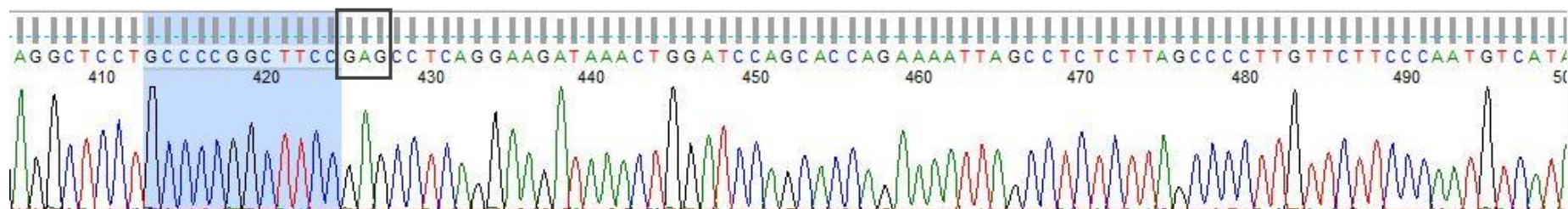


**312EE Stop codon**

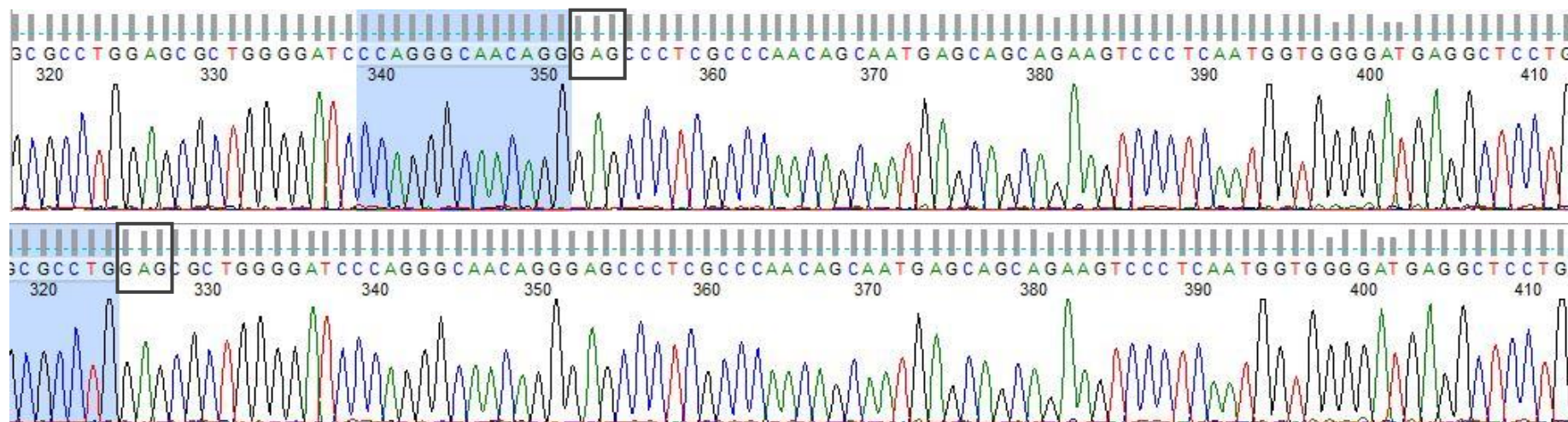
A) S580E, S581E, S590E&S597E

**B) 580E, S581E & S597E****C) S580E, S581E, S590E, S597E & S606E**

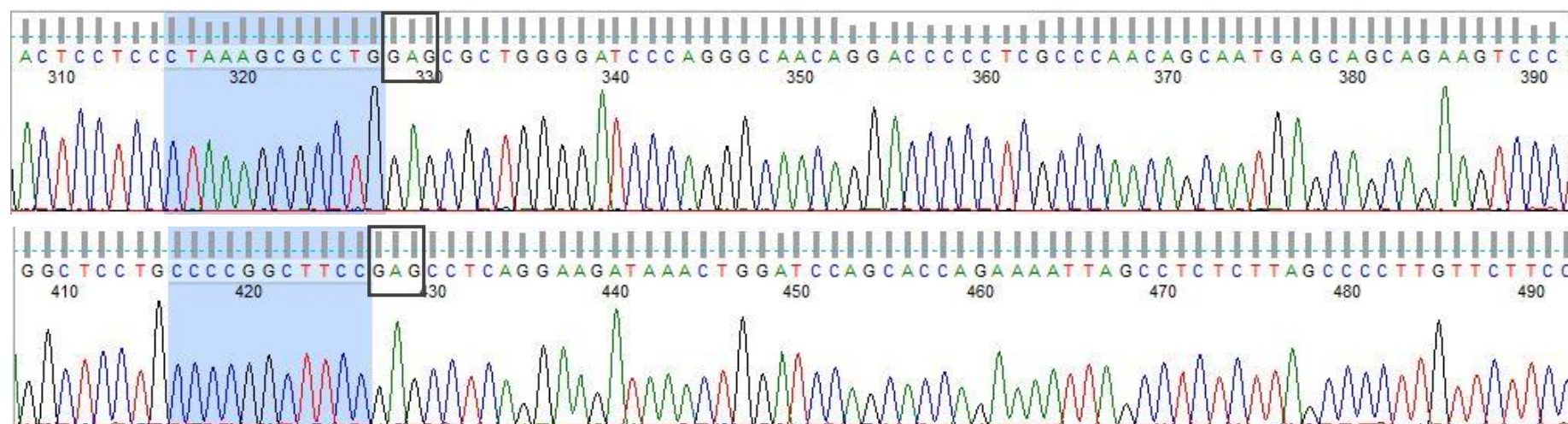


**T586E****T595E****T619E**

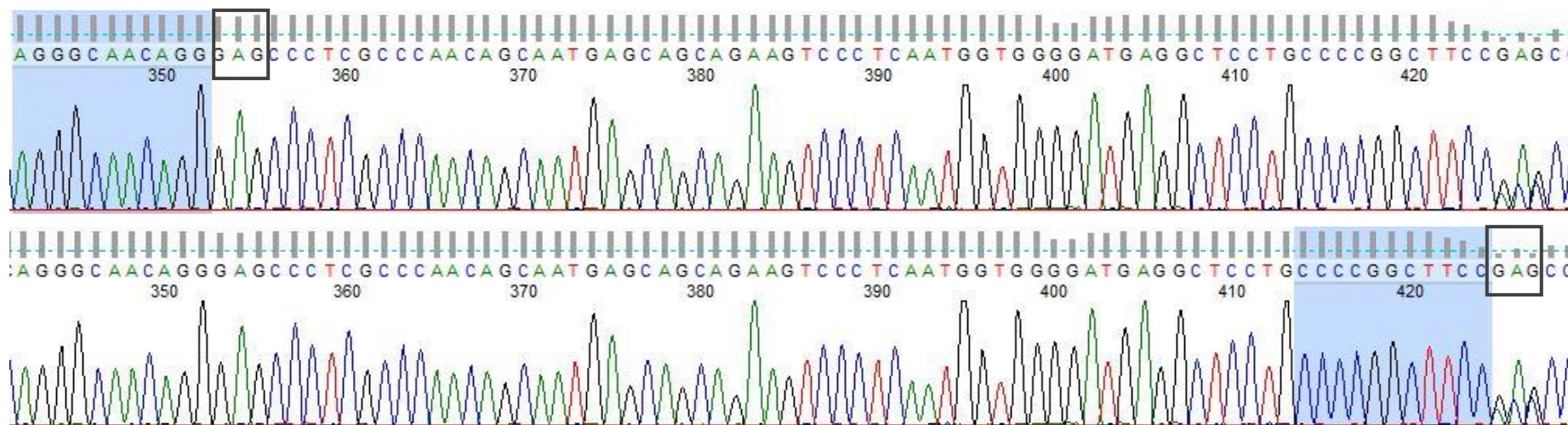
**T568E & T595E**



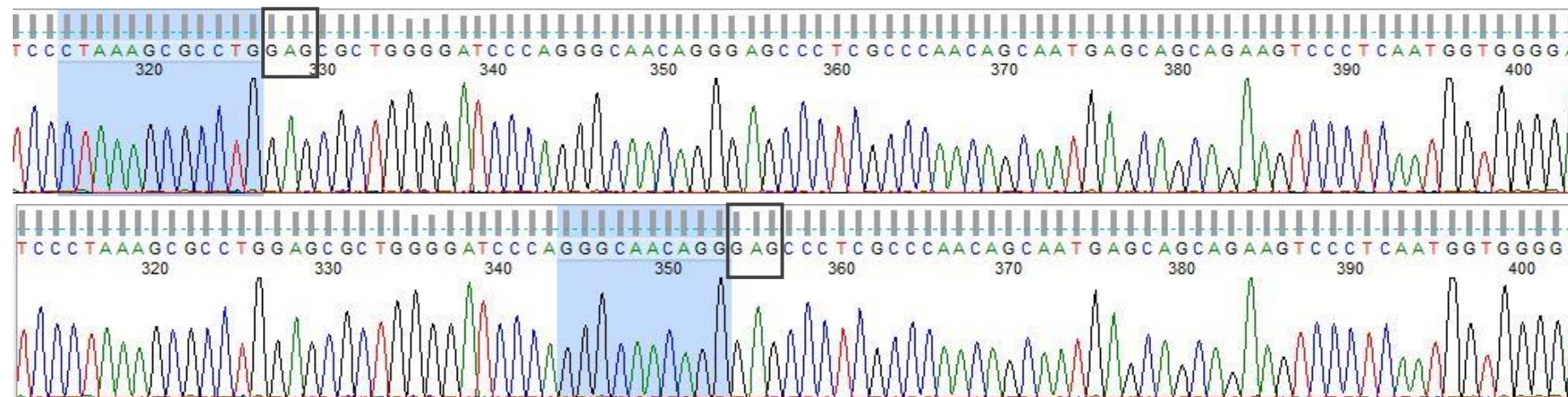
**T586E & T619E**

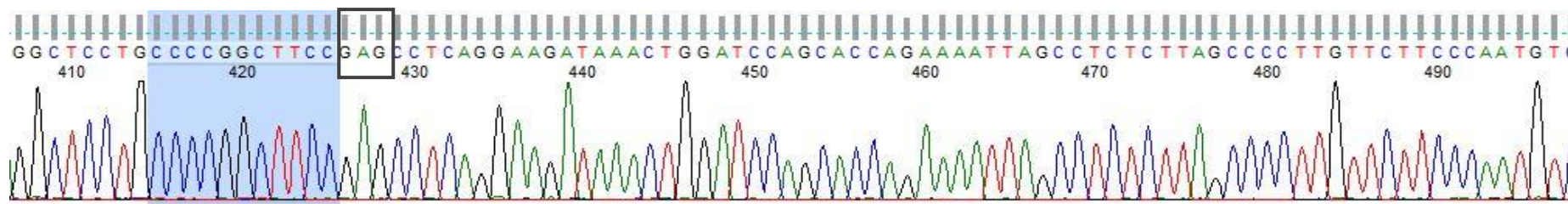


**T595E & T619E**

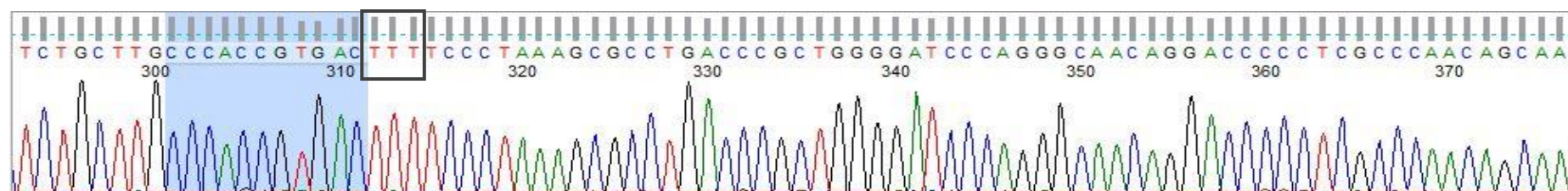


**T586E, T595E & T619E**

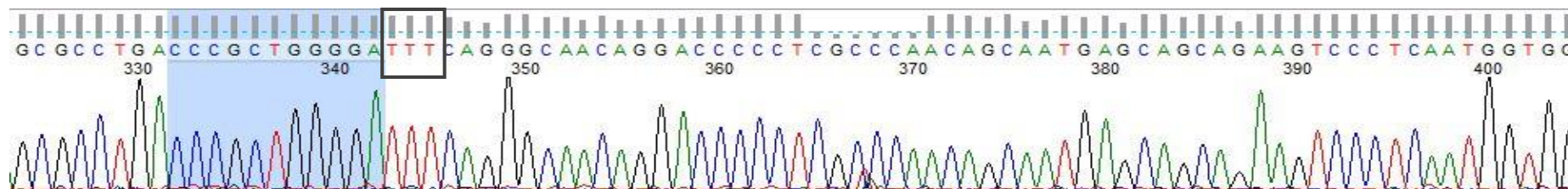




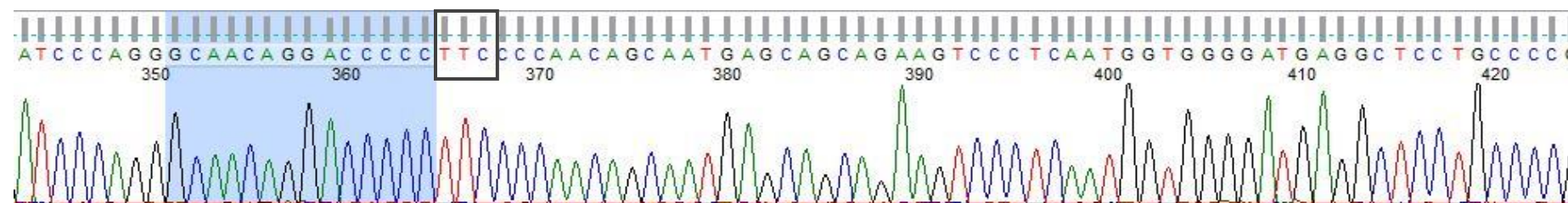
**S580F**

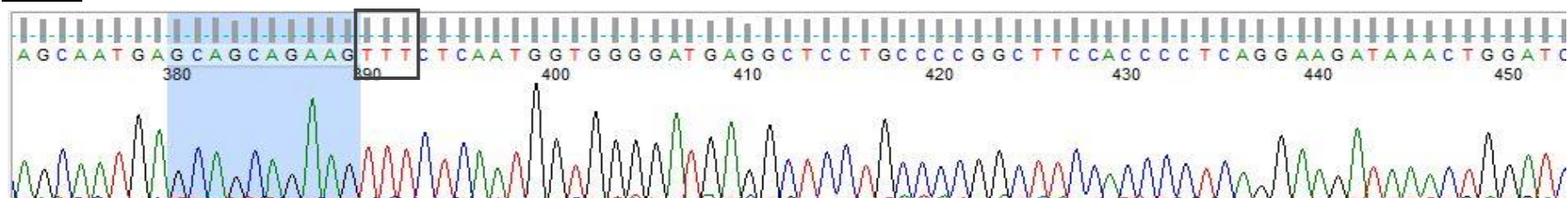
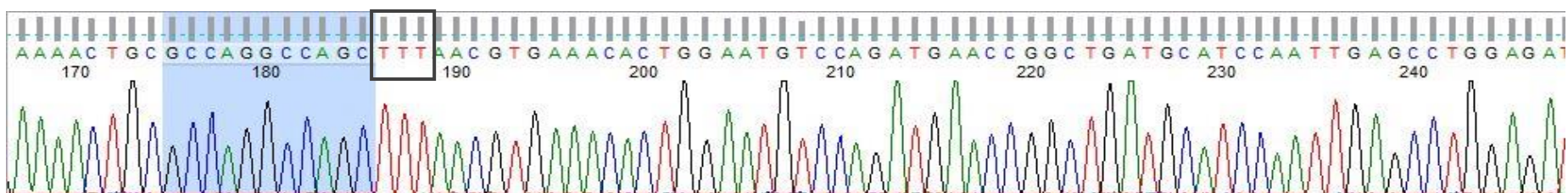
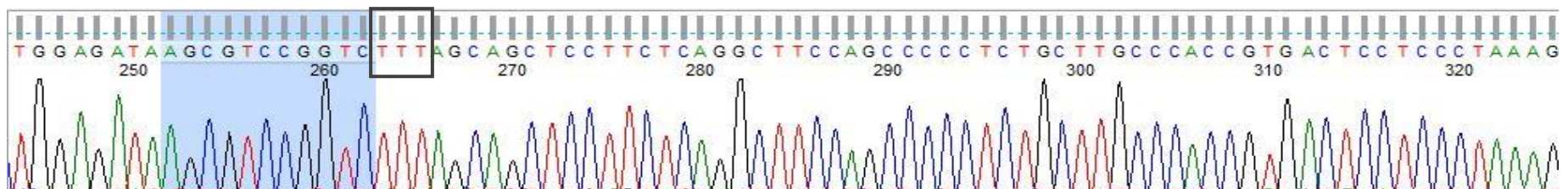
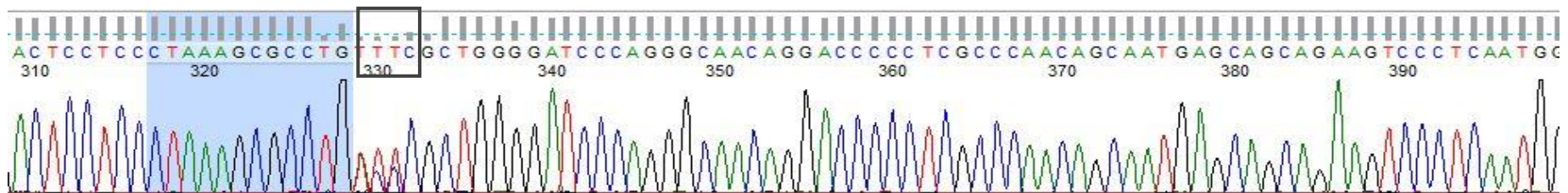


**S590F**



**S597F**



**S606F****T538F****T563F****T586F**

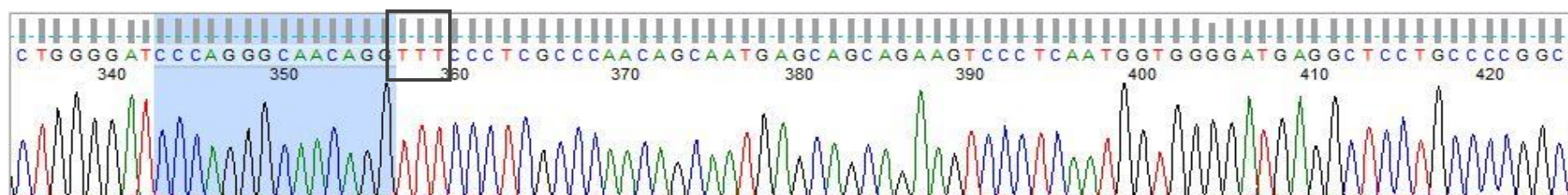
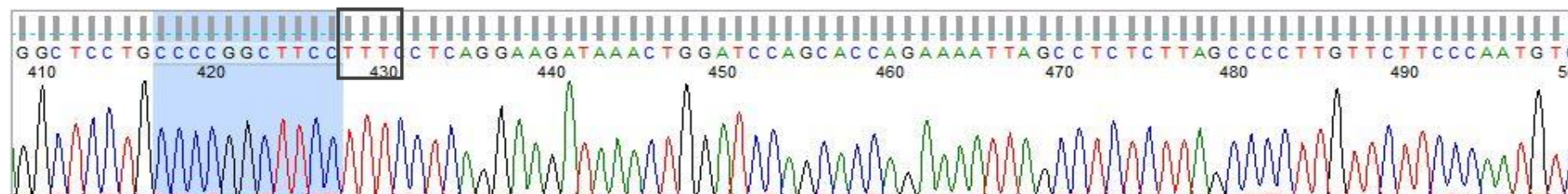
**T595F****T619F**

Figure 6.4: **Verification of DEF6 by DNA Sequencing:** Chromatographs for the DEF6-pEGFP-C2 serine and threonine to glutamic acid or phenylalanine mutants were read using Finch TV for the sequence alignment editor